Photoperiodic Encoding by the Neuronal Network of the Suprachiasmatic Nucleus

Henk Tjebbe van der Leest

Photoperiodic Encoding by the Neuronal Network of the Suprachiasmatic Nucleus

Proefschrift
ter verkrijging van
de graad van Doctor aan de Universiteit Leiden
op gezag van Rector Magnificus prof. mr. P.F. van der Heijden,
volgens besluit van het College voor Promoties
te verdedigen op woensdag 3 november 2010
klokke 13.45 uur
door
Henk Tjebbe van der Leest
geboren te Rotterdam
in 1979

Promotiecommissie

Promotor:
Prof. dr. J.H. Meijer

Overige leden:
Prof. H.D. Piggins (University of Manchester)
Prof. dr. B van der Horst (Erasmus Medical Center)
Dr. R. Hut (University of Groningen)

The research presented in this thesis was performed at the Leiden University Medical Center, group Neurophysiology, department of Molecular Cell Biology.

This work was supported by program grant "From Molecule to Cell" by the Netherlands Organization for Scientific Research (NWO), grant number 805.47.212 and by "Entrainment of the circadian clock" EUCLOCK program of the European Union.

Netherlands Organisation for Scientific Research
From Molecule to Cell

TABLE OF CONTENTS

CHAPTER 1

Introduction

Circadian Rhythms

The rotation of the earth around its axis causes differences in light intensity; temperature; food availability and wavelength composition of the light. Many organisms show rhythms in their behavior and physiology, which for long have been ascribed to environmental cycles. In 1926, Johnson concluded that there must be an internal clock. He based this conclusion on observations of mice, kept in constant conditions without environmental stimuli, which showed a sustained activity rhythm that deviated slightly from 24h (Johnson, 1926; Johnson, 1939). This is visible as a daily shift of the activity rhythm relative to the 24h cycle. Because of the deviation from 24h, it is unlikely that the rhythm is attributable to an external cycle. These rhythms in an organism of approximately 24h that continue to exist when environmental time cues are absent, are called circadian rhythms (circa = approximately; dies = day). The evolutionary advantage of circadian rhythms is that they allow an organism to anticipate to daily occurring events.

Advantage of a clock

For an organism that is able to anticipate the environmental changes, the fitness or reproductive success is thought to be enhanced. By studying unicellular cyanobacteria whose lifecycle is shorter than 24h but possess a circadian clock, the reproductive success can determined. The environmental time information, which exceeds the lifespan of these bacteria, is inherited by the offspring. When rhythmic and arrhythmic strains of these bacteria are exposed to a cyclic environment, the bacteria that express a circadian rhythm in metabolism are able to reproduce at higher rates than the arrhythmic strain, showing the adaptive significance of a clock that anticipates daily changes (Woelfle et al., 2004; Johnson et al., 2008). In higher organisms, it is much harder to find evidence for the functional evolutionary advantage of a circadian clock, although this concept has been studied in wild-caught animals. A number of animals received surgery that selectively abolished circadian rhythmicity. After surgery, the survival rate of these animals was monitored in their natural habitat. Despite a lack of a controlled environment, these studies presented compelling data that animals without circadian rhythms were more prone to predation than animals that did display a circadian rhythm (DeCoursey et al., 1997; DeCoursey and Krulas, 1998; DeCoursey et al., 2000). It is likely in the case of a nocturnal animal that it will have an advantage when it seeks refuge in its retreat before the sun rises, preventing predation by daytime hunters. Also, when an animal adjusts its timing so that it is foraging when a suitable food supply is more easily available, it can sustain a higher number of offspring, giving rise to a higher reproductive value.

Entrainment to environment

The research of circadian rhythms in mammals started with recordings of behavioral activity and many functions of the biological clock could already be investigated without knowledge of the actual location of such a clock, i.e. as a black box analysis. Although the internal clock continues to oscillate without environmental stimuli, it

is responsive to light and darkness. The internal free running rhythm, visible in the absence of time cues, can be phase advanced or phase delayed by presentation of a light pulse. The extend and direction of these phase shifts depend on the time of the light pulse. For instance, a nocturnal animal that is housed in darkness, responds to a light pulse at the beginning of the activity rhythm with a delay of its activity the following days. Light presentation at the end of its active period will phase advance the rhythm, in the resting phase of the animal, no phase shifts can be induced by light, even when the animal is awakened (DeCoursey, 1964; Daan and Pittendrigh, 1976a; Pittendrigh and Daan, 1976a; Takahashi et al., 1984). This time dependency of responses to light pulses can be represented in the form of a phase response curve (PRC). The PRC illustrates that the phase at which the light is presented, determines the response. Because of the time dependent responsiveness to light, animals will adjust their timing to the environment in natural conditions. Animals that have a free running period larger than 24h will return to their burrow too late and will therefore receive a phase advancing pulse in the morning. An animal with a period shorter than 24h will be entrained by the evening light at the start of the activity and will consequently delay its activity. This results in an adaptation of the internal clock to the environmental period. This process of adaptation to the external light dark cycles is called entrainment (Pittendrigh and Daan, 1976a).

Discovery of the suprachiasmatic nucleus

The clock is connected with the eyes

Because of the functional relation between the circadian oscillator and the environmental light conditions, a direct pathway was proposed between the optic pathway and the circadian clock. In an anatomical study the retino-hypothalamic tract (RHT) was identified (Moore and Lenn, 1972). The RHT is a tract that forms a direct connection from the retina to the hypothalamus. Because of this direct connection, the

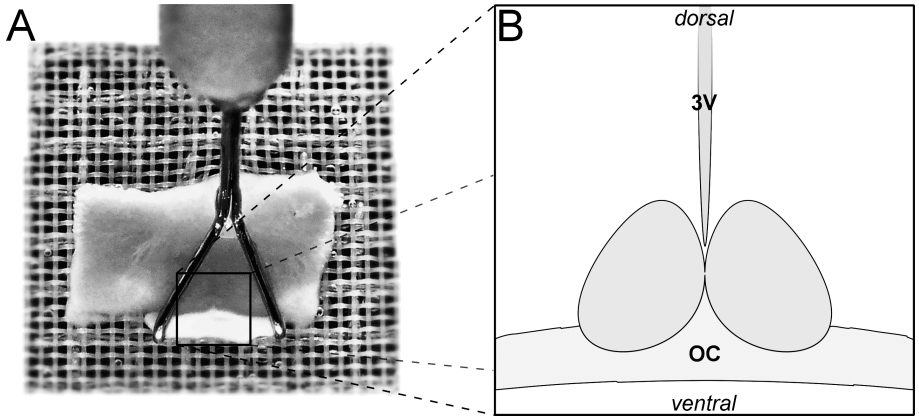

Figure 1.1

Coronal section containing the suprachiasmatic nucleus

(A) Photograph of a brain slice containing the SCN in an *in vitro* recording setup. The slice is stabilized by a fork and reaches from the dorsal part of the slice down to the ventral part, extending over the optic chiasm (OC, indicated in B). The area indicated by a black square is shown enlarged in B.
(B) Schematic drawing of a coronal hypothalamic section containing the SCN. On top of the optic chiasm (OC) the two suprachiasmatic nuclei are shown with the third ventricle (3V).

anterior part of the hypothalamus became a subject of great interest for a possible function in circadian rhythmicity.

Lesions along the optic tract were made and rhythmicity in wheel running, drinking and secretion of hormones, were recorded, to investigate at what point a lesion would induce a free-run of the circadian rhythm. It was hypothesized that, when no light-dark information from the eyes is transmitted to the clock, the clock will no longer synchronize to the environmental light dark cycles. As long as the lesions are upstream to the clock, this will be visible as a free-run of behavioral rhythms. When lesions of the optic nerve are performed downstream of the clock they do not affect entrainment. An experiment confirmed these hypothesis, lesions of the optic tract, downstream of the hypothalamus, rendering behaviorally blind animals, did not abolish entrainment capabilities (Moore and Klein, 1974; Klein and Moore, 1979).

Two research groups identified a paired structure just above the crossing of the optic nerve, the suprachiasmatic nucleus (SCN) as a possible location of the circadian oscillator at the same time (Moore

and Eichler, 1972; Stephan and Zucker, 1972). When the SCN was electrolytically lesioned, the rhythms in various output parameters were absent. This indicated that the SCN is critical for the generation of a circadian rhythm.

The SCN produces a rhythm

These findings certainly indicated that the SCN is involved in the rhythmic behavior but were not conclusive evidence that the SCN itself was producing the rhythm. The evidence that the SCN is in fact the main circadian pacemaker has accumulated throughout the years. Because of the neuronal nature of the SCN, electrical signals are the first parameter to study. The first electrophysiological recordings in the SCN *in vivo* were performed using an extracellular electrode, and multiunit electrical activity was recorded. The number of electrical impulses (action potentials) per time was used as a measure of activity. The electrical activity in the SCN appeared rhythmic and is high during the day and low during the night (Inouye and Kawamura, 1979). In animals where the SCN was partially isolated from the surrounding tissue, the electrical discharge rhythm inside the SCN remained high during the projected day, while in other brain areas it was oscillating in anti-phase, with high activity during the night. In animals where the connections with the surrounding tissue were completely removed, rendering an "SCN island", the rhythm in the surrounding tissue was lost while the SCN remained rhythmic with high electrical activity during the day. This shows that the SCN drives the rhythm that was recorded outside the SCN.

SCN rhythms are autonomous

This was the first positive evidence that the SCN is in fact a pacemaker for circadian rhythms, but still not conclusive as to whether it is an autonomous oscillator. The same recording technique used in the *in vivo* study, extracellular electrophysiological recordings, could be applied *in vitro* (Figure 1.1). Small brain slices can be kept alive *in vitro* for several hours (~48h) and the tissue and

characteristics of the neurons in the slice remain relatively unchanged. It is therefore possible to record the spontaneous electrical activity in the SCN *in vitro*. Three groups independently performed the same type of recording: Brain slices containing the SCN were prepared and the electrical activity of a single neuron was recorded with an extracellular glass microelectrode. The neuronal activity was sampled from different neurons and the activity was averaged to obtain a representation of tissue-level activity (Green and Gillette, 1982; Groos and Hendriks, 1982; Shibata et al., 1982). The averaged activity profiles all show that during the day (projected light period) the electrical activity is high, while during the night (projected dark period) the activity is low. These results could not have been the consequence of a certain day night variation in the recording since the same results were obtained from animals that had a reversed light-dark schedule. These findings indicate that the SCN does not require rhythmic input, but remains rhythmic, also when kept in constant conditions. These experiments were the first proof that the SCN oscillates endogenously.

These endogenous circadian oscillations in the SCN are present in individual cells, measurable as a circadian rhythm in electrical activity that can be measured *in vitro* (Welsh et al., 1995; Kuhlman and McMahon, 2006). When SCN cells are grown in a dispersed culture however the timing of electrical activity varies substantially between cells (Herzog et al., 1998). These results from dispersed cells show that it is important for SCN neurons to be able to communicate with each other in order to stay synchronized (Webb et al., 2009).

Circadian rhythms are generated by a molecular clock

Many cells either in the SCN or in downstream oscillators contain an intrinsic clock and have a day-night rhythm in their output. The internal cellular clock that generates these circadian oscillations has a genetic basis and functions through a molecular feedback loop. Identified genes involved in the primary negative feedback loop are *Clock* (Gekakis et al., 1998) and paralogue neuronal PAS domain-

containing protein 2, *nPas2*; *Bmal1* (Bunger et al., 2000); period homologue 1 (*Per1*) and *Per2* (Shearman et al., 1997), cryptochrome 1 (*Cry1*) and *Cry2* (Kume et al., 1999; Okamura et al., 1999; van der Horst et al., 1999). CLOCK and BMAL1 are transcription factors that together activate transcription of *Per* and *Cry* genes. PER and CRY in turn form a hetero-dimer and interact with the CLOCK-BMAL1 complex and thereby inhibit their own transcription (Shearman et al., 2000; Lee et al., 2001). The PER-CRY repressor complex is degraded over a period of time and CLOCK-BMAL1 can promote the transcription of *Per* and *Cry*. The secondary loop involves a feedback through *Rev-erbα*. Transcription of *Rev-erbα* is stimulated by the CLOCK-BMAL complex and the resulting REV-ERBα proteins complete the feedback by inhibiting transcription of the *Bmal1* gene (Preitner et al., 2002; Sato et al., 2004). The breakdown of PER and CRY is performed by casein kinase 1 delta (CSNK1D) and casein kinase 1 epsilon (CSNK1E). The speed at which PER is degraded by these kinases determines the speed of the circadian oscillation (Meng et al., 2008). These interactions between clock genes and their protein products lead to a rhythm in protein levels with a period of approximately 24h (Takahashi et al., 2008).

Interactions between Molecular clock and electrical activity

A circadian rhythm is furthermore present in membrane potential (Vm) and excitability. The circadian regulation of membrane potential and excitability in SCN neurons is controlled by the expression and modulation of different ionic channels (review see (Brown and Piggins, 2007). Membrane potential and excitability are often causally linked in neurons, but both are controlled by separate sets of ion channels. In the SCN the ionic channels known to regulate frequency of action potentials are mainly K^+-channels, like fast-delayed rectifier (fDR) K^+-channel (Itri et al., 2005), inactivating K^+-current (I_a) (Dudek et al., 1993) and Ca^{2+}-activated K^+-channels (BK and SK channels)(Pitts et al., 2006; Meredith et al., 2006; Belle et al., 2009), but Ca^{2+}-current can also affect action potential frequency (L-type

I_{Ca})(Pennartz et al., 2002). While these currents are rather well described in the SCN, the ionic mechanism of circadian membrane potential regulation has not fully been identified. Similar to molluscan circadian pacemaker neurons (Michel et al., 1999; Michel et al., 1993) a Tetraethylammonium (TEA)-sensitive K^+ current seems to form the basis of circadian Vm changes in the mammalian clock neuron (Kuhlman and McMahon, 2004). The isolation and characterization of these currents, that need to be active at resting potential, have yet to be performed, but possible candidates for this "background" current are cationic current, like Ba^{2+}-sensitive current (De Jeu and Pennartz, 2002) and currents carried by two-pore channels (Bayliss and Barrett, 2008; Linden et al., 2007). Studies on knockout models of clock genes suggest a correlation between circadian control of action potential frequency modulation and molecular machinery (Albus et al., 2002), but a real causal link has not been established and the pathways have not been identified yet.

Interestingly, there is more evidence for changes in excitability affecting clock gene expression than the other way around. Rhythmic expression of *Per* and *Tim* are suppressed in *Drosophila* pacemaker neurons when they are electrically silenced by over-expression of a leak current (Nitabach et al., 2002; Cao and Nitabach, 2008). Likewise, hyper-polarization of SCN neurons by low extracellular K^+ blocks rhythms in *Per1* and *Per2* expression (Lundkvist et al., 2005). Interestingly, not only Vm is affecting clock gene expression, also changes in excitability and synaptic input seem to have an effect on the amplitude of clock gene expression. The loss of peptidergic signaling in a knockout mouse model deficient of the receptor for vasoactive intestinal polypeptide (VIP) leads to severe loss of amplitude in the rhythmic expression of *Per2* (Maywood et al., 2006). The messenger or cytosolic pathway used to mediate membrane events to the regulation of gene expression is not yet known, but Ca^{2+} seems to be a good candidate involved in this pathway (Lundkvist and Block, 2005; Lundkvist et al., 2005).

The SCN is a pacemaker

From lesions to knock-outs

Circadian rhythms have been observed in many different physiological parameters, behavioral and cognitive functions. Moreover, many tissues and organs are able to generate a circadian rhythm (Schibler and Sassone-Corsi, 2002), provoking the question what the special role of the suprachiasmatic nucleus in this multitude of circadian oscillators may be. The prevalent view at the time is that the SCN represents a master pacemaker for the mammalian circadian system keeping most other peripheral oscillators in a strict temporal order, like a conductor giving the cue to the musicians in an orchestra (Davidson et al., 2003). To fulfill this function, the SCN rhythm itself is self-sustained and robust, well entrained to the environmental cycles and forms a uniform output signal.

In 1988, a hamster with an extremely short period of about 20h instead of the normal 24h was described (Ralph and Menaker, 1988). The mutation that this hamster carries was named tau, after the Greek letter τ, which is used to describe the period of an animal. The mutation is inherited by the offspring and a strain of these hamsters was bred for research. A spontaneously occurring mutation in the CSNK1E gene led to the shortening of the endogenous free-running period. Because of an enhanced degradation of *Per*, the duration of inhibition of its own transcription is reduced and therefore the loop is completed faster (Lowrey et al., 2000; Meng et al., 2008). The tau mutant hamsters were further studied, and used in an experiment that provides compelling evidence that the SCN is a pacemaker of circadian rhythms. SCN from these tau-mutant hamsters was transplanted into SCN lesioned wild-type hamsters and vice versa (Ralph et al., 1990). This resulted not only in a restoration of the circadian rhythm in locomotor activity, but also the free-running period and the phase of the rhythm was matching the one of the donor animal.

More evidence for the SCN as the master pacemaker comes from *in vitro* measurements of the rhythm in *Per1* gene expression in peripheral tissue compared to the SCN (Yamazaki et al., 2000). Transgenic rats were exposed to abrupt 6 h or 9 h shifts in the light-dark schedule, the tissue from SCN, liver skeletal muscle and lung was subsequently prepared and the phase of the *Per1* rhythm determined at different days after the shift. The circadian *Per1* rhythm in the SCN shifted more rapidly than the peripheral tissue rhythms supporting the idea of a hierarchically organized circadian system with the SCN as the master clock.

A number of lesion experiments have confirmed the early studies and have shown that the SCN seems to be required for a multitude of circadian rhythms in mammals. However, lesion experiments are not always conclusive, since other brain regions and pathways may be affected by the surgery complicating the interpretation of the results. While different research groups work on an SCN specific genetic deletion and have already generated a conditional knockout model for one of the clock genes (Hong et al., 2007), different models for dysfunctional SCN have been employed. The SCN can be made arrhythmic either by the use of constant light (Daan and Pittendrigh, 1976b; Witting et al., 1995; Ruby et al., 2008) or by depriving it of VIP, as an important neuro-modulator (Harmar et al., 2002; Colwell et al., 2003); review (Vosko et al., 2007). VIP is not widely distributed within the central nervous system, but predominantly found in the SCN and the cerebral cortex. This peptide seems to be critical for synchronization of neurons within the SCN and maintenance of a robust circadian rhythm in clock gene expression (Maywood et al., 2006). Mice deficient of either the peptide or its receptor show severe deficits in rhythms in behavior and physiology (Aton et al., 2005; Maywood et al., 2006).

SCN drives rhythms through electrical activity

The SCN generates different neuronal and humoral signals that could be used to transmit phase information to target tissues. Spontaneous

generation of action potentials and the circadian modulation of their frequency are hallmark features of SCN neurons. By chronically infusing tetrodotoxin (TTX), a pharmacological blocker of fast Na^+ channels, into the rat SCN, action potentials were presumably blocked, and thus electrical output was abolished (Schwartz et al., 1987). During blockage of the electrical output, behavioral activity became arrhythmic. When the blockage of electrical output was alleviated, the rhythm in behavioral activity returned in a manner that could be extrapolated from the free-running behavior before the blockage. This shows that electrical activity itself is not a prerequisite for the functioning of the clock since the rhythm during blockage was entirely free-running. Furthermore, the circadian clock in the SCN itself did not seem to be affected by the blockage of action potentials. During treatment with TTX, light entrainment capabilities were abolished. When a shift in the light dark cycle was presented during blockage of the Na^+ channels, the behavioral activity did not entrain to the new light dark regime. When the blockage was removed, normal entrainment was restored. This shows that the input to the SCN is electrical and the clock itself produces a rhythm that is synchronized to the environment through electrical communication and that electrical impulse frequency is the main output of the pacemaker (Schwartz et al., 1987).

Together it indicates that the clock mechanism functions at the molecular level, because it continues oscillating in the absence of electrical communication. On the other hand, electrical activity is necessary to reset the state and communicate the phase of the molecular clock. It was argued when the TTX experiments were performed that it is not likely that the circadian clock consisted of a single neuron with an internal clock, but instead that the neurons in the SCN communicate with each other to establish the clock output as a whole (Miller et al., 1996).

It should be noted however, that more recent studies confirmed that rhythm generation in SCN neurons can continue in the presence of TTX, but the lack of intercellular signaling does lead to de-

synchronization within the SCN and results in severe disturbances in phase accuracy in the output as a consequence (Yamaguchi et al., 2003).

Output of the SCN is electrical and humoral

The SCN has projections to many areas in the central nervous system and as a master pacemaker, it synchronizes the rhythms in peripheral tissues (Kalsbeek et al., 2006; Panda and Hogenesch, 2004). If the output pathway of the SCN is disrupted, many organs and brain areas can still express circadian rhythms as local pacemakers, although behavioral rhythms are absent. Circadian rhythms in peripheral tissues can become de-synchronized from each other and thereby overall circadian output can be abolished (Kalsbeek et al., 2008; Inouye and Kawamura, 1979; Honma et al., 1984; Eskes and Rusak, 1985; Abrahamson and Moore, 2006). These finding suggests that direct neuronal output of the SCN is important and that the SCN functions as a master circadian pacemaker.

On the other hand, in SCN lesioned, arrhythmic animals that received an encapsulated SCN graft, behavioral rhythms were restored (Silver et al., 1996). Humoral output of the SCN graft tissue can pass through the encapsulation, but electrical signaling is blocked. This shows that the humoral output drives or synchronizes the behavioral rhythms. The humoral output that is responsible for driving circadian behavioral rhythms may consist of two molecules, transforming growth factor-α (Kramer et al., 2001) and prokineticin 2 (Cheng et al., 2002; Zhou and Cheng, 2005). These two molecules have been identified as possible output from the SCN involved in regulating behavior and show that humoral output from the SCN is an important synchronizing agent for downstream structures.

Apart from these different output parameters, it is clear that the SCN control the timing of behavioral and physiological parameters through electrical and humoral output and synchronize the molecular state of peripheral oscillators (Schwartz et al., 1987; Silver et al., 1996; Kalsbeek et al., 2006). How these two different

SCN output parameters for controlling downstream oscillators interact is not clear. In the normal situation, the electrical activity within the SCN regulates the output in both electrical activity and the release of humoral factors. Therefore, the internal SCN electrical activity can be considered as a prerequisite for both output parameters.

Anatomy of the circadian visual system

The SCN in mice consists of about 10000 heterogeneous cells per nucleus (Abrahamson and Moore, 2001). By itself the clock has an endogenous rhythm close to, but not exactly 24 hours. Consequently, it needs to be adjusted to the environmental time cycle. If there are no external time cues, so-called Zeitgebers, the clock will free-run with its own period length of around 24h, and consequently shows a drift in the timing of the activity. To achieve the adjustment to the external environment, the system receives information from photic and non-photic Zeitgebers. The strongest and most obvious Zeitgeber is the light-dark cycle.

Photo receptors in the retina

The circadian system in mammals receives photic input exclusively from the eye (Nelson and Zucker, 1981; Meijer et al., 1999; Yamazaki et al., 1999). Other components are essential in communicating light information to the SCN: 1) photoreceptors in the eye, 2) retinal ganglion cells (RGC) and 3) retinal pathways.

Photoreceptors in the eye are sensitive to light of certain wavelengths and when stimulated by photic input, respond with a change in membrane potential. The change in membrane potential is transmitted to retinal ganglion cells, which in turn respond with a change in electrical discharge rate. The light information is then encoded in spiking frequency and communicated to the brain. In non-mammalian species, non-image forming photoreceptors, i.e. not involved in vision, have long been recognized (Menaker, 1971). In

many organisms, these photoreceptors play an important role in the regulation of circadian rhythms, coding for duration of light, i.e. photoperiod, and also entrainment to the environmental light dark conditions, pupillary responses and melatonin suppression. In mammals the existence of a similar, non-image forming photo pigment was predicted through experiments showing that genetically modified coneless and rodless rd/rd mice, that are visually blind and are devoid of rods and cones, were able to entrain to the external light-dark cycle and even retain a normal phase response to light (Foster et al., 1991).

Melanopsin

The expected non-image forming photo pigment was identified as melanopsin (Provencio et al., 2000). The gene coding for melanopsin was cloned and used to locate melanopsin-expressing cells in the retina. There were no melanopsin cells in the cells of the outer retina, where rods and cones are located, but instead melanopsin was present in a small number of cells in the retinal ganglion cell layer (Provencio et al., 2000; Berson et al., 2002). Although melanopsin is commonly referred to as a non-visual photo pigment, recent evidence suggests that it contributes to the functioning of the visual systems, since melanopsin containing RGCs also innervate brain nuclei where visual irradiance is encoded (Dacey et al., 2005; Barnard et al., 2006; Güler et al., 2008).

The melanopsin containing RGCs are photoreceptive at all portions of the cell and not just at a specialized photoreceptive location like in regular image forming opsins in rods and cones. The wavelength sensitivity peak appears to be at 484nm, which is comparable to the maximum sensitivity of the circadian system at the behavioral level (Takahashi et al., 1984; Provencio and Foster, 1995). The response to light is slow and the response latency decreases with increasing stimulus irradiance. When melanopsin is activated by light, it triggers a depolarization of the cell membrane through an inward current (Berson et al., 2002). The extend of the depolarization

is proportional to the stimulus energy, but the signal pathway triggering this inward current is not yet identified (Warren et al., 2003). The spike frequency seems to be related to the extend of the depolarization and maintains a plateau level during the full duration of the stimulus. After stimulus offset, the spiking activity remains for a short time while the frequency slowly decreases until the baseline membrane potential is reached (Warren et al., 2003; Morin and Allen, 2006). Besides its role as a circadian photoreceptor melanopsin also plays a role in a number of behavioral and physiological responses to light, like masking (Mrosovsky et al., 2001) and pupillary reflexes (Lucas et al., 2001). It seems that all the different photo pigments in, rods, cones and melanopsin containing cells, are required for proper functioning of these non-visual photic responses (Lucas et al., 2003; Panda et al., 2003), and that signaling from rods and cones through melanopsin containing RGCs shapes the output of the circadian photo response (Doyle et al., 2006; Güler et al., 2008).

Innervation of the SCN

The retinal ganglion cells communicate the light information via several pathways to the SCN. Most of the retinal ganglion cells directly project from the retina to the hypothalamus, and make up the RHT. The RHT consists of unmyelinated nerve fibers that project mostly to the ventral and lateral SCN cells (Morin and Allen, 2006). A small part of the RHT fibers also projects to other brain areas. Another pathway to the SCN is formed by the geniculohypothalamic tract (GHT). Some of the retinal ganglion cells that branch to the RHT also innervate the intergeniculate leaflet (IGL) and the ventral lateral geniculate nucleus (vLGN) via the retinointergeniculate tract. These parts of the geniculatum in turn project to the SCN via the GHT (Miller et al., 1996; Morin, 1994) Another part of the retinal ganglion cells project to the median and dorsal raphe nuclei. From the ventral raphe nucleus there are neural projections to the SCN but it is unclear whether these projections are directly connected to the

retinorecipient cells in the raphe nuclei (Morin, 1994; Morin and Allen, 2006).

Retinohypothalamic tract

The RHT is embedded in the optic chiasm and is a highly specialized pathway, in that it exclusively functions as a pathway mediating photic entrainment (Meijer and Rietveld, 1989). Unlike image-forming nerve fibers in the optic tract, the RHT projections to the SCN are not fully crossed in the optic chiasm but the extend is highly variable between species. The largest part of the RHT fibers end in the SCN but a small portion also innervates other brain areas (Hannibal, 2002). The RHT innervates the mouse SCN primarily in the rostral part of the ventral, ventro-medial and central portion of the nucleus, often referred to as the core. In the more caudal portion of the nucleus, the medial projections become sparse and projections primarily end in the ventro-lateral portion of the nucleus. The more dorsal part of the nucleus, or shell, receives no direct input from the RHT (Abrahamson and Moore, 2001). The communication by means of neurotransmitters between the nerve terminals originating from the RHT and the adjacent cells is also specialized; each different type of neuron has a selective range of neurotransmitters by which it communicates.

Neurotransmitters of the RHT

Neurotransmitters of the RHT are summarized by the following criteria: The neurotransmitters 1) are located in the RHT; 2) are released by light stimulation; 3) affect the cells in the SCN in a similar way as light. This functionally means that they should induce phase shifts of the endogenous rhythm, induce a change in electrical activity and stimulate light signaling pathways to induce a phase shift of the rhythm.

Glutamate and NMDA

The main neurotransmitter in the RHT is glutamate (Hannibal, 2002). Immunohistochemical studies identified glutamate immunoreactive projections from the RHT to the SCN. In the RHT the fibers that have projections to the SCN, contain glutamate, which is co-stored with pituitary adenylyl cyclase activating peptide (PACAP). Other excitatory amino acids also function as neurotransmitters like glutamate derivatives and other closely related molecules like N-methyl-D-aspartate (NMDA). L-aspartate, although not present in the RHT can also induce phase shifts in the SCN, N-acetyl-aspartylglutamate (NAAG) which is an endogenous ligand for glutamate receptors is found in the RHT but its functional significance is yet unclear.

Glutamate excites SCN cells *in vitro* and electrical stimulation of the optic nerve induces glutamate release. The circadian responses to glutamate or one of its agonists that bind to the NMDA receptor are comparable to the responses to light. This is true for both the direct electrical response and the phase response in behavior and *in vitro* (Colwell et al., 1991; Ding et al., 1994; Shibata et al., 1994). Light induced phase shifts can therefore also be blocked by application of NMDA receptor blockers (Colwell et al., 1990; de Vries et al., 1994).

PACAP

PACAP, a neuropeptide from the vasoactive intestinal polypeptide (VIP) / secretin family of peptides is co-stored with glutamate in a subset of retinal ganglion cells and in nerve terminals originating from the RHT in the ventro-lateral SCN, the retino-recipient zone (Hannibal, 2002). PACAP alters neuronal firing rate and most cells respond with a suppression in discharge frequency through the actions of PACAP on the VPAC2 receptor. A small number of cells however, respond with an excitation, probably mediated by the PAC1 receptor (Reed et al., 2002). PACAP enhances glutamatergic signaling in ventral SCN neurons. It increases glutamate release and enhances post-synaptic ionotropic glutamate receptor mediated currents

(Harrington et al., 1999; Michel et al., 2006). Functionally PACAP enhances light induced phase resetting, through the actions on glutamate release. Although PACAP by itself produces small light-like phase shifts, its primary action is most likely as a modulator of glutamate responses (Hannibal, 2006).

Substance P

Substance P, an undecapeptide is considered a neurotransmitter in both central as well as peripheral nervous system. It was thought to be a transmitter of the RHT but results are somewhat inconclusive, as it was found by tract tracing studies that Substance P containing fibers that innervated the SCN did not originate from the eye (Hannibal and Fahrenkrug, 2002). However Substance P does play a role in the SCN where it can phase shift the endogenous rhythm of the SCN *in vitro* (Shibata et al., 1992; Kim et al., 2001), however *in vivo* results are somewhat unclear as results are conflicting (Piggins and Rusak, 1997; Challet et al., 1998). Substance P is likely to play a role in mediating light induced phase shift, irrespective of whether this is intrinsic to the RHT or as an afferent transmitter in the SCN (Kim et al., 2001).

Geniculohypothalamic tract

The functional significance of the GHT in the circadian system has been studied in terms of visual properties in the SCN and behavioral consequences of disruption of the GHT. By several different techniques the input to the SCN by the GHT was disrupted, either by trans-section of the optic tracts or by bilateral lesions of the vLGN (Groos and Meijer, 1985; Inouye and Kawamura, 1982). In electrical activity recordings in the SCN of LGN lesioned animals, it was shown that SCN responses to visual stimuli were unaltered when compared to control animals with an intact GHT, therefore it can be concluded that the GHT is not necessary for tonic suppression and activation of SCN cells (Groos and Meijer, 1985). In behavior, it was shown that lesions of the LGN did not diminish normal entrainment to the light

dark cycle and show that the RHT suffices for normal entrainment. After a 12h shift of the light-dark cycle the entrainment capabilities of animals that had an LGN lesion was however significantly impaired (Rusak, 1977; Rusak and Boulos, 1981). Furthermore the magnitude of light induced phase shifts was reduced in animals with a destructed LGN (Harrington and Rusak, 1988; Harrington and Rusak, 1986; Pickard et al., 1987). In normal circumstances, the free-running period in nocturnal animals, is longer in constant light and increases with higher light intensities. In IGL ablated hamsters, these tonic effects of light are also reduced (Harrington and Rusak, 1988; Pickard et al., 1987). Taken together, these results show that the GHT is involved in controlling the phase of the SCN but do not alter the light-responses of single neurons.

In terminals of the vLGN, immunoreactivity for neuropeptide Y (NPY) was found, which suggests a possible mechanism of NPY induced phase shifts through activation of the GHT (Harrington and Rusak, 1986). It is possible that the GHT acts as a lights-off sensitive pathway (Miller et al., 1996), although the dark-pulse effects of NPY acting through the GHT are not yet fully understood.

Anatomy of the suprachiasmatic nucleus

In the SCN there are different types of cells that can be differentiated by the location in the clock, cell shape and most important transmitter content. Many receptor types that are present in SCN cells can be identified and have led to a characterization of different cell groups. Many types of glutamate receptors have been demonstrated in cells throughout the SCN but different subtypes are localized at different locations, showing that the role of different subtypes may also indicate a selective involvement in entrainment (Kopp et al., 2001).

Light response in the SCN

Retinorecipient cells in the SCN have been studied extensively by recordings of electrical activity. Retinorecipient neurons do not show a response to short light presentations but show a stable increase in

firing rate in response to a light stimulus which is maintained for the full duration of retinal illumination. Response latencies are high with an initial overshoot in spike frequency at the onset of the light stimulus (Meijer et al., 1986; Meijer et al., 1998; Drouyer et al., 2007). A small number of SCN cells are suppressed by light but show similar kinetics as light activated cells.

The response kinetics of SCN cells to light contrast those in visual brain areas involved in pattern recognition, but they are now known to correspond with the sustained increase in discharge rate in response to retinal illumination observed in melanopsin containing RGCs (Berson et al., 2002). Besides the sustained responses to light, SCN cells show a light induced increase or decrease in spike frequency as a function of the level of retinal illumination. The sensitivity of the system is dependent on the circadian time, with high sensitivity during the night and low sensitivity during the day (Meijer et al., 1986). The intensity–response curve has a sigmoid shape with no responses below a relatively high threshold. Above this lower threshold, there is an almost linear relation between increase in illumination and firing frequency. This linearity is maintained up to moderate light intensities, where the response becomes saturated (a horizontal asymptote), i.e. a further increase in luminance no longer increases the response. The relatively high intensity level of the lower threshold for a circadian light response and the saturating effects of light at moderate illumination levels suggest that SCN cells are best suited to differentiate between day and night and are most sensitive to light intensities occurring around dawn and dusk (Meijer et al., 1986; Meijer et al., 1998; Meijer, 2001).

Entrainment by light

The endogenous period τ of the circadian rhythm, which deviates slightly from 24h, is synchronized to the environment through the phase dependent shifting effects of light. The endogenous state of the pacemaker, in circadian time (CT) or phase φ of the pacemaker, can only be seen in the absence of external Zeitgebers. In the presence of

external synchronizers, the phase of the clock can be referred to as Zeitgeber time (ZT). In nocturnal animals, activity onset is defined as CT 12 when the animal is in constant conditions. ZT 12 is defined as lights off, which roughly corresponds to activity onset but may not reflect the true phase φ of the pacemaker. The phase shifting actions of light enable the organism to synchronize the internal timing to the environment. Phase shifts in behavior take several daily cycles to complete and show a transient transition to its new phase. The state of the pacemaker however is directly shifted after a light pulse, as was demonstrated by a double pulse paradigm (Best et al., 1999; Watanabe et al., 2001). Two discrete light pulses were administered and the resulting phase shift after the two pulses was used to calculate the shift induced by the first pulse. Depending on the direction, speed and magnitude of the phase shift induced by the first pulse, the second pulse will hit another area on the phase response curve when compared to a situation without the first pulse. More recently it was found that the phase of the SCN as a whole may not be fully shifted after application of a light pulse, as was found after a shift in the light-dark cycle. The circadian rhythm in the SCN showed regional differences (Vansteensel et al., 2003b; Albus et al., 2005) and even different phase shifting responses between clock genes (Reddy et al., 2002).

The phase shifting effects of light furthermore enable an organism to adapt to seasonal changes in the duration of light, or photoperiod. The duration of daylight in the different seasons has marked effects on the behavior and physiology in many mammals. The duration of light alone is sufficient for animals to show seasonal responses. These seasonal responses are mediated by the SCN and are independent of temperature changes. For instance hamsters that are kept on photoperiods with less than 12h light per day will develop a winter coat irrespective of ambient temperature and may go into some sort of hibernation, which is a physiological response to minimize energy expenditure (Goldman, 2001). Several photoperiodic responses are mediated by melatonin, primarily produced by the pineal gland.

These photoperiodic changes in melatonin excretion are driven by the SCN (Johnston, 2005). The photoperiodic changes in the SCN are visible as an increase or decrease of the duration of elevated electrical activity (Mrugala et al., 2000).

The SCN as a Neuronal Network

The circadian rhythm in the SCN has a single peak each circadian cycle. There are basically two approaches that can enable the clock to produce its monophasic output. One view is that all neurons in the SCN have synchronized phasing and produce a coherent rhythm in their output, small cellular differences in phasing would be averaged in the total clock output (Liu et al., 1997b; Low-Zeddies and Takahashi, 2001; Herzog et al., 1998). The other view is that the clock produces a rhythm based on the combined output from multiphasic rhythmic cells. Electrical discharge rhythms in the SCN entrain to the external light-dark cycle and reflect the photoperiod in duration of elevated electrical discharge. These rhythms are not constrained to a monophasic time-point but may also oscillate in anti-phase and the phase relationships between cells can be remodeled by the environment to enable entrainment (Pittendrigh and Daan, 1976b; Jagota et al., 2000; Mrugala et al., 2000). In 2003 the latter view of clock organization was confirmed by three research groups independently and has had great implications for future research on communication and organization of the biological clock.

Animals that were genetically altered to express a short half-life green fluorescent protein (GFP), that was coupled to the *Per1*-promotor, were recorded *in vitro* to investigate the organization of individual oscillators in the clock (Quintero et al., 2003). Quantitative imaging revealed that the per1 promoter had its peak activity 2 hours before lights off, regardless of the time of preparation. Therefore, these rhythms were not induced by the preparation procedure. The timing of the second peak after the first peak in fluorescence *in vitro* was about 23.5h. In the absence of Zeitgebers *in vitro*, the period

length was comparable to the period of behavioral rhythms in mice in constant darkness. Furthermore, electrical activity of *Per1* expressing cells was recorded and there was a strong positive correlation between spike frequency and *Per1* expression. In addition to the whole SCN recordings of fluorescence, individual neurons were imaged and it was observed that about 90% of the neurons showed rhythmic activity. A minority of 11% of the cells did not show any rhythmic *Per1* driven GFP when the slice was taken from a mouse kept in an LD cycle. When cells were taken from animals kept in DD, 26% of the cells did not show a rhythm in *Per1* expression. This shows that some of the cells recorded directly after an LD cycle may have been driven by the light-dark cycle. The percentage of rhythmic cells was different for different regions within the SCN. Further investigation of the timing of peak fluorescence revealed that about 50% of the cells had their peak in synchrony with the output of the whole SCN peak, both in LD as well as in DD. The timing of the peaks in slices from LD and DD differed somewhat and Per expression was delayed in slices from DD conditions, which may be due to the direct effects of light on *Per* (Asai et al., 2001). The single unit peaks that were outside the main peak were clustered in time and showed regional differences, with a medial to lateral gradient in peak times, early cells were mostly located in the medial SCN and peaked around ZT 5, whereas the latest peaks in Per1 fluorescence was in lateral cells around ZT18.

Another group recorded from organotypic brain slice cultures from mice carrying a firefly luciferase gene that was coupled to the *mPer1*-promoter (*mPer1-luc*), to investigate the network interactions of the autonomous molecular clocks in SCN cells and how they underlie the tissue oscillator (Yamaguchi et al., 2003). They were able to track the peak in *mPer1*-promoter activation of hundreds of cells simultaneously and found that about 99% of the cells showed a rhythm in bioluminescence. Furthermore, they found that peak and trough times in *Per* luciferase expression differed substantially between cells, even when they were located close to each other. These phase differences between cells remained constant over the cycles and

showed an anatomical preference, dorso-medial cells were first, then central cells and finally ventral SCN cells. To see if the dorso-medial cells were driving the ventral rhythm, a knife-cut was made to separate dorsal from ventral cells. In the dorsal part, the cells remained rhythmic, but lost synchrony. In the ventral part the cells remained rhythmic and synchronized. The data show that the dorsal cells are not driving the rhythm in the ventral part. The rhythmic properties of the clock are caused by an interlocked feed-back loop of protein levels that feed back on the transcription for other genes, thereby creating an oscillation in protein levels. When all protein synthesis, including luciferase, was blocked by application of cycloheximide (CHX) the level of bioluminescence decreased as a result. After full PER depletion, (36h of CHX), the entire clock was stopped and there were no detectable levels of clock proteins left. When the application of CHX stopped, and protein synthesis continued, all cells simultaneously started the molecular feedback loop, resulting in a completely synchronized rhythm. The first peaks in bioluminescence appeared 3h after restoration of protein synthesis, phase differences in peak expression between cells gradually restored over a time span of 4-5 days.

Because intracellular communication takes place via electrical activity, Na^+ channels were blocked by application of TTX, resulting in a loss of action potentials. After a few days, the individual *Per* oscillations continued at a lower amplitude and became desynchronized relative to one another, resulting in an overall lack of a rhythm. When TTX was removed, the preceding phase relations between individual clock cells were restored. These data together suggest that inter-neuronal signaling keeps stable phase relations between cells, and is needed for high amplitude molecular rhythms.

In another study performed in 2003 (see chapter 3) recordings of extracellular electrical activity were performed in rat brain slices. In these multiunit recordings, the peak in electrical activity was at midday. By an offline amplitude selection of action potentials, the area around the electrode could be selected and enabled the selection

of small populations of neurons. The subpopulation activity revealed short durations of increased electrical activity, for small populations and when a larger population was selected, the width of the signal increased and the peak phase stabilized towards midday. Furthermore, electrical activity of single units was extracted from the multiunit signal, and revealed that individual neurons display only short durations of activity. It was proposed that these short durations of activity and heterogeneous phasing might contribute to photoperiod encoding. Simulations were performed with an average single unit activity pattern, distributed linearly over the photoperiod. These simulations showed that the phase distribution of single units could explain the increase in peak width in an increased duration of light.

Together, these three studies showed that the SCN is composed out of differently phased autonomous clocks, and that the phase differences are an intrinsic property of the network of cells. The differences in timing, number of autonomously rhythmic cells and their anatomical location may have been due to differences in techniques. But what is consistent between these studies is that the phasing of individual neurons is the composite of many different phases and that these different phases are an intrinsic property with possibly differential coupling mechanism, that may be region specific. The observed phase differences may be an essential autonomous anatomical property, partly driven by light activation.

Introduction to research questions

In the present thesis, the functional significance of phase differences between SCN neurons is investigated. It is proposed that these phase differences are essential for photoperiodic encoding in the SCN. In chapter 2, we evaluate the acute brain slice recording methodology for circadian rhythm research. The acute brain slice preparation is extremely useful in the study of circadian properties as the aftereffects of environmental conditions can be evaluated *ex vivo*. The studies described in chapter 2, are aimed to elucidate whether the preparation of the brain slice introduces changes in the peak time and

waveform of the electrical activity rhythm. The results show that the peak time and waveform are robust and that he time of slice preparation, relative to the circadian cycle, does not affect the basic properties of the rhythm. The results are important for the chapters following chapter 2, in which the organization of the SCN in long and short photoperiods is evaluated ex-vivo.

In chapter 3, we investigated how the electrical activity of a single neuron contributes to the output signal of the large population of neurons in the SCN. We prepared hypothalamic brain slices from rats, containing the SCN with the technique covered in chapter 2. From the recorded multiunit data, we extracted the activity of subpopulations and single units. We found evidence of single units and subpopulations that are active for only a relatively short time and activity peaks are distributed over the 24h period. The output of the short active and differently timed subpopulations and single units together form a seemingly coherent, monophasic waveform at multiunit level. The observed short duration of electrical activity of single units and subpopulations is further explored and a simulation is presented on the basis of the recorded data. These simulations form the practical illustration of the hypothesis that the distribution over time of the observed single units lies on the basis of photoperiodic encoding in the SCN.

In chapter 4 we further investigated the hypothesis that the short duration of activity of single units and subpopulations play a role in encoding day length in the SCN. We recorded wheel-running activity of mice in long and short photoperiods and found that in behavior the day length is encoded. We furthermore recorded *in vivo* multiunit electrical activity and found that the *in vivo* multiunit electrical activity also reflects the photoperiod the animals are entrained to. Finally, *in vitro* recordings of multiunit electrical activity were performed to investigate the role of single units and subpopulations in photoperiodic encoding by the SCN.

In literature there has been a notion that the phase shifting capacity in long day length was significantly reduced and in short day

length it was enhanced. Systematic analysis of this phenomenon was lacking. In chapter 5, we present a functional mechanism underlying these observations. We created a phase response curve to light for mice entrained to short and long photoperiods. We found that in these mice the phase shifting capacity in short days was indeed enhanced whereas in long day length it was reduced. We then investigated whether these changes in responsiveness may have been caused by a desensitization of retinal input to the SCN or are an intrinsic property of the SCN. We adjusted the light exposure during entrainment so that the animals from both day lengths received an equal amount of photons each day, and found that this did not change the responsiveness to a light pulse in any circumstance. To study this effect in more detail, we recorded electrical activity in brain slices from animals entrained to both photoperiods and applied NMDA to mimic a light pulse. We found that the different responses are intrinsic to the SCN and we present a functional mechanism that underlies these changes.

In chapter 6, we discuss the preceding chapters in the context of more recent findings. We look into possible research perspectives and link our findings to other research. A major conclusion is that the neuronal network of the suprachiasmatic nucleus is of key importance to its function, and that the network properties of the SCN shape the output.

CHAPTER 2

Phase of the Electrical Activity Rhythm in the SCN *in vitro* not Influenced by Preparation Time

VanderLeest,H.T., Vansteensel,M.J., Duindam,H., Michel,S., and Meijer,J.H. (2009). Phase of the electrical activity rhythm in the SCN *in vitro* not influenced by preparation time. **Chronobiol. Int**. *26*, 1075-1089.

Summary

The mammalian circadian clock, located in the suprachiasmatic nucleus (SCN) of the hypothalamus, drives daily rhythms in behavioral, physiological, and endocrine functions. The SCN has a genetic basis for rhythm generation and remains rhythmic when it is isolated and kept in constant conditions. This allows for an *in vitro* analysis of circadian attributes, which is a powerful approach in the study of SCN cellular mechanisms. For studying the phase of the SCN rhythm *in vitro*, it is important to assess whether preparation of the tissue itself introduces phase shifts. In the present study, we investigated whether preparation of hypothalamic brain slices affects the phase and waveform of the rhythm in electrical impulse frequency of the mouse SCN. Mice were kept under a 12:12h light-dark cycle, and slices were prepared at six timepoints distributed over the 24h cycle. We used the peak time and the time of the half-maximum levels in electrical activity as markers for circadian phase. The peak time in electrical activity was observed during the mid-subjective day, irrespective of the time of preparation, at a mean ZT of 5.18 ± 0.20h (n = 39). After preparation in red light at the end of the subjective night, the circadian phase appeared slightly advanced. When slices were prepared in the dark, using infrared illumination, the ANOVA showed no significant differences in peak times and time of half-maximum values between preparation times. The results affirm the value of the slice preparation for studying the phase of the SCN *in vitro*. We conclude that the phase and waveform of the electrical activity in the SCN *in vitro* is unaffected by the time of slice preparation but may be influenced by short light presentation when preparation is performed during the subjective night.

Introduction

In mammals, circadian rhythms in physiological, endocrine, and behavioral functions are driven by the suprachiasmatic nucleus (SCN) (Stephan and Zucker, 1972; Meijer and Rietveld, 1989; Ralph et al., 1990). The SCN is located at the base of the anterior hypothalamus and receives light input via the retinohypothalamic tract (Morin and Allen, 2006). The ability of the SCN to generate circadian rhythms can be explained at the molecular level by a transcriptional-translational feedback loop (Takahashi, 1993; Kume et al., 1999; Reppert and Weaver, 2002; Dardente and Cermakian, 2007) Several genes have been identified that play an essential role in the generation of circadian rhythmicity, including Period (Per), Cryptochrome, Clock, and Bmal (Albrecht et al., 1997; Shearman et al., 1997; Hastings et al., 1999; van der Horst et al., 1999; Vitaterna et al., 1999; Vitaterna et al., 1994; Bunger et al., 2000; Hastings and Herzog, 2004). Electrical activity is a major signal of the SCN pacemaker (Schwartz et al., 1987) and shows clear circadian modulation in discharge rate, with high frequencies during the day and low frequencies during the night (Meijer et al., 1998). Neuronal and humoral pathways distribute this temporal information to other parts of the central nervous system (Abrahamson and Moore, 2001; Kalsbeek et al., 2006; Silver et al., 1996). Circadian rhythms in e.g. gene expression (Nakamura et al., 2005; Yamazaki et al., 2000), neurotransmitter content (Shinohara et al., 2000b), and electrical activity (Brown et al., 2006; Gillette et al., 1995; Schaap et al., 2003) persist in *in vitro* preparations, such as in dissociated cells (Welsh et al., 1995), in organotypic slice cultures (Herzog et al., 1997) and acutely prepared hypothalamic slices (Groos and Hendriks, 1982). The *in vitro* brain slice preparation offers the valuable possibility to investigate circadian rhythms under constant conditions and in the absence of influences from other parts of the central nervous system. Moreover in acutely prepared slices, it is possible to evaluate after-

effects of previous manipulations of the light-dark (LD) cycle, such as different photoperiods, constant light, or shifts of the environmental LD cycle (Albus et al., 2005; Jagota et al., 2000; Mrugala et al., 2000; Nagano et al., 2003; Nakamura et al., 2005; Ohta et al., 2005; Schaap et al., 2003; Shinohara et al., 1995; VanderLeest et al., 2007; Vansteensel et al., 2003b; Yannielli and Harrington, 2000).

For all such *in vitro* studies, it is important to determine whether the time of preparation of the slice affects the phase of the SCN rhythm, such as the time of maximal activity. However, detailed studies on this issue are scarce. One study reported that in Per1-luc transgenic rats, the time of preparation largely determines the peak time of the Per1 rhythm *in vitro* (Yoshikawa et al., 2005). These results prompted us to analyze potential phase-shifting effects of slice preparation on the electrical activity rhythm *in vitro* in more detail. We used three phase markers to evaluate the influence of slice preparation on the SCN rhythm: the time of maximum activity, the time of half-maximum discharge level on the rising slope, and the time of half-maximum activity on the declining slope. We also measured the broadness of the recorded electrical activity peaks. The results of the present study show that the time of preparation of brain slices has no influence on the different phase markers of the electrical activity rhythm in the SCN.

Methods

Animals

All experiments were performed under the approval of the Animal Experiments Committee of the Leiden University Medical Center and in accordance with the journals' ethical standards (Portaluppi et al., 2008). Male C57Bl6/J mice (Harlan, Horst, The Netherlands) were individually housed in clear plastic cages that were equipped with a running wheel, in a sound-attenuated and temperature-controlled room. Food and water were available ad libitum. The animals were entrained to a 12:12 LD cycle for at least two weeks, with the time of lights-off defined as Zeitgeber time 12 (ZT) and the time of lights-on as ZT 0. The animals were sacrificed at ZT 2, 6, 10, 14, 18, or 22. Additional experiments were performed at ZT 0, immediately after lights-on, because preparation at ZT 2 did not allow for a reliable estimation of the peak. Decapitation during the subjective day (at ZT 0, 2, 6, and 10) as well as subsequent brain dissection occurred under normal room light. Dim red light (10μW/cm^2) was used when the animals were taken from their dark period (ZT 14, 18, and 22). Additional experiments were performed at ZT 22 in the dark, with the aid of infrared light viewers.

In vitro Electrophysiology

Preparation of brain slices and recordings were performed as described earlier (VanderLeest et al., 2007). After decapitation, brains were rapidly dissected and placed in ice-cold bicarbonate buffered artificial cerebrospinal fluid (ACSF), containing (in mM): NaCl 116.4, KCl 5.4, NaH_2PO_4 1.0, $MgSO_4$ 0.8, $CaCl_2$ 1.8, $NaHCO_3$ 23.8, and glucose 15.1, as well as 5 mg/l gentamycine. Coronal, hypothalamic slices (~400μm) containing the SCN were prepared with a tissue chopper and transferred to a laminar flow chamber, where they were kept submerged in ACSF (35°C), and stabilized by a tungsten fork. The slice chamber was continuously perfused with ACSF at a rate of

1.5ml/min and oxygenated with warmed, humidified O_2 (95%) and CO_2 (5%). Before the recording was started, slices were equilibrated in the chamber for ~1h. One slice per animal was used and contained at least 50% of the rostro-caudal extend of the SCN. Recording electrodes (insulated 90% platinum and 10% iridium, 75μm) were placed in the ventro-medial aspect of the left and right SCN in order to obtain multiunit neuronal activity recordings from both nuclei. The electrical activity was amplified (×100k) by a high-impedance amplifier and subjected to a band-pass filter (0.3-3 kHz). A hardware spike trigger was set so that the threshold was above noise level. The action potentials crossing this threshold were counted in 10s bins with the aid of custom-made software. The electrodes and spike threshold settings were left unaltered during the experiment. Data were excluded from analysis if the fluid levels were unstable or when the phase markers could not unambiguously be determined.

Data Analysis

The data were analyzed offline in MATLAB (The Mathworks). The multiunit data were plotted against ZT and smoothed using a least squares algorithm (Eilers, 2003). Peak time, determined as the time of maximum firing, as well as minimum and half-maximum levels, were determined in these smoothed recordings. To estimate the influence of the smoothing parameter on the observed peak times, we applied both a weak and stronger smoothing procedure (weak: average $\lambda = 1 \times 10^{9}$; stronger: average $\lambda = 8 \times 10^{10}$). When both recordings of the slice were successful, we took the average from both channels, resulting in a more robust estimate of circadian phase of the whole slice (see statistical analysis); otherwise, we used the data of one recording. In all experiments, the first peak in multiunit activity was used as a primary marker of clock phase. Additionally, the times of half-maximum activity levels on the rising and declining slope of the multiunit activity patterns were calculated. We also calculated the width of the electrical activity peak, on the basis of the half-maximum values.

Statistical Analysis

Statistical analysis was performed in Origin7 (OriginLab Corporation, One Roundhouse Plaza Northampton, Massachusetts, USA). Before averaging the peak phases of two recordings from a single slice, we performed a two-sided, paired t-test on the peak phase between both recording channels from all successful experiments and found that peak times within a slice were not significantly different (paired t-test, $p > 0.06$). The influence of a stronger smoothing on the time of the maximum electrical activity was also tested using a two-sided, paired t-test. To test for differences among preparation times, one way ANOVAs with post-hoc Tukey and Bonferroni tests were used. We applied ANOVAs for time of maximum activity, half-maximum values and width of the peak. All provided values are means ± standard error of the mean (SEM). Data were considered significantly different when $p < 0.05$.

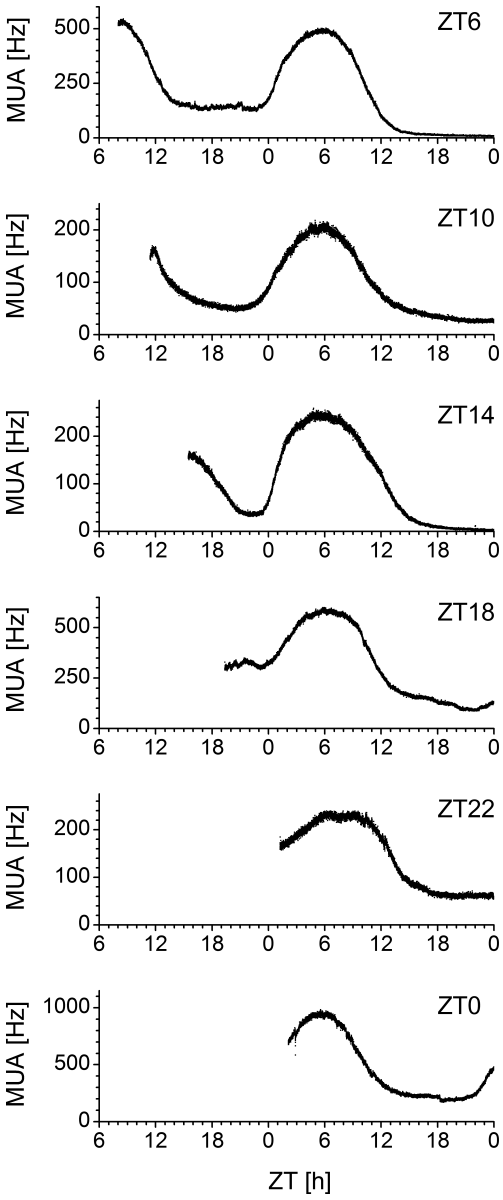

Figure 2.1

Extracellular multiunit electrical activity rhythms in the SCN following different preparation times.

Raw data plots of multiunit electrical activity as a function of Zeitgeber time. Preparation was started, from top to bottom, at ZT 6, ZT 10, ZT 14, ZT 18, ZT 22, and ZT 0, respectively. The timing of the peak and shape of the rhythm in spontaneous action potential firing rate is consistent between preparation times.

Results

We successfully recorded rhythms in spontaneous electrical activity in the SCN in a total of 51 acutely prepared hypothalamic slices. We obtained successful recordings from both SCN nuclei in 36 slices and from one nucleus in the other 15 slices. Our recordings following preparation at ZT 0, 6, 10, 14, 18, and 22 showed increased electrical activity during the projected day and decreased activity during the projected night (see Figure 2.1). All of our individual electrical activity peaks occurred during the projected light at a mean ZT of 5.18 ± 0.20h (n = 39; see Figure 2.2).

The mean peak times for preparations during the dark period of the animal were ZT 14: 5.76 ± 0.58h (n = 5), ZT 18: 5.43 ± 0.48h (n = 5), and ZT 22: 3.92 ± 0.53h (n = 6). The mean peak times obtained for preparations during the day were ZT 6: 4.36 ± 0.35h (n = 11) and for ZT 10: 5.97 ± 0.54h (n = 5). We performed additional experiments and prepared slices at ZT 0, because preparation at ZT 2 (n = 6) appeared too close before peak time and interfered with the estimation of the peak. The mean peak time after preparation at ZT 0 was 5.19 ± 0.25h (n = 6).

An ANOVA on the peak times obtained for the different times of preparation reached significance ($p < 0.02$), showing that the data were not homogeneous; however, neither a post-hoc Tukey nor a post-hoc Bonferroni test on the data used in the ANOVA revealed significant differences in peak time between any of the groups. Although not significantly different, the average peak time after preparation at ZT 22 appeared relatively early, with four of the ten experiments that displayed a peak before ZT 4 following preparation at ZT 22. Therefore, we performed additional experiments and prepared slices at ZT 22 in the dark with the aid of an infrared light viewer. This resulted in a mean peak time of 5.30 ± 0.62h (n = 7), which was not different from the results obtained in red light at ZT 22 (t-test, $p > 0.12$). Moreover, when we used these results in the

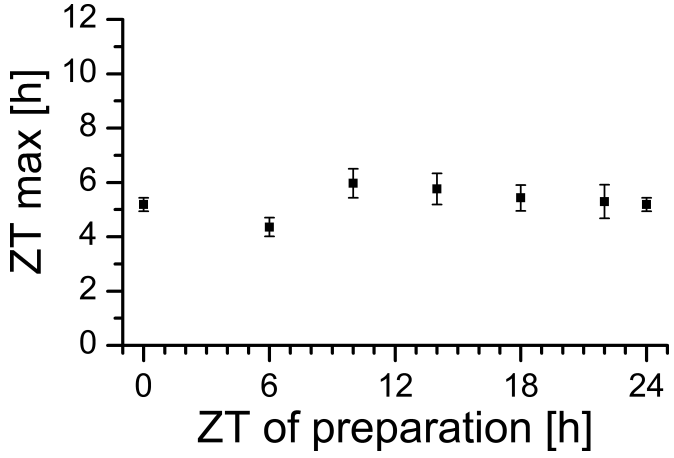

Figure 2.2

Peak phase in multiunit electrical activity following different preparation times.

The time of maximal MUA, or multiunit electrical activity (ZTmax ± SEM), is plotted against the time of brain slice preparation. All peaks in MUA occurred during the projected light period. No significant differences were observed in peak time when preparation in the subjective night was performed in the dark using infrared viewers (ANOVA, p > 0.15). Note that the ZT 0 and ZT 24 data points are repeated and thus are the same values.

ANOVA, no significant effect of the time of preparation was observed ($p > 0.15$).

Furthermore, we determined the peak times of all successful recordings after applying a higher smoothing parameter (Supplemental Figure 2.1). The stronger smoothing did not result in a consistent earlier or later peak time, but the SEM in peak time decreased slightly (weak smoothing: 5.17 ± 0.19h; stronger smoothing: 5.08 ± 0.17h; paired t-test, $p > 0.22$, n = 51).

During the rising and declining phase, the electrical activity changed rapidly (21.5 ± 1.3%/h and 16.9 ± 1.0%/h respectively, n = 24), offering a precise marker for circadian phase. We analyzed the times of the half-maximum levels at the rising and declining phase of the electrical activity rhythm; in this analysis, we used data from ZT 22 that were obtained in darkness (see Figure 2.3). The mean half-maximum level of the rising phase occurred at ZT 0.96 ± 0.17h (n = 24), and at the declining phase it occurred at ZT 10.28 ± 0.22h (n = 38). The mean peak width was 9.24 ± 0.29h (n = 24). No significant effects of preparation time were observed at any of the circadian

phases on the half-maximum values or peak width (ANOVA, rising slope: $p > 0.07$, n = 24; falling slope: $p > 0.06$, n = 38; peak width: $p > 0.61$, n = 24).

Discussion

We prepared coronal hypothalamic slices containing the SCN at different Zeitgeber times from mice kept under a 12:12 LD cycle. From these slices, we recorded the spontaneous electrical activity with stationary extracellular multiunit electrodes. In all experiments, the electrical activity showed high levels during the animals' subjective day and low levels during the night (see Figure 2.1). This is consistent with previous multiunit electrical activity recordings in the SCN using stationary electrodes (Albus et al., 2002; Bouskila and Dudek, 1993; Brown et al., 2006; Gribkoff et al., 1998; Liu et al., 1997a; Mrugala et al., 2000; Prosser, 1998). Electrical activity rhythms of the SCN have also been investigated by sampling the electrical activity rate from many individual neurons for short durations of time. These sampling procedures yielded similar electrical activity patterns of the ensemble, with a peak during the mid-subjective day (Akiyama et al., 1999; Burgoon et al., 2004; Mason and Rusak, 1990; Prosser, 1998; Saeb-Parsy and Dyball, 2003; Soscia and Harrington, 2004). One study showed influences of time of preparation on the phase of the *in vitro* rhythm. In that study, preparation of the brain slices during the animals' dark period was performed under brief (20 - 30s) light exposure, which may have caused the observed phase shifts (Gillette, 1986). Surprisingly, no other studies have systematically analyzed the influence of preparation time on the peak of the electrical activity rhythm.

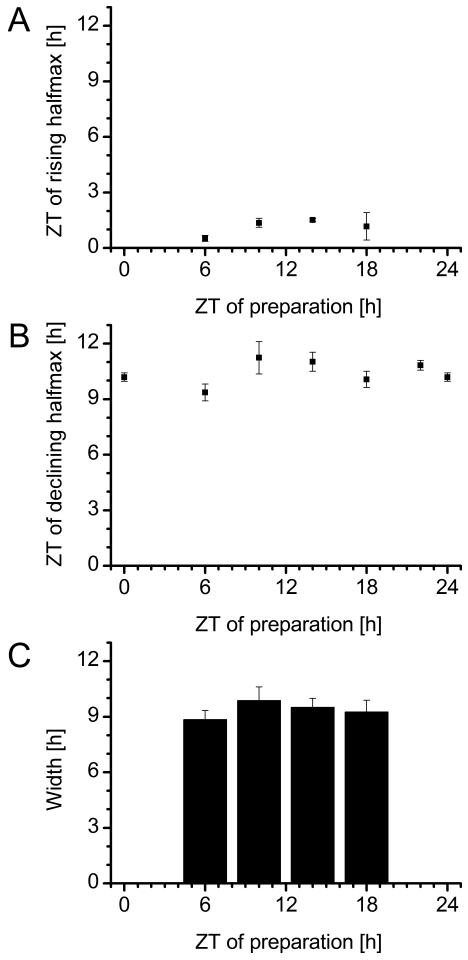

Figure 2.3

Properties of multiunit electrical activity rhythms in the SCN.

(A) Average Zeitgeber time (± SEM) of the half-maximum levels on the rising slope of multiunit electrical activity as a function of time of preparation. No significant differences were observed between preparation times (ANOVA, $p > 0.07$). Note that for some preparation times, the rising phase of the first peak in electrical activity could not be determined.
(B) The average time (± SEM) of the half-maximum levels on the declining phase of the peak as a function of time of preparation. It was consistent for all times of preparation, and no significant differences were found between any of the preparation times (ANOVA, $p > 0.06$). Note that the ZT 0 and ZT 24 data points are repeated and are the same values.
(C) The width of the multiunit peak as a function of time of brain slice preparation. Width of multiunit electrical activity was also unaffected by the time of preparation (ANOVA, $p > 0.61$).

When we obtained two successful recordings from one slice, we averaged the peak times to obtain the best possible estimate for the phase of the SCN as a whole. It is well known that populations within the SCN differ in phase. Simultaneous recordings from populations of

the left and right SCN of the rat can show phase differences of up to 4h, with a mean difference of about 1h (Schaap et al., 2001; Schaap et al., 2003). Populations from the dorsal and ventral rat SCN show mean phase differences of 0.9h (Schaap et al., 2003). Regional differences have also been observed in the mouse SCN (VanderLeest et al., 2007; Brown and Piggins, 2009). Recordings of single mouse SCN neurons in acutely prepared slices show phase differences in Per1 GFP and luciferase expression (Quintero et al., 2003; Yamaguchi et al., 2003). In the present study, we found a range in peak times for each preparation time. Most peaks of the electrical rhythm occurred around mid-day (between ZT 4 - 8), but some were observed outside this range.

We noticed that the data from ZT 2 were influenced by the relatively short interval between slice preparation and determination of the peak time. After preparation at ZT 2, and subsequent settling of the slice for 1h, we started the actual recording at around ZT 3.5. Because of the lack of a clear rising phase at this time of the cycle, a number of peaks could not unambiguously be determined. We concluded that preparation at ZT 2 is not suitable for determination of the first peak, and we performed additional recordings at ZT 0 to obtain data for preparation at the early day. The peak time for preparation at ZT 0 was at ZT 5.19 ± 0.25h (n = 6).

For preparation at ZT 22, the mean peak time occurred relatively early, which was attributable to a very early peak time in four out of the six recorded slices at this preparation time. Light exposure during the beginning of the night causes delays of the circadian pacemaker of the mouse, while light exposure at the end of the night causes advances. As we prepared our slices under dim red light, we wondered whether the short exposure to light may have caused a phase advance. While an exposure time of 3 - 5min of red light may not trigger large behavioral phase shifts, it has been shown that the phase shifting response *in vitro* is larger than the response *in vivo* (Vansteensel et al., 2003b) and is measurable within several hours after slice preparation (Yannielli and Harrington, 2000;

Gillette, 1986). When we repeated the experiments in the dark at ZT 22, using infrared viewers, no differences were detected by ANOVA between any of the preparation times. The obtained peak times at ZT 22, however, were not significantly different from the ones obtained in red light. Therefore, we cannot distinguish whether the early peaks were really due to red-light exposure or to variability in the dataset. The latter would also be in accordance with the finding that no shifts were observed at ZT 14, where phase delays are induced by light. Although the effect is minor or negligible, we suggest that care should be taken with preparations started at ZT 22.

The main focus of our analyses in this article is the peak phase in multiunit electrical activity in the SCN *in vitro*, following preparation at different Zeitgeber times. We also analyzed other parameters of the extracellular multiunit electrical activity peak, such as the phase of half-maximum levels and the width of the peak. Half-maximum levels on the rising slope of the multiunit peak were not significantly different between preparation times, and the half-maximum levels on the falling slope and the width of the peaks were also not different. Taken together, the results show that the waveform of the multiunit electrical activity in the SCN is robust and comparable between preparation times.

There have been a great number of *in vitro* studies in the field of circadian rhythms in which the peak time of the electrical activity rhythm was quantified. The precise time of preparation, however, often has not been provided. To evaluate the time of peak activity observed in the various studies, we restrict ourselves to those studies that provided the preparation time in some detail. Studies performed in rats that were kept on LD 12:12 and were prepared during the light period report average peak times between ZT 5 - 8 (Bergeron et al., 1999; Gillette, 1986; Gillette and Prosser, 1988; Liu and Gillette, 1996; McArthur et al., 1991; McArthur et al., 2000; Prosser, 1998; Rangarajan et al., 1994; Shibata and Moore, 1993). Hamsters housed under a 14:10 LD cycle, also prepared during the light period, showed a narrow range of peak times between ZT 6 and ZT 7 h (Biello et al.,

1997; McArthur et al., 2000; Schak and Harrington, 1999; Yannielli et al., 2002). No phase shifting effects were found in hamsters following preparation at different circadian times (Yannielli and Harrington, 2000). In mice, slice preparation during the second half of the day (ZT 6 - 12) resulted in a peak in SCN activity at ZT 6.3h (Soscia and Harrington, 2004) and when prepared at ZT 2 - 4.5 peaks were observed at ZT 6.8h (Liu et al., 1997a). Multiunit recordings performed in brain slices from mice kept in constant darkness and prepared at circadian time 2 (CT 2) showed activity peaks at CT 5.4h (Albus et al., 2002). Despite differences in techniques, strains, and species, the range of peak times is remarkably narrow. Studies in which the preparation time was provided in a more general way (i.e., preparation was performed during the day) also yielded very similar peak times (for a review, see Gillette, 1991). Together, the findings of these studies indicate a relative robustness in the time of the electrical activity peak *in vitro*.

At the molecular level, the Per1 gene is involved in translational-transcriptional feedback (Albrecht et al., 1997; Yamazaki et al., 2000). Transgenic rats that carry a firefly luciferase gene that is under control of the mouse Per1 promoter (Per1-luc rats) can be used to follow the circadian expression of Per1 both *in vivo* (Yamaguchi et al., 2001) and *in vitro* (Yamazaki et al., 2000). Studies on Per1-luc expression recordings from the SCN show inconsistent results with regard to the effect of preparation time on the phase of the circadian rhythm. Yamazaki et al. (2000) showed no difference in the phase of the rhythm in bioluminescence in the SCN when prepared at ZT 3 or ZT 9. Preparation of slices, with an interval of 2h, showed no consistent effects on the phase of Per1-luc expression rhythm, although a large range in peak times was observed (Abraham et al., 2005). Yoshikawa and coworkers (2005), however, observed consistent delays, of up to 6h, for preparations during the animals' dark phase and at the start of the light period (ZT 1, 17, or 23) (Yoshikawa et al., 2005). No visible light was used when preparations

were started during the dark period of the animal, which suggests that the observed shifts were not induced by light.

It is unlikely that species differences explain the differences in results, as electrophysiological recordings show comparable peak times for rats, mice, and hamsters. One possibility could be that the Per1 expression rhythm may not always parallel the electrical activity rhythm but may dissociate from it as a consequence of the preparation procedure. Differences between electrical activity and Per1-luc expression rhythms were found in one study that compared Per1 luciferase activity with electrical activity following a phase shift of the LD cycle (Vansteensel et al., 2003b). It is possible, therefore, that slice preparation induced shifts in Per1 bioluminescence rhythms, but no shifts in electrical activity. Given the difference in results between studies on Per1 expression, it is possible that the phase of the Per1 rhythm is more susceptible to phase shifting effects than the electrical activity rhythm.

Our data do not imply that the characteristics of the electrical activity rhythm measured *in vitro* are similar to those *in vivo*. In fact, a number of differences have been observed (Meijer et al., 1997). Some of these differences may be due to the absence of incoming pathways in the slice preparation. In our study, the slices are 400μm thick, while the SCN in mice is ~600μm from the anterior to the posterior side (Abrahamson and Moore, 2001). As a consequence, connections within the SCN are disrupted to some extent by slicing. An analysis of *in vivo* versus *in vitro* characteristics revealed that the *in vivo* autocorrelation of electrical impulses is lower than *in vitro*, leading to an increment in variability *in vivo*. Part of this may stem from incoming information from sleep and activity regulatory areas, as both have been shown to alter SCN electrical impulse frequency (Deboer et al., 2003; Schaap and Meijer, 2001; Yamazaki et al., 1998). In addition, it has been observed that the phase of the SCN rhythm *in vitro* shifts to a larger extent than the SCN *in vivo* (Vansteensel et al., 2003b; van Oosterhout et al., 2008). Furthermore, the electrical

activity peaks *in vivo* are somewhat broader (~2h) than those observed *in vitro* (VanderLeest et al., 2007).

In the present study, we investigated whether the time of preparation affects the phase of the rhythm in the electrical activity in the SCN *in vitro*, and, thus, whether results from different preparation times are comparable. This question is important, as different experimental procedures require different preparation times. We conclude that the peak of the electrical activity rhythm of the SCN renders a robust marker for circadian phase, especially when preparation during the subjective night is performed in darkness, and that the time of the peak is consistent between preparation times.

Supplemental Data

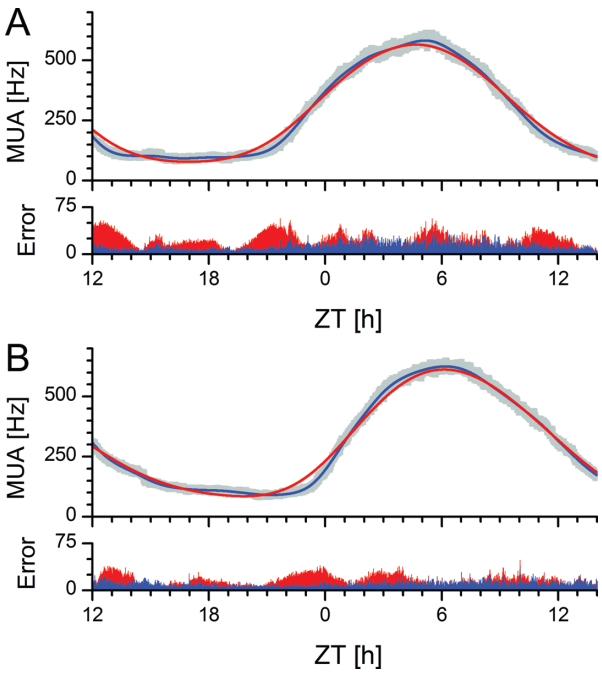

Supplemental Figure 2.1

Effect of applying a higher smoothing parameter

(A, B) Two examples of extracellular multi unit activity plotted as a function of Zeitgeber Time with on the lower axis the deviation of the smoothed data from the raw data (in Hz). Raw data is indicated as grey dots. Weak smoothing (blue line, $\lambda = 1 \times 10^{9}$) provides a low error and a good form estimate of the raw data, i.e. the smoothed line stays within the range of raw data points. Application of a higher smoothing parameter (red line, $\lambda = 1 \times 10^{11}$) introduces a larger error and the shape deviates from the raw data, i.e. at some parts of the curve it is outside the range of the raw data and it renders a more symmetrical peak. Application of a higher smoothing parameter however did not significantly influence the determined time of maximum activity (paired t-test, $p>0.22$).

CHAPTER 3

Heterogeneity of rhythmic suprachiasmatic nucleus neurons: Implications for circadian waveform and photoperiodic encoding

Schaap,J., Albus,H., VanderLeest,H.T., Eilers,P.H., Detari,L., and Meijer,J.H. (2003). Heterogeneity of rhythmic suprachiasmatic nucleus neurons: Implications for circadian waveform and photoperiodic encoding. **Proc. Natl. Acad. Sci. U. S. A.** *100*, 15994-15999.

Summary

Circadian rhythms in neuronal ensemble, subpopulations, and single unit activity were recorded in the suprachiasmatic nuclei (SCN) of rat hypothalamic slices. Decomposition of the ensemble pattern revealed that neuronal subpopulations and single units within the SCN show surprisingly short periods of enhanced electrical activity of ~5h and show maximal activity at different phases of the circadian cycle. The summed activity accounts for the neuronal ensemble pattern of the SCN, indicating that circadian waveform of electrical activity is a composed tissue property. The recorded single unit activity pattern was used to simulate the responsiveness of SCN neurons to different photoperiods. We inferred predictions on changes in peak width, amplitude, and peak time in the multiunit activity pattern and confirmed these predictions with hypothalamic slices from animals that had been kept in a short or long photoperiod. We propose that the animals' ability to code for day length derives from plasticity in the neuronal network of oscillating SCN neurons.

Introduction

The suprachiasmatic nuclei (SCN) contain a major pacemaker of circadian rhythms in mammals (Meijer, 2001; Ralph et al., 1990). The SCN control circadian rhythms in the central nervous system and peripheral organs and as such ensures that organisms are able to anticipate and adjust to predictable changes in the environment that occur with the day-night cycle (Moore and Eichler, 1972; Yamazaki et al., 2000; Abe et al., 2002). The SCN is also involved in adaptation of the organism to the annual cycle by monitoring seasonal changes in day length (Gorman et al., 2001). As an example, animals will accommodate their daily behavioral activity to the photoperiod. A multi oscillator structure has been proposed to fulfill this dual task (Pittendrigh and Daan, 1976b).

At least nine candidate genes have been identified that play a role in rhythm generation on the basis of a transcriptional-translational feedback loop (Allada et al., 2001; Lowrey and Takahashi, 2000). A number of additional genes may be involved to further refine or shape circadian rhythms Shimomura (Shimomura et al., 2001). Although great progress has been made in understanding the molecular basis for circadian rhythm generation, it is unknown how individual neuronal activity rhythms are integrated to render a functioning pacemaker that is able to code for circadian and seasonal rhythms. The SCN each contain ~10,000 neurons, which are small and densely packed (van den Pol, 1980). After dissociation, isolated SCN neurons express circadian rhythms in their firing patterns (Welsh et al., 1995; Liu et al., 1997b). The free-running periods of the individual neurons vary from 20 - 28h. The average period matches the behavioral activity pattern of ~24h. In these cultured dispersals, synaptically coupled neurons can sometimes be observed with synchronized firing patterns (Shirakawa et al., 2000). In SCN tissue explants cultured on multi-electrode plates, the variation in free-running period is considerably smaller (Herzog et al., 1997; Herzog et

al., 1998; Nakamura et al., 2001). In these explants, firing patterns can be observed which are in phase, or 6 - 12h out of phase. The range of phase relationships observed within the SCN *in vitro* suggests a level of temporal complexity that challenges our understanding of how a singular phase and period is obtained for control of behavior.

In the present study we measured the circadian discharge pattern of small neuronal subpopulations on the basis of spike amplitude. Additionally, we applied cluster analysis to determine the circadian activity profile of single units that were extracted from the multiunit signal on the basis of their waveform. The data show that the multiunit signal of the SCN consists of the concerted activity of small neuronal subpopulations or single units that differ substantially from each other in phase and that express by themselves only short durations of increased electrical activity. The summed neuronal activities resembled the ensemble activity pattern and showed consistent peak times during mid-day. On the basis of these results, we propose that phase relations between oscillating neurons may provide information that can code for day length.

Methods

Electrophysiological Recording

The multiunit activity rhythms of SCN neurons were measured as described (Meijer et al., 1997). Male Wistar rats were entrained to a light-dark cycle (e.g., LD 12:12). Coronal slices (500μm) were prepared at the beginning of the subjective day and kept submerged (100 - 150μm) with a thin fork in a laminar flow chamber (35.5°C). The slices contained at least 50% of the rostro-caudal extent of the SCN, and all of the ventro-dorsal extent. Extracellular electrical activity of populations of SCN neurons were simultaneously measured from left and right or dorsal and ventral SCN by platinum/iridium electrodes and subsequently amplified, bandwidth-filtered, and sampled at a rate of 25kHz for more than one circadian cycle (Schaap et al., 2001; Albus et al., 2002). Action potentials with signal-to-noise ratio of 2:1 (noise $\leq$ -5μV from baseline) were selected by spike triggers, counted electronically every 10s and stored for off-line analysis. The positions of the electrodes and spike trigger settings were not changed during the experiment. Spikes larger than a preset amplitude were discriminated online and the spike amplitude and time of occurrence were stored on disk. The same signal was sampled in parallel on another channel at 56kHz. On this channel, the waveform of individual spikes (> -12μV from baseline) were saved (Power1401 with SPIKE2 software, CED, Cambridge, U.K.).

Data Analysis

The phase of circadian discharge rhythms were determined by analyzing the time of maximal discharge rate as described (Schaap et al., 2001). In short, raw discharge patterns were moderately smoothed with *P* splines (smoothing parameter = 10^9 unless stated otherwise) to remove noise. Data are given ± standard error of the mean (SEM). The significance of phase differences between recordings was determined by Monte Carlo simulations.

Subpopulations in the multiunit recordings were constructed on the basis of spike amplitude, sorted by using the B-tree sorting algorithm of BERKELEYDB (Sleepycat, Lincoln, MA), and correlated with distance to electrode tip. When, alternatively, subpopulations were determined on the basis of an equal number of discharges per subpopulation, qualitatively similar results were obtained.

For each subpopulation, circadian activity patterns were determined. The width of the activity pattern was defined as $2(T_{50\%} - T_{max})$ with T_{max} being the time of maximal activity and $T_{50\%}$ being the time of half maximum activity at the declining slope.

We applied cluster analysis on the spike waveform data to isolate and verify single unit activity from the multiunit signal (see Figure 3.5 and 3.6). The validity of the clusters was determined by using interval histograms and autocorrelograms. A clear refractory period, seen as a zero beginning in the autocorrelogram, was used to validate the cluster being a true single unit.

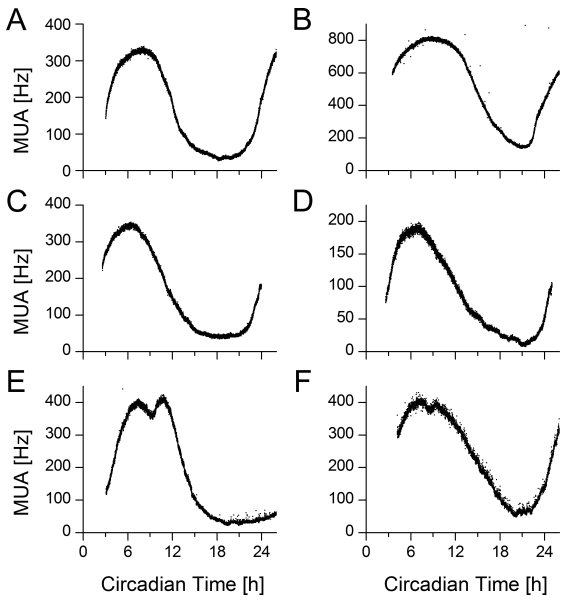

Figure 3.1

Four examples of multiunit activity patterns of SCN neurons recorded with stationary electrodes.

Electrical discharge is shown as a function of CT. CT 0 corresponds with the onset of the projected light phase and CT 12 with the onset of the projected dark phase. Circadian discharge patterns show a peak in electrical activity during the mid-subjective day.

Results

Phase Differences between SCN Regions

We performed dual recordings of multiunit activity in 26 experiments. All experiments yielded raw data traces with low variability (Figure 3.1) and showed high activity during the mid of the projected light phase (mid-subjective day) and low activity during the projected dark phase (mid-subjective night). Simultaneous recordings from the left and right SCN revealed that activity patterns showed small but significant phase differences (1.13 ± 0.2h, range: 0.25 - 3.4h, n = 18, $p < 0.001$). Unilateral recordings in dorsal and ventral SCN revealed similar phase differences within SCN regions (0.89 ± 0.17h, range: 0.3 - 1.65h, n = 8, $p < 0.001$). There was no significant preference for any of the investigated areas to be consistently advanced or delayed (left advanced vs. right, 9:9; dorsal advanced vs. ventral, 3:5).

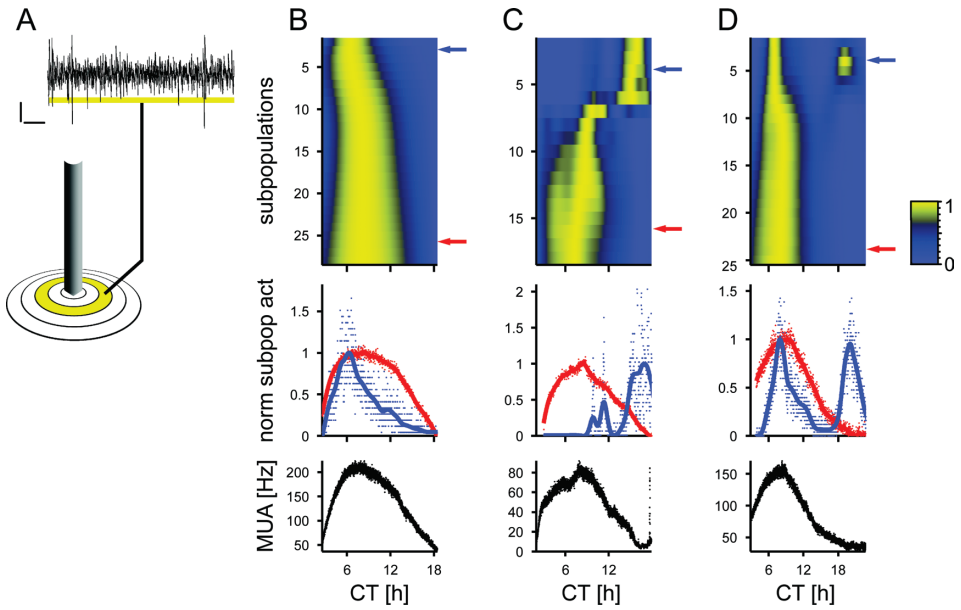

Figure 3.2

Subpopulations within SCN regions show phase differences in electrical activity.

(A) Spikes with amplitudes that fell in a certain range were grouped together.(Scale bars are 10ms by 10μV.)
(B) Color bands represent smoothed neuronal activity rhythms, with high activity plotted in yellow and low activity in blue (see normalized scale bar). Color bands on top represent subpopulations with large amplitude spikes (close to the electrode tip), whereas toward the bottom they represent subpopulations with smaller amplitudes (that are farther away). Normalized discharge patterns of two selected subpopulations (marked by a blue and red arrow) are plotted separately. Dots represent averaged discharge rate per minute. Smoothed activity is indicated by a line; the smoothing parameter was set to 10^5. The peak in firing rate with large amplitude spikes (blue arrow) was relatively advanced in time, and its peak was narrow. The sum of the neuronal activity rhythms of all subpopulations is plotted versus CT at the bottom in black. The shape of this pattern resembled that of the subpopulation marked with the red arrow.
(C) The neuronal activity close to the electrode tip (large amplitudes) showed a maximal firing rate at CT 16.1, whereas farther away from the tip, a discontinuous shift in peak time is visible and peaks occurred around CT 8. Plotting conventions are as in B.
(D) A second peak of multiunit activity is visible that is in antiphase with the main peak. Plotting conventions are as in B.

Phase and Shape Differences within SCN Regions

Subpopulations were selected from multiunit signals on the basis of the amplitude of spikes (Figure 3.2A) in 18 recordings. The circadian discharge pattern and times of maximal firing appeared to vary considerably (Figure 3.2 B-D). Subpopulations with large spikes, consisting of relatively few contributing neurons, showed large phase differences and in some cases sudden transitions in phase occurred or

subpopulations in antiphase were visible. In contrast, subpopulations with small spikes, that consist of more contributing neurons, showed a maximal firing rate at the mid of the subjective day (Figure 3.2 B-D), corresponding with our multiunit activity data. The decreasing variability in time of maximal firing suggests that the circadian discharge patterns are stabilized when more neurons from a larger area within the SCN contribute to the recording (SD vs. spike amplitude, r =-0.907, $p < 0.001$; Figure 3.3B).

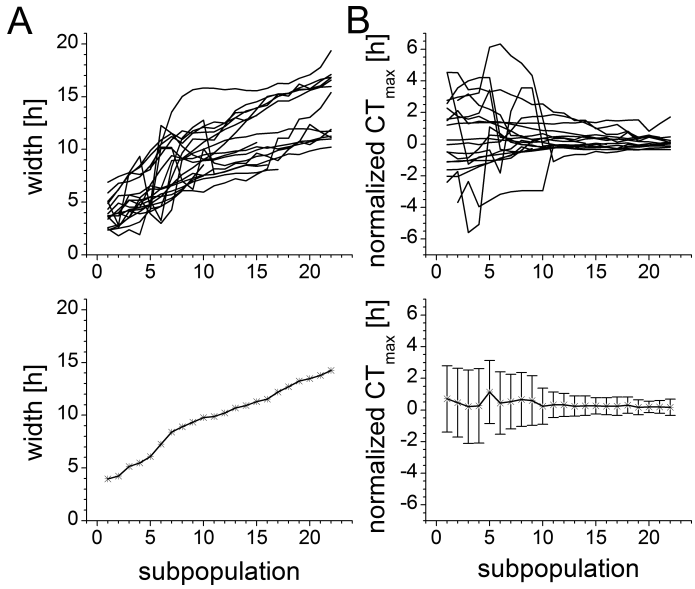

Figure 3.3

Width and phase of neuronal subpopulations.

(A)(Upper) The width of neuronal activity patterns of subpopulations in each experiment is plotted on the y-axis as a function of the spike amplitude of the recorded population. Subpopulation 1 corresponds with the highest amplitude spikes, which originate from small neuronal populations close to the electrode tip. Smaller amplitude spikes are generated by larger groups of neurons, further away from the tip. Data from a single recording are connected with a line. (Lower) The mean width of the populations is plotted against the spike amplitude of the population. The data illustrate that neurons that are located close to one another (large amplitude spikes) show synchronized activity and render narrow peaks as a result.
(B)(Upper) The time of maximal firing rate of each subpopulation from each experiment is plotted and connected with a line. The times are relative to the peak-time in the subpopulation with the smallest spikes. The peak times appeared to vary considerably between subpopulations, and showed large phase jumps (see also Figure 3.2). (Lower) The mean and standard deviation of the times of maximum firing are plotted. The standard deviation was larger in the subpopulations with large spikes than in those with small spikes.

A second difference between the small and large subpopulations existed with respect to the width of the circadian peaks in electrical activity. Subpopulations in the vicinity of the electrode tip showed narrow peaks of neuronal activity (Figure 3.2 B-D, middle plots). These subpopulations expressed peaks in electrical activity of 3.97 ± 0.36h (range: 2.36 - 6.9h, n =18) indicating that the subpopulations showed electrical activity > 50% of their maximum for only very short periods of time. In contrast, subpopulations with small amplitude spikes showed broader peaks, corresponding with the multiunit activity data (width versus spike amplitude, r =-0.699, $p < 0.001$; Figure 3.3A). The broadening of the peaks that is visible when more neurons are being recorded can be best observed by plotting the subpopulation electrical activity in a cumulative way. When an increasing number of neurons around the electrode tip is included, it becomes clear that the ensemble electrical activity is built up from multiple components, and stabilizes with a broad peak at around circadian time 6 (CT 6) (Figure 3.4).

Neuronal Activity Patterns of Single Units

In seven experiments we successfully isolated single unit activity (n = 10) from the multiunit signal after cluster analysis (see Figure 3.5 and 3.6). The single unit activity peaks were narrower than the multiunit population peaks (single: 4.4 ± 0.6h, range: 0.5 - 6.8h; multiunit: 12.38 ± 0.42h, $p < 0.001$) and the times of maximal firing rate of the single units occurred at different phases of the circadian cycle (Figure 3.7). Some units peaked during the subjective night, in antiphase with the peak in multiunit activity, whereas other units peaked at mid-subjective day. The circadian discharge pattern of single units resembled the patterns of the small subpopulations close to the electrode tip (as shown in Figure 3.2) with respect to the narrow peak width, and the large range in peak times.

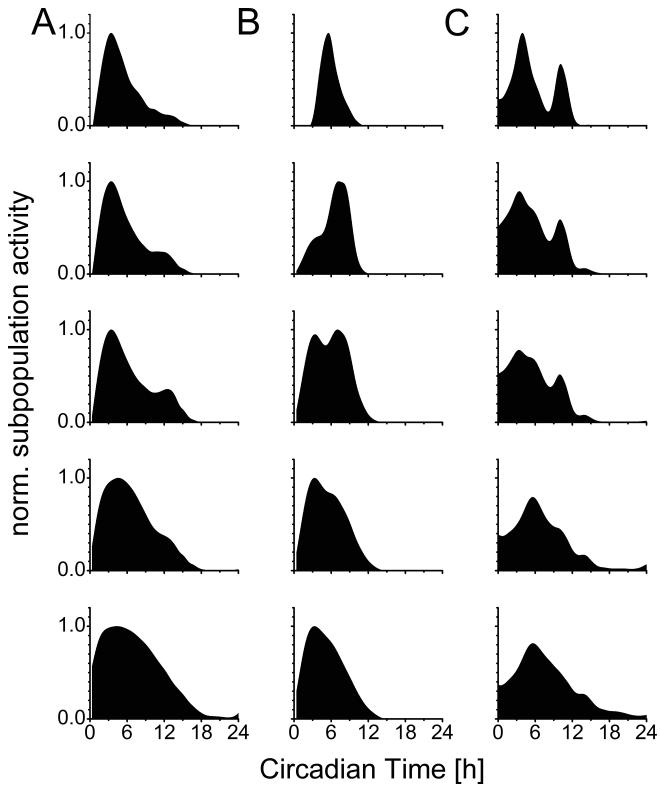

Figure 3.4

Three examples of cumulative electrical activity of SCN subpopulations.

(A)(Top) Normalized activity of a small subpopulation close to the electrode tip. From top to bottom, an increasing number of neurons is recorded, by decreasing the minimum amplitude of the accepted spikes (-29, -24, -20, -15, and -9μV, respectively).
(B) Minimum spike amplitude from top to bottom: -28, -19, -17, -15, and -10μV.
(C) Minimum spike amplitude from top to bottom: -22, -18, -16, -15, and -8μV. Data illustrate how the neuronal ensemble activity is build up from heterogeneous components in the SCN.

Simulations of Neuronal Discharge Patterns

To investigate whether the decrease in peak width is a trivial finding when gradually fewer neurons located close to one another are recorded, multiunit circadian discharge patterns were simulated on basis of the recorded single unit patterns. We simulated 1,000 drawings from a population of 3, 9, 40, and 1,000 neurons and measured the obtained peak width and variance (Figure 3.8 A-D). The average width of the simulated peaks appeared to decrease only slightly with decreasing number of units in the simulated population, whereas the standard deviation in peak widths showed a strong

increase (Figure 3.8E). Although the results presented here are based on a Gaussian distribution, other statistical distributions result in identical trends. In the recordings, however, the width of the peaks declined with a decreasing number of contributing units whereas the standard deviation remained roughly the same (Figure 3.8F). The discrepancies between the simulated and measured patterns demonstrate that SCN neurons are not randomly distributed in phase but are more synchronized when located close to one another.

Phase Differences Contribute to Photoperiod Adaptation

On the basis of our single unit recordings, we calculated an average pattern of single unit activity. We used this average to simulate multiunit activity patterns under different photoperiods (Figure 3.9 A-C). The phase distribution was related to the duration of light in the simulated photoperiod. The phases of the neurons were equally distributed over 8, 12, and 16h to simulate a short, normal, and long photoperiod, respectively. On the basis of these simulations, we found three differences in the multiunit activity pattern. (1) Peaks of the population patterns increased in width with the longer photoperiods and decreased with simulated short photoperiods. (2) The amplitude of the peaks decreased in long photoperiods and increased in short photoperiods. (3) The time of maximal firing (relative to Zeitgeber time 12; light off) advanced in long photoperiods and delayed in short photoperiods. We used the outcomes of the simulation to serve as predictions for a next series of experiments.

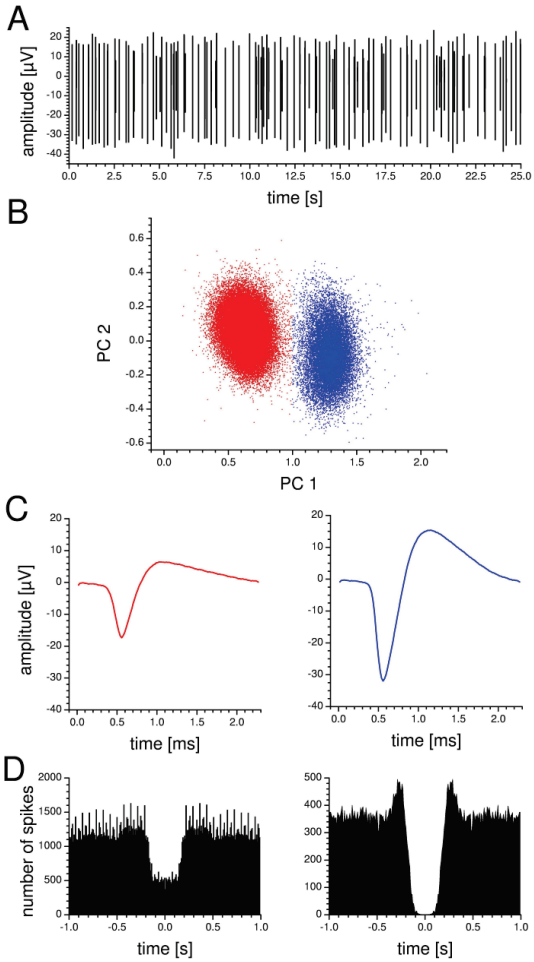

Figure 3.5

Identification of single units in multiunit recordings.

To identify single units in a multiunit signal, the waveform of individual spikes in the signal was sampled and clustered. Clusters of spike waveforms were evaluated to meet criteria for single units.
(A) Spikes sampled from a multiunit recording. Spikes larger than a preset amplitude were sampled at 56kHz, resulting in 126 points to characterize a spike waveform.
(B) In the cluster analysis, spikes were regarded as vectors of a high dimensionality (126). The dimensionality of the data set was reduced by calculating the first few principal components (see Methods). These components were plotted against each other to obtain a cluster plot. The clusters were separated on the basis of the first principal components.
(C) Average waveforms of the clusters in B.
(D) Autocorrelograms were used to evaluate the clusters. A cluster is characterized as a single unit if its autocorrelogram has a clear refractory period around the zero interval. In this case, the right cluster was characterized as a single unit but the left cluster was not. The single units' circadian activity pattern has been plotted in Figure 3.7A.

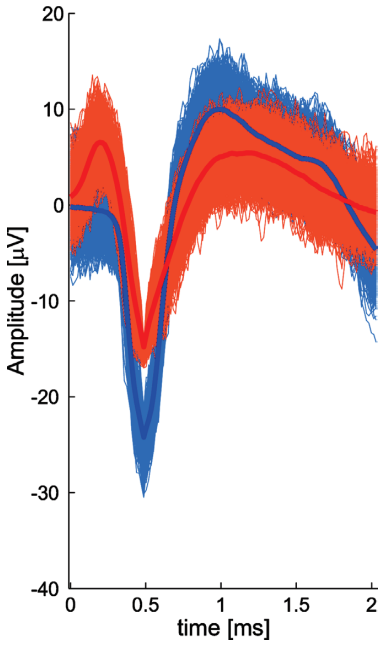

Figure 3.6

Individual waveforms of two identified single units.

The first two or three principal components were calculated to construct a scatterplot from which clusters were readily visible. The clustering resulted in groups of spike waveforms that were homogeneous in shape and distinguishable from other groups.

Neuronal activity of populations of SCN neurons were recorded in slices from animals that had been entrained to a long or short photoperiod and showed a clear response in their behavioral activity pattern. For animals that had been exposed to long photoperiods (n = 5), the population discharge pattern appeared to have increased in width, decreased in amplitude, and advanced in the time of maximal firing. For animals that had been exposed to short photoperiods (n = 5), the multiunit peak width was narrower, the amplitude was increased and the time of maximal firing was delayed. All differences between the long and short day animals were significant (ANOVA, $p < 0.05$). These results are consistent with the changes that were predicted by the simulations (Figure 3.9 D-G).

Discussion

With an innovative recording technique, we were able to simultaneously record the activity of many subpopulations derived from one multiunit electrode. In this study, the technique was successfully applied to describe the transitions from near single unit to population discharge patterns. Because the electrical signal decays with distance, large amplitude spikes are generated by neurons that are in close proximity to the recording electrode.

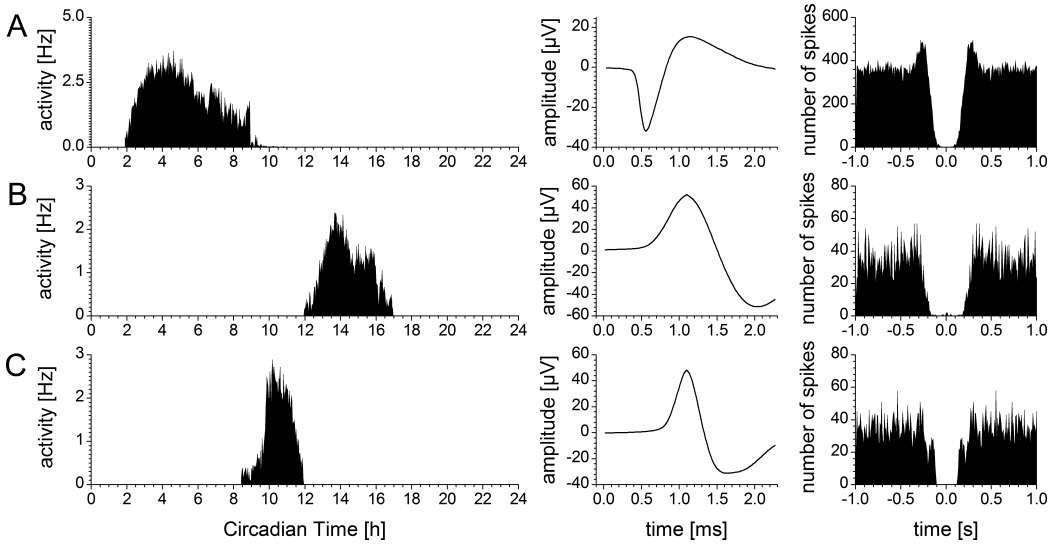

Figure 3.7

Three examples of single unit activity recordings.

Single unit circadian activity patterns are narrow and are found throughout the circadian cycle mainly during the day. Neuronal discharge of single units were isolated on the basis of cluster analysis.
(Left) Neuronal activity was determined in 2min bins and plotted in Hz as a function of CT.
(Right) The autocorrelogram was computed for each single unit over the whole recording period and show a clear refractory period around the zero interval. It is apparent that individual SCN neurons show asynchronous circadian activity rhythms with short durations of electrical activity.

It can be calculated that intercellular distance of SCN neurons is ~25µm, rendering at most seven neurons under the flat surface of the 75µm electrode tip. Subpopulations in the vicinity of the tip were found to vary considerably in phase and shape (Figures 3.2 – 3.4). With decreasing spike amplitude, the subpopulations became larger and consisted of neurons that were also located at larger distance from one another. The concomitant circadian discharge pattern became increasingly wider (the peak in electrical activity broadened) and eventually resembled the ensemble population pattern. The time of maximal firing stabilized at around CT 6 (or mid-subjective day) in these groups. These results are also consistent with the rather small phase differences that we measured between the left and right SCN (Nakamura et al., 2001) and the dorsal and ventral SCN, as these recordings involved large neuronal populations.

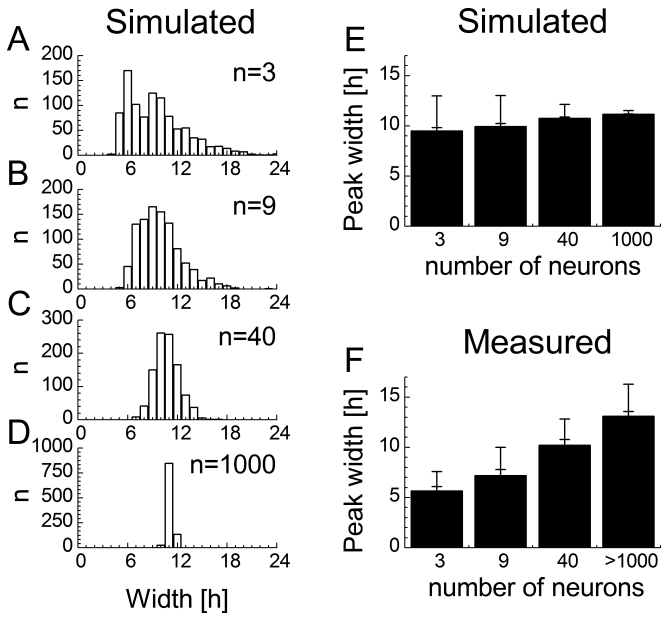

Figure 3.8

Simulated peak width and its standard deviation (SD) as a function of population size.

The simulations were based on the measured average single unit activity pattern.
(A-D) After 1,000 drawings, the resulting width at half-maximal height is plotted for groups consisting of 3, 9, 40, and 1,000 neurons.
(E) Summary of results from A-D, with SEM and SD. The SD in obtained peak widths depends strongly on the number of neurons, and the average width is minimally dependent upon the number of units in the simulation.
(F) Summary of measured peak widths with SEM and SD. The numbers of neurons in the subpopulations were estimated on the basis of the measured integrated single unit frequency.

Single Unit Discharge Pattern

Recording of waveform and subsequent cluster analysis is an experimentally verified method. When this method was used, single unit activity could be extracted out of a multiunit signal. The overall success rate of this technique was low because 7 of 26 experiments yielded verified single unit activity for a long recording period and led to the characterization of 10 units. In the remaining 19 experiments, clusters were either not well separated (n = 10) or did not meet the criteria (n = 9). The strict criteria for cluster validation on the other hand resulted in single units of high quality. The peak times of neuronal activity varied strongly between the recorded neurons and were observed during both subjective day and night. The measured

neurons were active for relatively short periods, up to 7h. Their peak widths are very similar to the widths observed in the smallest subpopulations, indicating that these may have been near single neuron recordings as well. On the basis of both findings, we conclude that neurons in the SCN have short durations of increased neuronal activity.

With simulations of neuronal activity patterns we verified that the observed trend in peak width is not a trivial result when gradually more (or fewer) neurons are recorded. The simulations showed that a random distribution of phases within the SCN cannot account for the decrease in peak width when small numbers of neurons are recorded (Figure 3.8). The interpretation of our experimental results is that the phase of neurons that are located close to one another is correlated, i.e., that groups of neurons in the SCN show some synchronization as a function of interneuronal distance. On the other hand we observed discontinuous changes in phase when we scanned through subregions of the SCN on basis of spike amplitude. This would be in agreement with the existence of small patches of relatively synchronized neurons. We conclude that SCN neurons show synchronized activity as a function of interneuronal distance, but only to some extent.

It is unknown whether the results obtained *in vitro* match those obtained *in vivo*. At present, we are unable to perform long-term single unit recordings with similar criteria *in vivo*. We consider that the acute slice preparation contains 50 - 100% of the anterior-posterior plane of the SCN and has left intact most of the integrity of inter-SCN communication. However, most of the afferent connections have been cut off, which strongly diminishes the effects of extra SCN areas on SCN functioning. With respect to our finding that single units and subpopulations are active for only short durations of activity, we consider it unlikely that the *in vivo* situation changes this result drastically such that neurons become active for the full duration of the photoperiod.

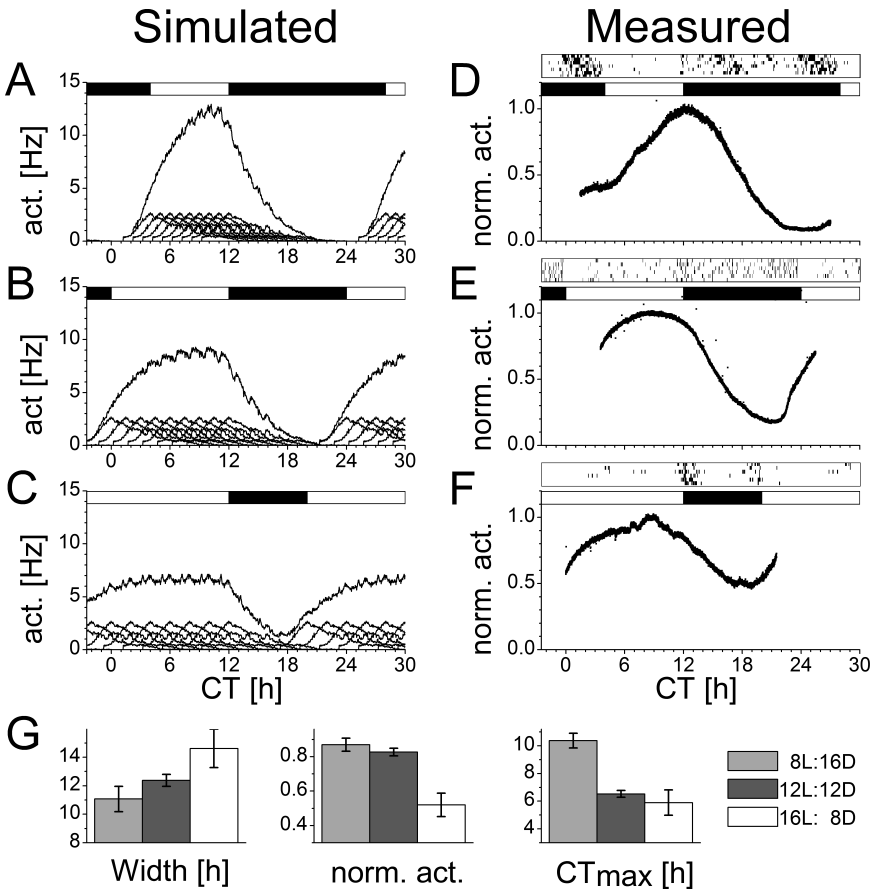

Figure 3.9

Phase differences between neurons contribute to photoperiod adaptation of the SCN.

(A-C) Simulated effects of day length on SCN neuronal activity. Simulations were based on the average firing pattern of recorded single units. Nine individual firing patterns are plotted on the abscissa together with the resulting multiunit pattern. (A-C) Simulations of photoperiods LD 8:16, 12:12, and 16:8, respectively. White bars represent daytime, and black bars represent nighttime. Simulation of a short photoperiod by a small distribution in phase of constituting neurons (A) resulted in a narrow population pattern with a high amplitude rhythm. Simulation of longer photoperiods by larger phase distribution of the neurons (B and C) rendered lower-amplitude rhythms with a broader peak. Maximum firing rate shifts from later to earlier times when day length increases relative to onset of darkness (CT 12).
(D-G) Measured effects of day length on SCN neuronal activity. (D) Example of neuronal activity pattern recorded in a slice from an animal kept on a short photoperiod. The animal's running wheel activity pattern in the 6 days preceding slice preparation is indicated above the recording. (E) Example of a recording of an animal kept in a normal photoperiod. (F) Example of a recording from a long photoperiod. Width, relative amplitude, and peak time of the simulated (G) and measured (H) discharge patterns ± SEM are shown (see text for significance).

This view is supported by the findings that many neurons in the SCN, when sampled for short periods of time *in vivo*, are in their silent phase (Saeb-Parsy and Dyball, 2003). We conclude that circadian waveform of electrical activity in the SCN is determined by heterogeneity in oscillating neurons and that multiunit discharge patterns are build up from subpopulations or individual neurons that exhibit narrow activity peaks and differ from one another in phase.

Phase Differences Contribute to Day Length Adaptation

Our data prompted us to investigate whether changes in phase differences between neurons could underlie adaptation to photoperiodic changes. To test the implications of changing phase relationships for the ensemble population pattern, we performed simulations by using the average recorded single unit activity pattern with a homogeneous distribution of these units over the day (Figure 3.9). Multiunit activity patterns were then recorded from animals entrained to a long and short photoperiod to investigate whether the multiunit discharge patterns that were predicted by the simulations could be observed. We found that 1) the width of the multiunit peaks was increased in long photoperiods and decreased in short photoperiods, 2) the amplitude of multiunit activity peaks was decreased in long photoperiods and increased in short photoperiods, and 3) the CT of maximal firing was advanced after entrainment to a long photoperiod and delayed after entrainment to short photoperiods. These changes were consistent with our predictions. We conclude that alterations in phase differences between oscillating SCN neurons can explain photoperiodic adaptation.

Mechanisms for synchronization between SCN neurons may be nonsynaptic (Shinohara et al., 2000a) or synaptic (Shirakawa et al., 2000). Nonsynaptic synchronization may involve electrical coupling via gap junctions and ionic mechanisms (Shinohara et al., 2000a; van den Pol and Dudek, 1993; Jiang et al., 1997) or paracrine factors such as nitric oxide (Ding et al., 1994), whereas synaptic coupling may involve γ-aminobutyric acid (Liu and Reppert, 2000). Potentially,

these mechanisms may also account for photoperiodic regulation of synchronization between SCN neurons.

A valid question is whether other explanations exist that can also account for the observed changes in SCN neuronal ensemble activity. To that purpose, we performed additional simulations in which we supposed that it is not the phase relationship between neurons that varies with photoperiod, but the width of the single unit peak. However, a change in duration of single unit activity alone could not account for the observed trends in peaks width or amplitude. However, we cannot exclude that single units adjust their activity period under different photoperiods, and that this serves to further support photoperiodic adaptation. The very short periods of increased neuronal activity measured both in single units and in small neuronal populations (mean: < 5h) from rats on a 12h light regimen demonstrates that single unit activity by itself provides an insufficient explanation for photo-periodic adaptation.

The changes in amplitude and time of maximal firing have not been addressed before when evaluating the effects of photoperiod on SCN neuronal ensemble activity. The increased width in multiunit activity patterns that we observed is consistent with the increased peak width in multiunit activity in the hamster (Mrugala et al., 2000), in patterns of c-fos and arginine vasopressin mRNA expression in the rat (Jac et al., 2000; Sumova et al., 2000), in clock gene expression in the rat (Sumova et al., 2003), and in patterns of Per expression in the hamster (Messager et al., 1999; Messager et al., 2000; Nuesslein-Hildesheim et al., 2000). The data on protein and mRNA expression are comparable with the multiunit data in that they represent responses of grouped neurons to different photoperiods. Our data have indicated that individual neurons or small neuronal populations show activity patterns that deviate from the ensemble pattern. Possibly, individual neurons show relatively short periods of increased gene expression, whereas between neurons, these periods do not necessarily overlap. Molecular evidence has been obtained that populations within the SCN show regional heterogeneity (Aida et al.,

2002; Dardente et al., 2002; King et al., 2003; Kuhlman et al., 2003; Reed et al., 2001; Schwartz et al., 2000) and multiple phase relationships among SCN cells have been shown by recording Per1-driven GFP fluorescence.

Our hypothesis that the SCN consists of multiple components that show plasticity in their mutual phase relationship to adopt the photoperiod is conceptually new and of importance for molecular research on photoperiodic encoding at the subpopulation or single unit level.

CHAPTER 4

Seasonal Encoding by the Circadian Pacemaker of the SCN

VanderLeest,H.T., Houben,T., Michel,S., Deboer,T., Albus,H., Vansteensel,M.J., Block,G.D., and Meijer,J.H. (2007). Seasonal encoding by the circadian pacemaker of the SCN. **Curr. Biol.** *17*, 468-473.

Summary

The circadian pacemaker of the suprachiasmatic nucleus (SCN) functions as a seasonal clock through its ability to encode day length (Mrugala et al., 2000; Sumova et al., 2003; Schaap et al., 2003; Nuesslein-Hildesheim et al., 2000; Messager et al., 1999; Sumova et al., 1995). To investigate the mechanism by which SCN neurons code for day length, we housed mice under long (LD 16:8) and short (LD 8:16) photoperiods. Electrophysiological recordings of multiunit activity (MUA) in the SCN of freely moving mice revealed broad activity profiles in long days and compressed activity profiles in short days. The patterns remained consistent after release of the mice in constant darkness. Recordings of MUA in acutely prepared hypothalamic slices showed similar differences between the SCN electrical activity patterns *in vitro* in long and short days. *In vitro* recordings of neuronal subpopulations revealed that the width of the MUA activity profiles was determined by the distribution of phases of contributing units within the SCN. The subpopulation patterns displayed a significantly broader distribution in long days than in short days. Long-term recordings of single-unit activity revealed short durations of elevated activity in both short and long days (3.48 and 3.85h, respectively). The data indicate that coding for day length involves plasticity within SCN neuronal networks in which the phase distribution of oscillating neurons carries information on the photoperiod's duration.

Results and Discussion

In vivo Multiunit Recordings

Exposure to long and short photoperiods had marked effects on the circadian pattern of wheel-running activity in mice (Figure 4.1). In short days, animals showed long durations of nocturnal activity, whereas in long days, animals exhibited short intervals of activity. These data agree with previous reports on the wheel-running activity of mice under long or short photoperiods (Pittendrigh and Daan, 1976b; Refinetti, 2002). *In vivo* multiunit recordings from SCN neurons of freely moving mice in long and short days revealed high discharge rates during the day and low levels during the night, for both photoperiods (Figures 4.2A and 4.2B). During exposure to light-dark (LD) cycles, the mean duration of elevated electrical activity, calculated as the width of the peak at half of its amplitude, was 10.48 ± 0.61h (n = 4) in short days and 14.88 ± 1.13h (n = 4) in long days. Peak times during the last two days in LD occurred at "external time"

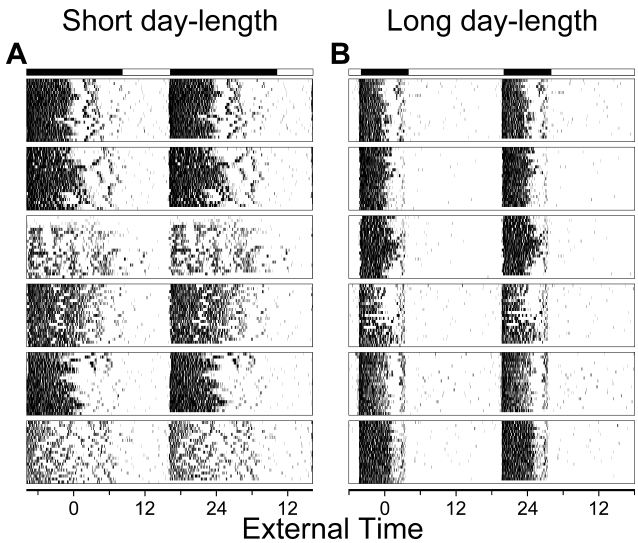

Figure 4.1

Double Plotted Actograms of Mice Kept under a Short Day and Long Day Light Regime

The light regime is plotted on top as a bar with the black part representing the dark period. The animals showed expanded (A) or compressed (B) durations of activity in accordance with the light dark cycle.

(ExT) 11.45 ± 0.27h (n = 4) for the short-day group and at ExT 15.68 ± 0.65h (n = 4) for the long-day group (ExT 12 = midday). In both photoperiods, these peaks occurred 4 - 5h before lights off. Half-maximum values were reached 5.89 ± 0.31h (n = 4) and 10.29 ± 1.34h (n = 4) before the peak time and 4.60 ± 0.28h (n = 4) and 4.60 ± 0.57h (n = 4) after the peak time in short and long days, respectively. The results show that the expansion in electrical activity is asymmetrical with respect to the peak times, and lengthening in long days occurs during the rising phase of the electrical activity pattern.

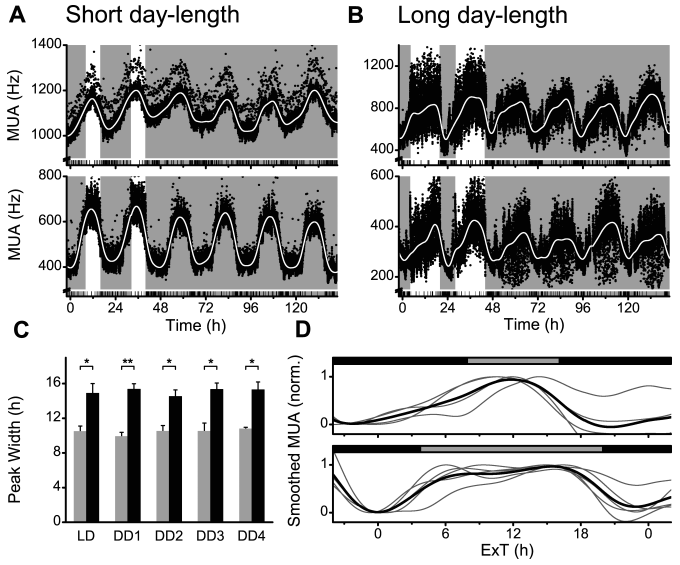

Figure 4.2

SCN Neuronal Activity Measured *In vivo* after Entrainment to Short or Long Day Photoperiods

(A and B) Two typical examples of recordings showing the last two days of multiunit electrical activity of freely moving mice in an LD 8:16 (A) or LD 16:8 (B) photoperiod and the first 4 subsequent days in DD (dark indicated by gray background). Individual data points represent 10s epochs. Smoothed data are indicated by a white line. Drinking activity is shown at the bottom of each plot.
(C) Mean width of the peak, measured at half maximum electrical activity (± SEM) during LD and the first 4 days in DD. Gray bars represent data from animals kept in short day photoperiod, and black bars represent data from long day animals (short day length, n = 4, 4, 4, 4, and 2 on the consecutive days, and long day length, n = 4, 5, 5, 5, and 4 on the consecutive days). Asterisks indicate a significant peak width difference between the recordings (t-test, *$p < 0.05$, **$p < 0.001$).
(D) Smoothed waveforms of the recorded MUA on the first day in constant darkness. The x-axis represents extrapolated external time (ExT 0 = midnight, ExT 12 = midday).
The top bar indicates the prior light dark cycle, and the gray coloring represents lights on. Data are normalized by setting the first trough value to 0 and the first peak value to 1. Gray lines represent individual recordings, and black lines are the averaged waveform (short day length n = 4, long day length n = 5).

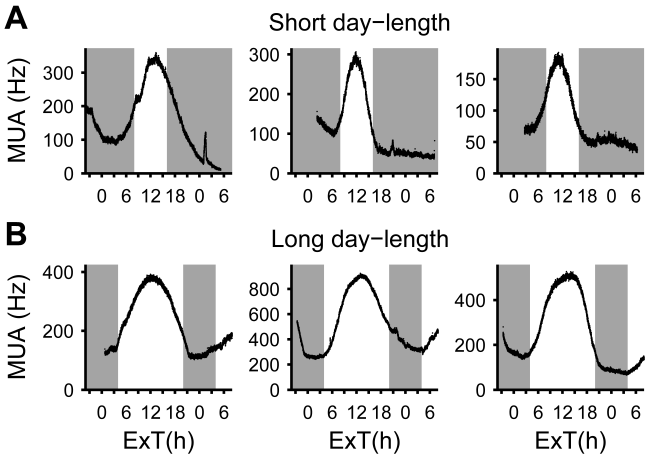

Figure 4.3

***In vitro* Multiunit Activity of Animals Housed under Short and Long Photoperiods**

Raw data traces of electrical impulse frequency, plotted per 10s. The 36h x-axis represents external time (ExT 12 = midday). The gray background represents the dark period of the previous light dark cycle. The widths of the peaks for animals in short day length (A) were narrower than those obtained in long days (B).

After the mice were released in constant darkness, the peak widths remained significantly different and stable for at least 4 days of recording, without evidence of adaptation (Figure 4.2C; two-way ANOVA, $p < 0.0001$, with post-hoc t-tests). The sustained waveform generated by the SCN (Figure 4.2D) indicates that photoperiodic information is present in the electrical output signal of the SCN *in vivo*.

In vitro Multiunit and Subpopulation Recordings

To investigate whether changes in circadian waveform are caused by a change in phase relationships among oscillating neurons, or due to photoperiod-induced changes in the neuronal activity pattern of individual cells, we explored the multiunit, subpopulation, and single-unit activities of SCN cells *in vitro*. Exposure of animals to short or long days resulted in narrow or broad multiunit discharge patterns in slices, respectively (Figure 4.3). These findings are consistent with previous *in vitro* recordings in rats and hamsters (Mrugala et al., 2000; Schaap et al., 2003) and with *in situ* measurements in the SCN of rat, hamster, and sheep (Sumova et al., 2003; Nuesslein-

Hildesheim et al., 2000; Messager et al., 1999; Sumova et al., 2002; Messager et al., 2000; Lincoln et al., 2002; Tournier et al., 2003; Carr et al., 2003; de la Iglesia et al., 2004; Johnston et al., 2005). The maximum frequency of electrical-impulse activity occurred at approximately ExT 12 for both photoperiods. Peak time occurred at ExT 11.09 ± 0.24h (n = 19) for the short-day group and at ExT 12.47 ± 0.21h (n = 24) for the long-day group. The peak times were not different between the ventral and dorsal SCN (Table 4.1) or between anterior and posterior SCN (Table 4.2); thus, this finding contrasts with the anterior-to-posterior differentiation observed *in situ* in the hamster SCN for clock-related genes per2, rev-erbα, and dbp (Hazlerigg et al., 2005).

Table 4.1
Time of Maximum Multiunit Activity *In vitro* within the Ventral and Dorsal SCN

	Ventral			Dorsal			
	PeakTime (ExT)	SEM	n	PeakTime (ExT)	SEM	n	Significance
Short day	10.72	0.36	11	11.11	0.13	13	$p > 0.3$
Long day	13.11	0.89	7	12.74	0.21	20	$p > 0.4$

The peak times were not different between the ventral and dorsal SCN (Table 4.1) or between anterior and posterior SCN (Table 4.2); thus, this finding contrasts with the anterior-to-posterior differentiation observed *in situ* in the hamster SCN for clock-related genes per2, rev-erbα, and dbp (Hazlerigg et al., 2005).

Table 4.2
Time of Maximum Multiunit Activity *In vitro* within the Anterior and Posterior SCN

	Anterior			Posterior			
	PeakTime (ExT)	SEM	n	PeakTime (ExT)	SEM	n	Significance
Short day	11.3	0.15	7	10.92	0.16	12	$p > 0.1$
Long day	12.71	0.23	12	12.87	0.26	9	$p > 0.6$

We did not observe any relation between the time of maximal firing and recording location (t-test).

The peak width of multiunit activity showed significant differences between short days (8.14 ± 0.33h, n = 20) and long days (11.76 ± 0.37h, n = 22, t-test, $p < 0.0001$). The difference in peak width between short and long days *in vitro* (4h) was consistent with the difference obtained *in vivo* (5h). This indicates that photoperiodic information is preserved in the isolated mouse SCN, *in vitro*, and this finding allows for a more detailed cellular-level investigation of the underlying mechanism.

Subpopulation activity analysis was performed by an offline analysis of spike amplitude in which we gradually increased the threshold and thereby decreased the size of the recorded unit population (Schaap et al., 2003). By including fewer neurons in the recording, the results revealed a narrower peak in electrical activity (Figure 4.4). The duration of activity for the smallest subpopulations, measured at half-maximum amplitude, was 3.72 ± 0.31h (n = 31) on short days, and 4.31 ± 0.33h (n = 34) on long days (Figure 4.5). These durations were not significantly different from one another (t-test, $p > 0.25$). A gradual increase in population size resulted in an increase in peak width (Figure 4.6). The increase in peak width occurred especially in the range of more negative, high amplitude, spike threshold levels (between -19 and -10μV).

Small subpopulations were recorded at all phases of the circadian cycle, and especially in long days, a broad distribution in phases was observed. In short days, the mean peak time, determined by a fitted Gaussian distribution, was at ExT 11.00 ± 0.04h, and the mean peak time for long days was at ExT 12.24 ± 0.23h. Although the majority of subpopulations peaked during the projected light period, a considerable number of subpopulations showed maximal activity in the projected dark (Figure 4.5). The distribution of subpopulation peak times (with the median of both groups at zero) was significantly broader in long than in short days (Quartiles, χ^2 test, $p = 0.04$). Furthermore, the distribution of the peak times was significantly different from a uniform distribution in the short days but not in the long-days condition (Rayleigh test, short days' $p = 0.0001$; long days' p

= 0.39). In addition, the Watson two-sample test comparing the distributions of the short and long days was significant ($p < 0.01$). The data indicate that differences in circadian waveform of SCN multiunit activity observed under short and long photoperiods result from the different spacing of subpopulation activity patterns.

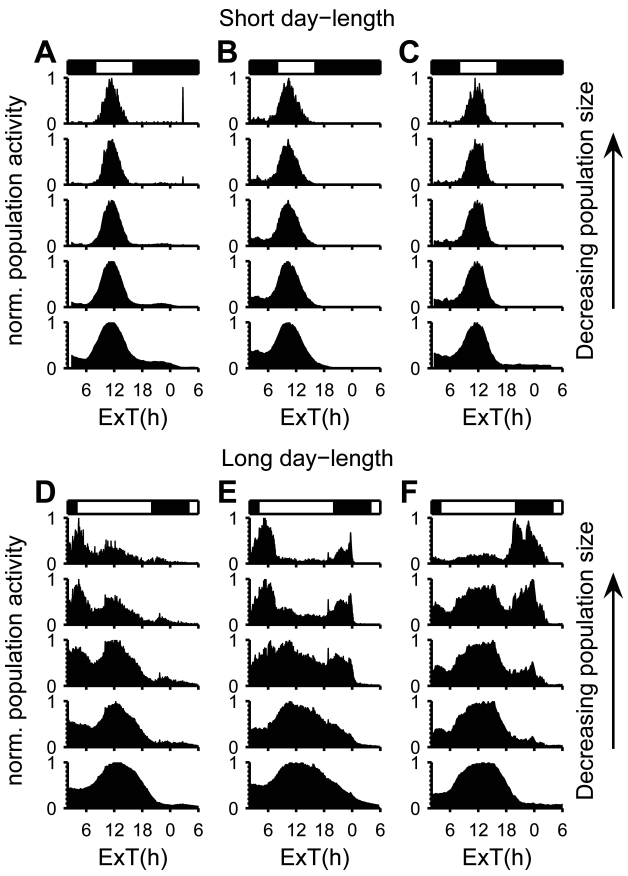

Figure 4.4

Three Examples of Normalized Cumulative Electrical Population Activity for Mice Housed under a Short Day and a Long Day Light Regime

The bars on top of each set of graphs represent the light cycle to which the animals were exposed. Population activity was calculated by a count of all threshold crossing action potentials in 2min bins over the 24h cycle, as a function of external time (ExT 12 = midday). Maximum spike frequency is normalized to 1 for enabling comparison between the graphs. The top graphs show the electrical activity pattern at near single unit level. The lower graphs contain increasingly larger populations as we lowered the threshold for action potential selection. The data show that the electrical activity pattern of the SCN is composed of out of phase oscillating neuronal populations. In long days (D F), we observed a larger phase distribution between the populations than in short days (A C).

Circadian Single-Unit Activity Patterns

Single units were distinguished with the aid of a cluster analysis of spike waveform and were verified by the additional criterion that the interval distribution must be empty at approximately time zero (i.e., units cannot fire with infinite short time intervals). When performing the single-unit analysis, we recognized that the single-unit patterns we measured may not reflect the intrinsic firing patterns of the individual neurons such as the signals recorded in dispersed cell cultures (Welsh et al., 1995; Honma et al., 1998; Herzog et al., 2004) but, rather, are the functional patterns of neurons interacting within the network. In short days, we recorded 26 single units (out of 21 slices) and in long days, 26 units (out of 18 slices). The analysis of most recordings yielded one single unit, but in some cases (seven short-day and five long-day recordings) two to three units were distinguishable in the same recording with waveform and interval characteristics (Figure 4.7). The peak times of the single-unit patterns occurred at various phases of the circadian cycle (Figure 4.8). In short as well as long days, single-unit patterns were broader during the day than during the night (Figure 4.8). Some neurons displayed regular firing patterns (n = 6 out of 26, both in long and short photoperiods). The mean duration of single-unit activity was 3.48 ± 0.29h (n = 26) on short days and 3.85 ± 0.40h (n = 26) on long days (Figure 4.8 and Figure 4.9) with no significant difference (t-test, $p > 0.4$). Single-cell recordings of mPer1 gene expression in cultured mouse SCN at the molecular level (Quintero et al., 2003; Yamaguchi et al., 2003) have shown phase differences, which could be changed by light input (Quintero et al., 2003). Narrow single-unit electrical activity patterns have been described for the SCN of rat and mouse that were kept in 12:12h LD conditions (Schaap et al., 2003; Brown et al., 2005). For different photoperiods, however, single-cell recordings have not been performed.

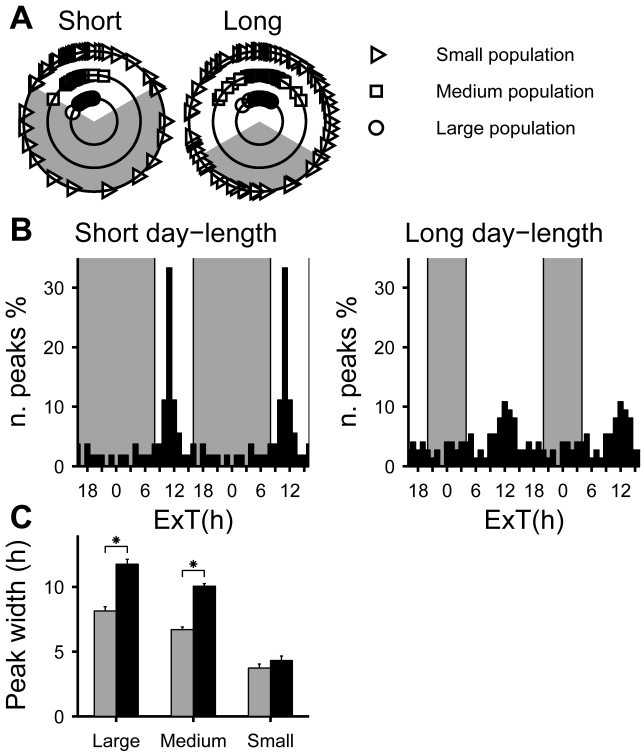

Figure 4.5

Differences in Distribution of Large, Medium, and Small Population Peak Times in SCN Neuronal Activity

Circular 24h plots of the distribution of peak times in electrical activity at the multiunit population level (inner circle, large population of about 600 units), medium population level (middle circle, about 250 neurons), and small population level (outer circle, five neurons or less).
(A) The circles are centered with midday at the top, and the gray part represents the dark. The peak times at the small population level are widely distributed.
(B) Double plotted histogram of SCN neuronal subpopulation activity peak times in short and long day length. The x-axis represents external time. The percentage of populations that peak around the middle of the day (ExT 12) is greater under short days than under long days.
(C) Bar graph showing the width (± SEM) of the activity peaks in short (shown in gray) and in long days (shown in black) for large, medium, and small populations. Asterisks indicate significance (t-test, $p < 0.0001$).

We now show that single units are active at all phases of the circadian cycle and that activity waveforms of individual units do not compress or decompress significantly in short and long days. The presence of neuronal activity during the night is consistent with previous recordings in which sampling of electrical activity for brief periods of time revealed night-time activity (Gillette et al., 1993).

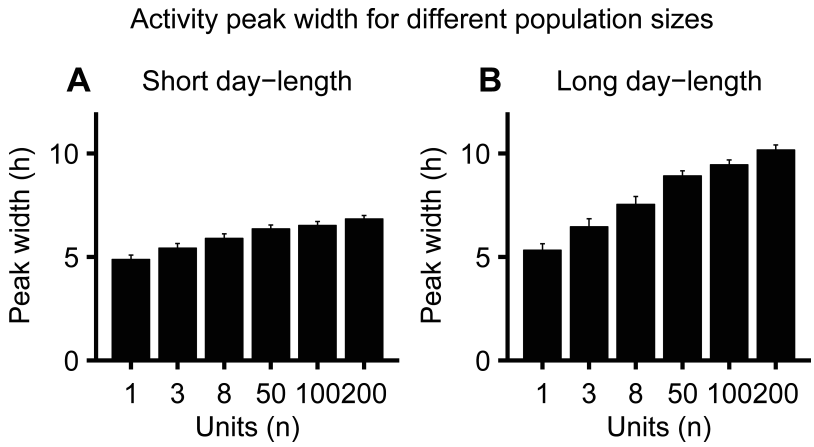

Figure 4.6

Peak Widths for Different Estimated Population Sizes

In both day lengths the spike threshold levels were set at -19, -15, -13, -10, -9, and -8μV, respectively. These threshold levels corresponded roughly to the following number of neurons: < 1, ~3, ~8, ~50, ~100, and ~200. The number of units contributing to the signal was determined by a calculation of the area under the single unit activity curve (Figure 4.8) and the area under the subpopulation activity patterns. In short days, the increase in width caused by the inclusion of more neurons is relatively small (A), whereas in long day length, the increase in width of the peak is large (B). The data indicate that phase distribution of neuronal populations provides a mechanism to code for day length.

Although small differences in the width of the single-unit activity pattern in short and long days are not significant, they may exist. Simulation studies, however, have shown that small differences are insufficient to account for 4 - 5h changes in multiunit peak width (Rohling et al., 2006b).

Furthermore, we cannot rule out that other parameters such as clock gene expression or membrane potential show differences between short and long days. However, we should emphasize the fact that electrical-impulse activity is a major output of the clock (Schwartz et al., 1987); i.e., we strongly suspect that this is the information that is transmitted to downstream processes that would translate photoperiod information into changes in physiology and behavior.

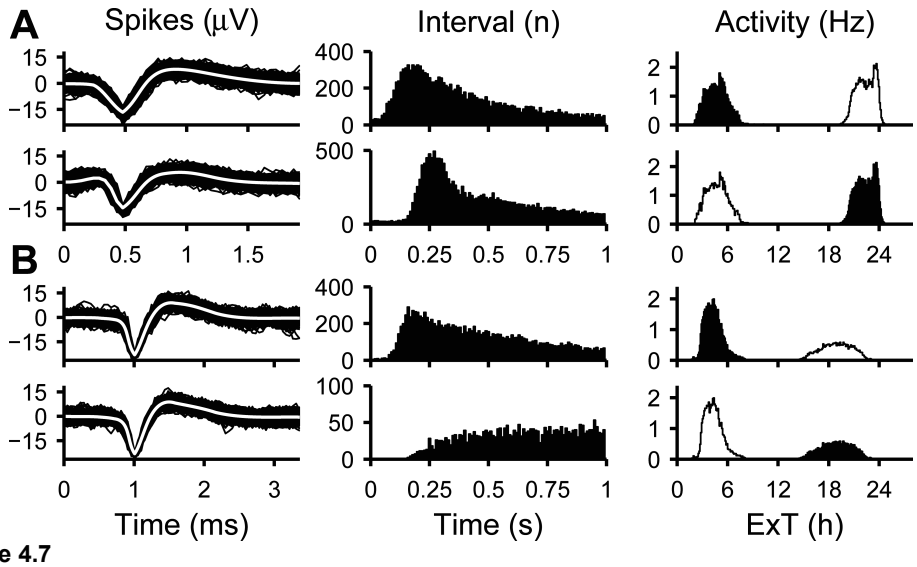

Figure 4.7

Distinct Activity Patterns of Two Single Units in One Recording

Action potential waveforms, their corresponding interspike interval histograms, and circadian activity pattern, as a function of external time, are shown in black. The secondary circadian activity pattern was recorded in the same experiment.
A) Two units were separable by their spike waveform and reflect the activity pattern of two single units.
B) Two units showed different interval characteristics but were not separable by spike waveform. The difference in interval distribution suggests that these bimodal patterns reflect the activity pattern of two different neurons or that one neuron showed a combination of its intrinsic discharge pattern at one phase and a driven pattern at another phase

Based on the single-unit activity patterns obtained in this study, it can be calculated that our smallest subpopulations consisted of less than five neurons (Figures 4.6 and 4.8). This calculation is based on the area under the subpopulation activity curve and the area of the mean single-unit activity pattern in short and long days, respectively (Figure 4.6). Most of the increase in peak width occurs when neuronal populations are increased from about 1 to 50 neurons (Figure 4.6). With 50 neurons, approximately 75% of the full peak width is obtained, both in short and in long days, and a further raise in population size resulted only in small increments in peak width. This leads us to conclude that relatively small groups of SCN neurons can carry substantial information on day length.

The *in vivo* recordings of SCN activity suggest that the phase distribution remains stable for some time even in the absence of

photic information. This corresponds with behavioral aftereffects observed in mice after exposure to different photoperiods (Pittendrigh and Daan, 1976b; Refinetti, 2002). It will be interesting to investigate whether recently identified coupling mechanisms such as VIP receptors or electrical synapses (Colwell et al., 2003; Long et al., 2005; Colwell, 2005; Aton et al., 2005) are involved in the regulation of phase relations between SCN neurons. In the present paper, we observed that plasticity in the phase differences between neurons is the primary mechanism encoding for day length.

Experimental Procedures

Animals and Recording of Behavioral Activity

Male black 6 (C57B/6JOlaHSD) mice (Harlan, Horst, the Netherlands) were entrained to 24h light dark (LD) cycles with either long (16h) or short (8h) days. The animals were housed separately with food and water ad libitum. The cages were equipped with a running wheel for recording locomotor activity of the animals in 1 min intervals. Entrainment to short and long photoperiods for less than 30 days did not lead to consistent waveform changes in the circadian rhythm of electrical activity, either *in vivo* or *in vitro*. For that reason, all animals in this study were entrained for 30 days or longer and were 9 - 14 weeks old when taken for electrophysiological recordings. Of note, C57 mice show photoperiodic responses in their behavioral activity patterns despite their melatonin deficiency, indicating that melatonin is not involved in the regulation of wheel running activity duration (Goldman, 2001). All experiments were performed under the approval of the Animal Experiments Ethical Committee of the Leiden University Medical Center.

In vivo SCN Multiunit Recording

Recording techniques have been described in detail previously (Meijer et al., 1998; Meijer et al., 1996). In brief, tripolar stainless steel electrodes (125µm, Plastics One, Roanake, Virginia) were implanted with a stereotactical instrument in the brain of animals that were under Midazolam / Fentanyl / Fluanisone anesthesia. Under a 5° angle in the coronal plane, electrodes were aimed at the following stereotaxic coordinates: 0.46mm posterior to bregma, 0.14mm lateral to the midline, and 5.2mm ventral to the surface of the cortex (Paxinos and Franklin, 2001). Two of these electrodes (Polyimide insulated) were used for differential recordings of multiunit activity from SCN neurons. The third electrode was placed in the cortex and used as reference. After a recovery period of at least 1 week, the animals were placed in the recording chamber, where drinking

activity was monitored and stored per min. The animals were connected to the recording system with a counter balanced swivel system allowing the animals to move freely. After amplification and filtering (0.5 - 5kHz) of the signal (signal to noise ratio 3:1 to 8:1), the action potentials were detected by a window discriminator and counted electronically in 10s bins. Simultaneously, drinking activity was monitored and stored in 10s epochs. After at least 30 days in the light regime and approximately 5 days of multiunit recording in the LD cycle, the animals were released into constant darkness in order to assess the properties of the neuronal activity rhythm in the absence of light. At the end of each recording, the animals were sacrificed and the recording tip was marked with a small electrolytic current for enabling histological verification of the electrode location. The iron deposition from the electrode tip was stained blue with a potassium ferrocyanide containing fixative solution in which the brain was immersed. Only recordings where the electrode location was verified to be inside the SCN were taken into account.

In vivo Data Analysis

Multiunit activity data were smoothed with a penalized least squares algorithm (Eilers, 2003). The time of maximal activity was determined in the smoothed curve, and the peak width was determined by measurement of the width at half maximum values determined bilaterally. The peak widths for the last two cycles in LD were averaged for each photoperiod. After the mice were released into constant darkness, the peak widths were averaged per day for the first 4 days for evaluation of the stability of the SCN waveform. For obtaining an average waveform for the first day in DD, the amplitude between first trough and peak was normalized in each experiment.

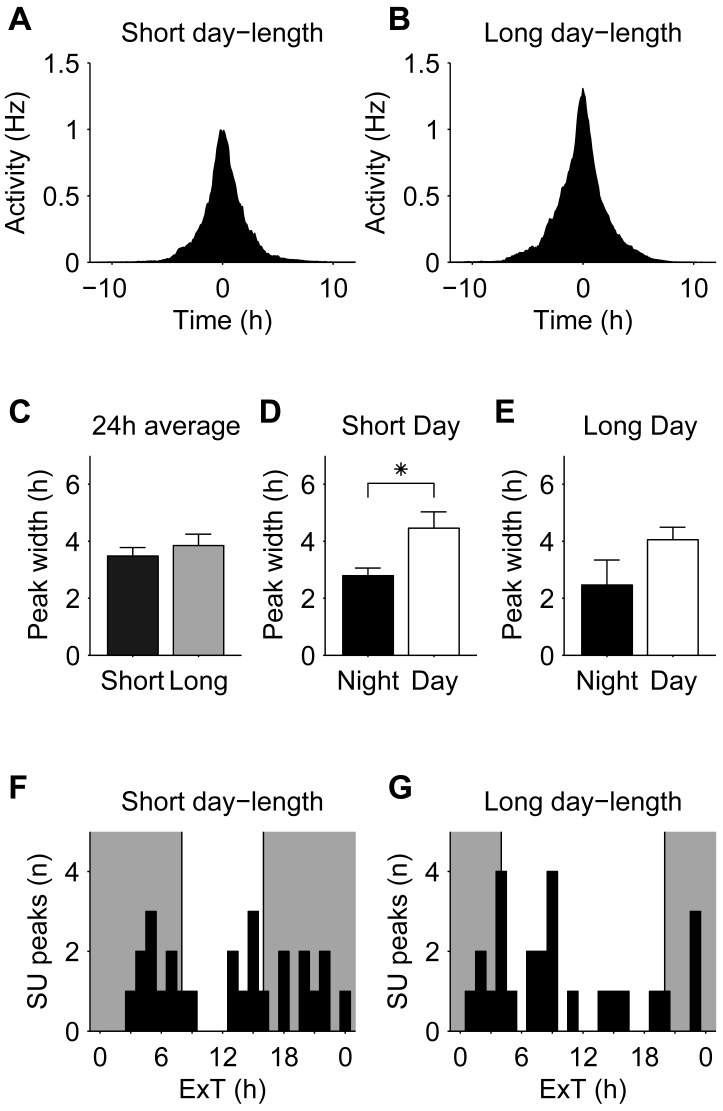

Figure 4.8

Average Single Unit Activity and Distribution of Peak Times.

(A,B) When all single unit activity peaks are centered with the peak at zero and averaged, we obtained a mean circadian activity pattern for short days (A) and for long days (B).
(C,D,E) The width of the mean single unit activity pattern (± SEM), average of the 24h circadian cycle, is shown in (C). (D) and (E) show the mean width (± SEM) of the single unit activity pattern obtained during the day and night in short and long days, respectively $*p = 0.013$, t-test.
(F,G) The histogram with a number of peaks in 1h bins indicates that peaks were distributed throughout the day for both short and long days.

In vitro Electrophysiology

Electrical activity rhythms of SCN neurons were recorded as described previously (Albus et al., 2002). In brief, coronal hypothalamic slices (400µm) containing the SCN were prepared from mice of the long day and short day group, 8h and 4h before lights on, respectively. Only one slice per animal was used for the recording. For the long day group, additional experiments were started at 9h before lights on (this is 1h before lights off) for excluding effects of the time of preparation on the phase and waveform of the rhythm in electrical activity. During the night, preparations were performed under dim red lighting. The slices were kept submerged in a laminar flow chamber and continuously perfused (1.5ml/min) with oxygenated artificial cerebrospinal fluid (35°C, 95% O_2, and 5% CO_2). Population and single unit electrical activity was recorded by two extracellular stationary platinum / iridium metal electrodes (50µm diameter, insulated) placed in the SCN. The signals were amplified (×10,000) and bandpass filtered (0.3 - 3kHz) by a high impedance amplifier. Action potentials were selected by a window discriminator (Neurolog system, Digitimer, Hertfordshire, UK, signal to noise ratio > 2:1) and counted electronically in 10s bins for at least 26h. In addition, the amplified signals were digitized and recorded by a data acquisition system (Power1401, Spike2 software, CED, Cambridge, UK). Amplitude and time of all action potentials crossing a threshold of approximately -6µV were recorded as a measure for subpopulation activity (see below). With thresholds above -9µV, spike templates were generated and thus isolated the activity of several units. The complete waveforms and time of occurrence of the events crossing the threshold were stored for offline analysis.

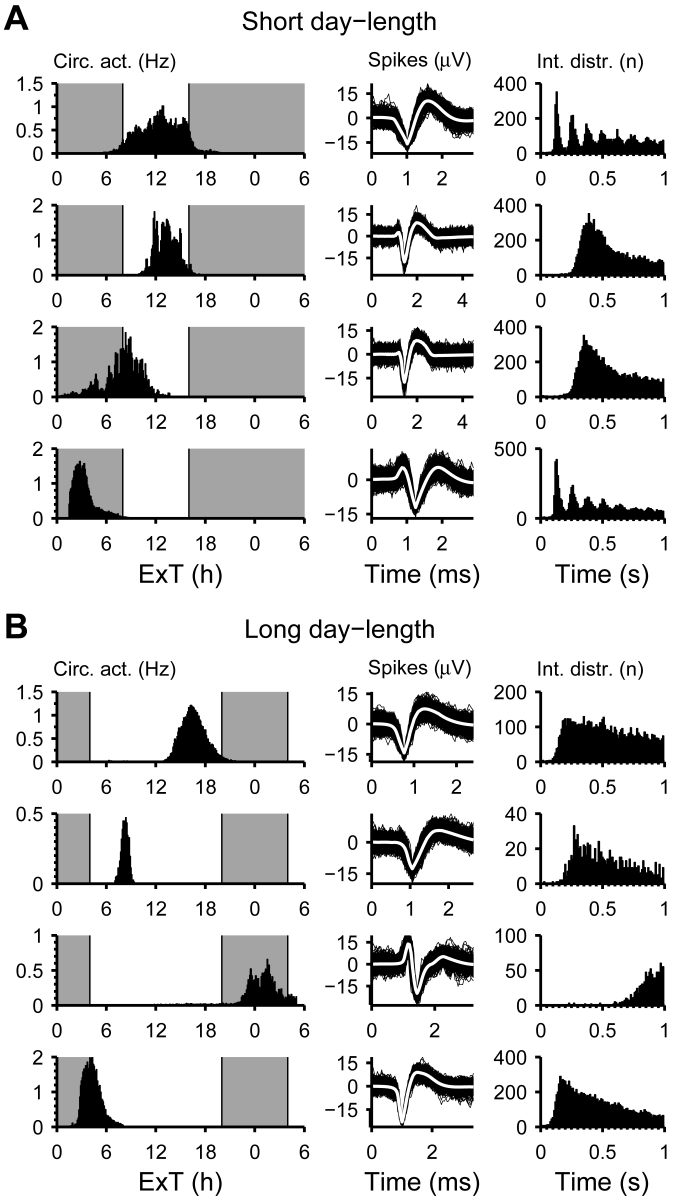

Figure 4.9

Single Units in Short and Long Day Length

Four representative examples of single unit electrical activity for animals housed under a short day (A) and long day (B) light regime. On the left, circadian activity patterns with the gray background indicating the projected dark period are shown. In the middle, the corresponding spikes with mean spike waveform (indicated by white lines) are shown. On the right, interspike interval histograms are shown. The data indicate that single units show short activity patterns in long and short days.

In vitro Data Analysis

Multiunit Activity

Multiunit activity data were smoothed with a penalized least squares algorithm (Eilers, 2003). Peak times were determined in the smoothed data and are given in external time (ExT) with ExT 0 de fined as the middle of the night. Consequently, ExT 12 is midday in both photoperiods (Daan et al., 2002). The duration of the elevated SCN activity was defined as the width of the peak at half maximum amplitude, with the values of the peak and the following trough. The location of the recording electrode was visually assessed. We distinguished between ventral and dorsal recordings and divided the rostro-caudal extend into five portions. We compared peak times of the anterior 40% with the posterior 40% and left out the middle 20% of the SCN. We also compared peak times of the ventral and dorsal 50% of the SCN.

Activity of Neuronal Subpopulations

Activity of neuronal subpopulations in the SCN was analyzed with MATLAB (The Mathworks). Amplitude data recorded from action potentials were divided into 50 equally sized bins starting at a low spike threshold level, representing a large number of neurons, to the highest threshold including only a few units (Figure 4.6). Population and subpopulation activity were smoothed and characterized by their width and peak time of the daily patterns. The width was measured in the smoothed data as the distance between the half maximum amplitude values with peak and troughs on both sides of the peak. Other values were determined as described for the multiunit data.

Single-Unit Analysis

The digitized action potential waveforms were further analyzed with MATLAB. First, the data were reduced by an increase of the thresh old. Next, a combination of principal components (PC) analysis and waveform feature selection was applied for separating the units. Clusters were generated with an expectation maximization Gaussian

model (Lewicki, 1998) with the original templates built by the Spike2 program as a starting point. In some experiments, clusters were bisected into a large number of smaller clusters and were fused together if the shape and interval of the spike would stay the same (Fee et al., 1996). This helped to reduce the number of spikes coming from multiple units and improved single unit clusters. During the mid-subjective day, the isolation of single units appeared more difficult than during the silent phases of the cycle because of the high number of spikes generated by the different neurons. The validity of single units described by the clusters was confirmed with their interspike interval (ISI) histogram, showing a lack of events in the first 50-100ms. The timing and width of single-unit activity were also calculated on smoothed data.

Statistical Analysis

The width of *in vitro* multiunit, subpopulation, and single unit activity between long and short days were compared with a two tailed independent samples t-test in SPSS and were considered to be significant if $p < 0.05$. Distribution of peak times for the small populations was compared between long day and short days with a quartile cross tabulation. We compared the middle two groups (center of the distribution) with the outer two groups (tails of the distribution). Differences in distributions were tested with a χ^2 test. We also per formed a Rayleigh test that compares the observed circular distributions with the uniform distribution in both photoperiods. In addition, we compared the two circular distributions of the short and long day conditions with the Watson two-sample test. Peak widths of *in vivo* multiunit were compared with a two way ANOVA in SPSS and then post hoc independent samples t-tests and were considered to be significant if $p < 0.05$. All values are mean ± SEM.

CHAPTER 5

Phase Shifting Capacity of the Circadian Pacemaker Determined by the SCN Neuronal Network Organization

VanderLeest,H.T., Rohling,J.H., Michel,S., and Meijer,J.H. (2009). Phase shifting capacity of the circadian pacemaker determined by the SCN neuronal network organization. **PLoS One**. *4*, e4976.

Summary

Background In mammals, a major circadian pacemaker that drives daily rhythms is located in the suprachiasmatic nuclei (SCN), at the base of the hypothalamus. The SCN receive direct light input via the retino-hypothalamic tract. Light during the early night induces phase delays of circadian rhythms while during the late night it leads to phase advances. The effects of light on the circadian system are strongly dependent on the photoperiod to which animals are exposed. An explanation for this phenomenon is currently lacking. **Methodology and Principal Findings** We recorded running wheel activity in C57 mice and observed large amplitude phase shifts in short photoperiods and small shifts in long photoperiods. We investigated whether these different light responses under short and long days are expressed within the SCN by electrophysiological recordings of electrical impulse frequency in SCN slices. Application of N-methyl-D-aspartate (NMDA) induced sustained increments in electrical activity that were not significantly different in the slices from long and short photoperiods. These responses led to large phase shifts in slices from short days and small phase shifts in slices from long days. An analysis of neuronal subpopulation activity revealed that in short days the amplitude of the rhythm was larger than in long days. **Conclusions** The data indicate that the photoperiodic dependent phase responses are intrinsic to the SCN. In contrast to earlier predictions from limit cycle theory, we observed large phase shifting responses in high amplitude rhythms in slices from short days, and small shifts in low amplitude rhythms in slices from long days. We conclude that the photoperiodic dependent phase responses are determined by the SCN and propose that synchronization among SCN neurons enhances the phase shifting capacity of the circadian system.

Introduction

The daily revolution of the earth causes 24 hour cycles in the environmental conditions, while the annual cycle of the earth moving around the sun brings about seasonal changes. Many organisms possess an endogenous 24 hour or 'circadian' clock, which allows them to anticipate and adapt to the daily and annual environmental changes (Takahashi et al., 2001). In mammals, a major pacemaker for circadian rhythms is located in the suprachiasmatic nuclei (SCN) of the anterior hypothalamus (Ralph et al., 1990). The ability of the SCN to generate circadian rhythms is present at the single cell level and is explained by a molecular feedback loop in which protein products of period and cryptochrome clock genes inhibit their own transcription (Reppert and Weaver, 2001; Ko and Takahashi, 2006). The SCN control circadian rhythms in molecular, endocrine and physiological functions, as well as in behavior (Kalsbeek et al., 2006). Besides their role as a daily clock, the SCN are an integral part of the photoperiodic time measurement system and convey day length information to the pineal gland and other parts of the central nervous system (Carr et al., 2003; Sumova et al., 2003; Bendova and Sumova, 2006).

The SCN are synchronized to the environmental light-dark cycle via the retina. Light information reaches the SCN directly via the retino-hypothalamic tract, which innervates the SCN with glutamate and pituitary adenylate cyclase activating peptide containing fibers (Morin and Allen, 2006). Synchronization to the environmental light-dark cycle is based on a time-dependent responsiveness of the SCN to light, which is most easily demonstrated in "perturbation experiments" in which animals are kept in constant darkness and subjected to discrete pulses of light. Light pulses presented during the early night induce phase delays of the rhythm, while at the end of the night, they induce advances. The characteristic phase dependent light responsiveness is a prerequisite for animals to

entrain to the environmental cycle, and is a common property of many organisms (Pittendrigh et al., 1984).

The maximum advancing and delaying capacity depends strongly on the photoperiod to which animals are exposed (Pittendrigh et al., 1984; Refinetti, 2002; Evans et al., 2004). This finding has received surprisingly little attention, given the robustness of the photoperiodic modulation and potential functional significance. For instance in the hamster, the phase shifting effects of a 15min light pulse on behavioral activity rhythms are about 2 - 3 fold larger in short winter days than they are in long summer days (Pittendrigh et al., 1984). One possibility is that increased light exposure in long days desensitizes the system to light at the level of the retina (Refinetti, 2002). Recently, it has become known that the organization of the SCN shows plasticity under influence of changes in day length (Schaap et al., 2003; Johnston et al., 2005; Rohling et al., 2006b; Inagaki et al., 2007; VanderLeest et al., 2007; Naito et al., 2008). The variation in light response over the seasons could therefore also result from different response properties brought about by plasticity within the SCN itself. We performed behavioral and electrophysiological experiments and found evidence that the phase shifting magnitude is determined by the SCN. The large phase shifts observed in high amplitude rhythms in short days versus the small shifts in long days leads us to propose that synchronization among individual oscillator components enhance the phase resetting capacity.

Results and Discussion

We performed behavioral experiments to establish phase shifting effects of light under long and short photoperiods. Running wheel activity was recorded from C57 mice kept in short and long day length (light:dark 8h:6h and 16h:8h). After at least 30 days of entrainment to the light-dark cycle, the animals remained in continuous darkness for 3 days (Figure 5.1). On day 4 in darkness, the animals received a saturating 30 min white light pulse which was aimed at different phases of the circadian cycle. The onset of behavioral activity was used as a marker of circadian phase, and defined as circadian time 12 (CT 12). Maximum delays were observed for pulses given 3 hours after activity onset in both animals from short days (shift: 22.68 ± 0.19h, n = 6) and animals from long days (shift: 20.62 ± 0.28h, n = 5). The magnitude of the delays was however significantly larger for animals in short days ($p < 0.001$). Light pulses towards the end of the night produced small phase advances which were not significantly different between the groups (short day advance: 0.61 ± 0.26h, n =8; long day advance 0.50 ± 0.11h, n = 9; $p > 0.6$).

To investigate whether the small phase delays in long days may have resulted from a decrease in photic sensitivity of the circadian system as a consequence of higher photon stimulation during entrainment, we reinvestigated the phase delaying effects of light in short days, and doubled the amount of photons to which we exposed the animals during the entrainment period. Thus, the short day animals received the same amount of photons as the long day animals, but now distributed over 8 instead of 16 hours. We found that the phase delaying effects of light were large (shift: 22.95 ± 0.19h, n = 8) and not different from those observed in short days under normal light conditions ($p > 0.1$). The shifts were, however still significantly larger than those observed in long days ($p < 0.001$). The results indicate that the difference in shift between long and short day animals is not attributable to an increment in photon stimulation during entrainment to long days.

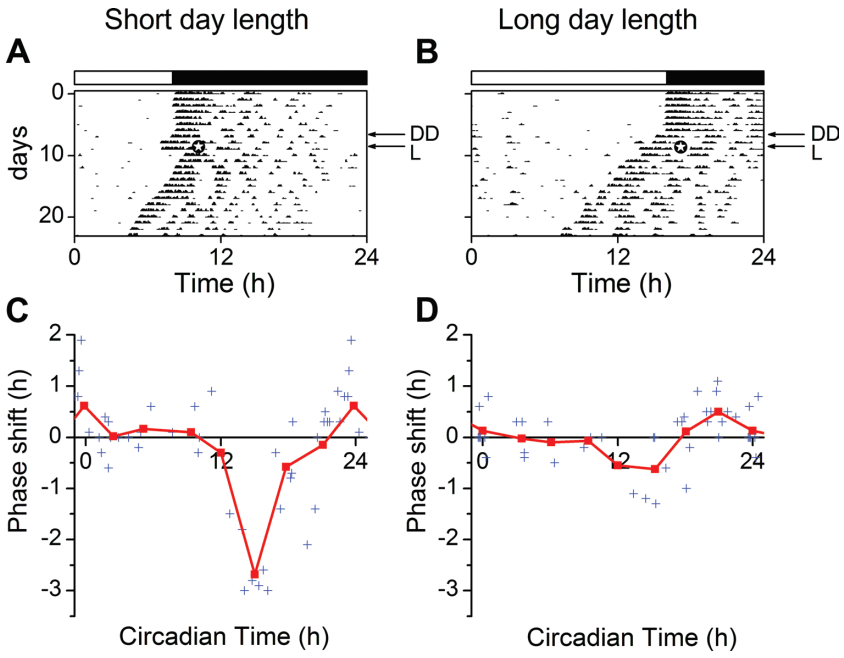

Figure 5.1

Phase shifts of wheel running behavior in mice induced by 30 minutes light pulses.

(A, B) Examples of wheel running actograms from animals kept in short (A) and long photoperiods (B). The actograms show the wheel running activity of the mice over the 24h day. Consecutive days are plotted on successive lines. The top bar indicates the light-dark schedule before transfer to continuous darkness (DD, indicated with an arrow). A light pulse was given on day four in DD (L, indicated with an arrow), 3 hours after activity onset (indicated by ✪ in the actogram). Activity onset was defined as circadian time 12.
Phase response plots to 30 minute light pulses in short (C) and long (D) photoperiod. Phase responses are plotted as a function of the circadian time of the light pulse. Individual phase shifts are indicated by a plus symbol. The results were grouped in 3h bins centered at CT 0, 3, 6, 9, 12, 15, 18 and 21. The average phase responses of the light pulses are indicated by squares and connected with a solid line. The time of maximal delay is at CT 15 for both long and short photoperiods and is significantly different between both day lengths ($p < 0.001$). The large magnitude of the delays observed in short days is consistent with other studies (Pittendrigh et al., 1984; Refinetti, 2002).

To investigate whether the difference in the magnitude of the phase shift in long and short days is retained in the SCN *in vitro* we kept animals under long and short day length and prepared hypothalamic slices containing the SCN on the third day after release in constant darkness (Figure 5.2). We recorded electrical impulse frequency in the SCN by stationary electrodes and applied NMDA pulses (10µM, 30min duration) by switching from regular artificial cerebrospinal fluid (ACSF) to NMDA containing ACSF. The NMDA

receptor is of crucial importance in mediating phase shifting by light and application of the glutamate receptor agonist NMDA to brain slices *in vitro* generates phase shifts of the circadian rhythm resembling photic phase responses (Colwell et al., 1991; Ding et al., 1994; Shibata et al., 1994). The timing of the NMDA pulse was based on the extrapolated behavioral activity of the animal before slice preparation, and was aimed 3 hours after activity onset, where the largest shifts in behavior were observed in both photoperiods.

NMDA induced a sustained increment in SCN electrical discharge in slices from both photoperiods (Figure 5.3). The relative increase in electrical activity was 32.2 ± 9.1% (n = 5) of baseline discharge in short days and 43.9 ± 8.0% (n = 5) of baseline discharge in long days. No significant differences in responsiveness to NMDA were observed ($p > 0.1$). Despite the similarity in acute NMDA responses, the resulting phase shifts were significantly larger in short days (23.2 ± 0.50h, 6 control and 5 experimental slices) compared to long days (0.0 ± 0.89h, 6 control and 5 experimental slices; $p < 0.006$; Figure 5.2). We also calculated the phase shift based on a secondary phase marker, the time of half maximum value on the rising slope of the electrical discharge peak. With this phase marker we found the same difference in phase shift between long and short day length, indicating the robustness of the measured differences in phase shift (difference in phase shift between day lengths: 3.2 ± 0.86h; $p < 0.002$).

The data indicate that the phase shifting capacity of the circadian system under long and short photoperiods is determined by the SCN itself. The absence of a difference in the magnitude of the NMDA response underscores this interpretation and shows that the same increase in neuronal activity of the SCN results in a different phase shifting response.

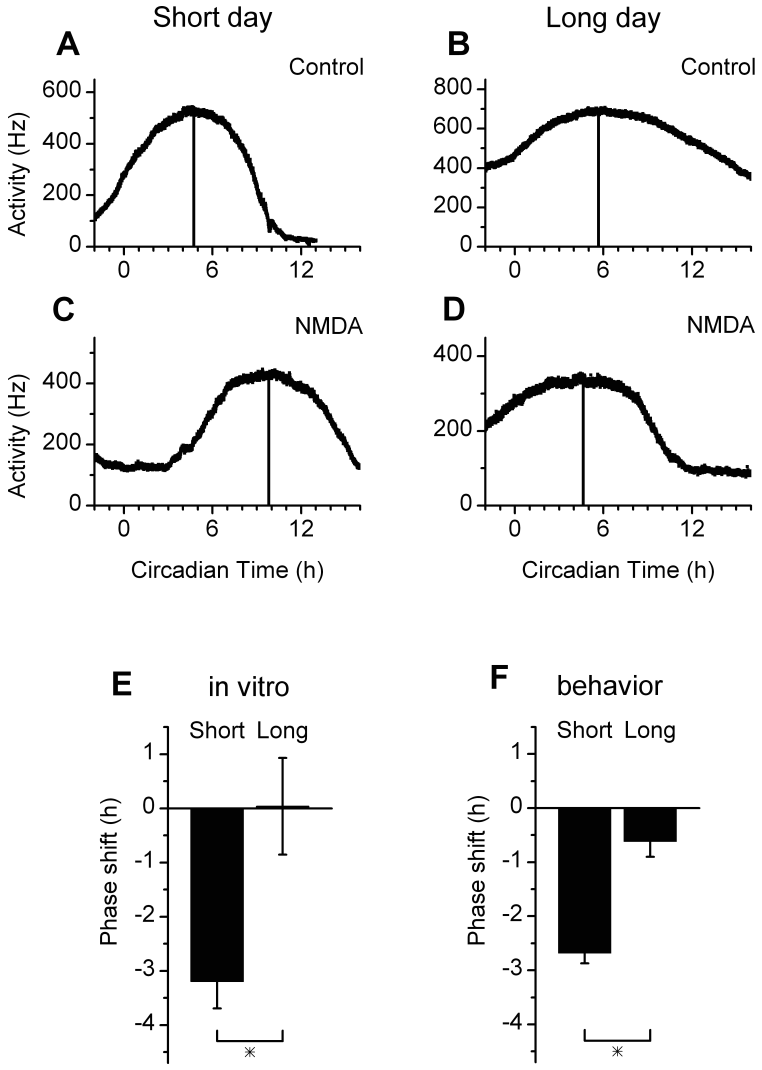

Figure 5.2

Phase shifts of multiunit electrical activity rhythms in brain slices from mice kept on a short and long photoperiod.

Examples of extracellular multiunit recordings from the SCN in mice kept on a short photoperiod (A, C) and on a long photoperiod (B, D).
Action potentials were counted in 10s bins, and are plotted as a function of circadian time, determined by activity onsets from the mice prior to slice preparation. NMDA pulses were given 3 hours after the activity onset (CT 15), on the first cycle *in vitro*, in slices from both short (C) and long (D) day animals. In slices obtained from short day animals these pulses induced a delay in the peak time of the rhythm on the day following the application. Peak times are indicated by a vertical line.
(E) Delays obtained at CT 15 from short day animals were significantly larger than delays obtained from long day animals. The magnitude of the delay after an NMDA pulse at CT 15 was significantly different between day lengths ($p < 0.01$).
(F) The magnitude of the behavioral delay was not different from the delay observed *in vitro*, for both day lengths (short day *in vitro* vs. behavior $p > 0.3$, long day *in vitro* vs. behavior, $p > 0.4$).

In an additional series of experiments we treated 7 slices from long day animals with 25μM NMDA at CT 15. The acute increase in electrical activity in response to 25μM NMDA was 123 ± 16.0% as compared to baseline, which is three times larger than the response to 10μM NMDA ($p < 0.003$). The phase-shifts in electrical activity rhythms were however not significantly different from untreated or 10μM NMDA treated slices (shift: 20.29 ± 0.72h; $p > 0.68$ in both cases). These results show that for long day length, the phase shifting response is not enhanced by an increment of the pharmacological stimulus. The preservation of the small shifts in slices from long days indicates an intrinsic incapability of the SCN to shift in long photoperiods.

The question arises what mechanism in the SCN underlies the photoperiodic modulation of the phase shifting capacity. Recently it has become clear that photoperiodic encoding by the SCN (Sumova et al., 2003; Mrugala et al., 2000) is accomplished through a reconfiguration of cellular activity patterns (Schaap et al., 2003; Inagaki et al., 2007; VanderLeest et al., 2007; Naito et al., 2008; Hazlerigg et al., 2005). In long days, the activity patterns of single SCN neurons are spread in phase, rendering a broad population activity pattern, while in short days, the neurons oscillate highly in phase, which yields a composite waveform with a narrow peak (Schaap et al., 2003; VanderLeest et al., 2007). Molecular studies have shown regional differences in gene expression patterns within the SCN that increase in long days and decrease in short days (Inagaki et al., 2007; Naito et al., 2008; Hazlerigg et al., 2005).

Theoretically, it follows from such a working mechanism, that the amplitude of the SCN rhythm in short days is larger than the amplitude in long days. That is, when neurons overlap in phase in short days, the maximum activity of each neuron will be at similar phases, leading to a high frequency in multiunit activity due to the summed activity of overlapping units during the peak, while during the trough, non-overlapping units lead to low activity (Rohling et al., 2006b). We measured the frequency of the multiunit activity of SCN

neurons in long and short day slices and found that indeed, the maximum discharge levels are higher in short day animals (Figure 5.4). A general assumption in the field of circadian rhythm research is that high amplitude rhythms are more difficult to shift than low amplitude rhythms (Pittendrigh et al., 1991), which stands in contrast to our present findings. To critically test the observed amplitude differences, we analyzed the amplitude under long and short days in more detail, by an off-line analysis of subpopulation activity. To test if the amplitude differences are inherent to a change in photoperiod and are not influenced by threshold settings, we analyzed the amplitude at different threshold settings, reflecting the activity of different sizes of populations of SCN neurons (c.f. (Schaap et al., 2003; VanderLeest et al., 2007)).

In this analysis, we could reliably compare subpopulation activity rhythms, with an equal number of action potentials contributing to the circadian waveform. The results showed that in short days, the amplitude of the rhythm was larger than in long days for any given number of spikes in the recording (Figure 5.4D).

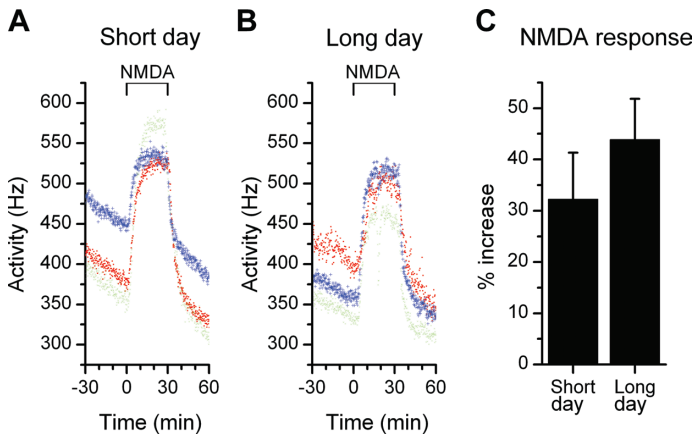

Figure 5.3

Acute responses in multiunit electrical activity to NMDA application at CT15.

(A, B) NMDA application (10μM) at CT 15 induced an increase in firing rate that was recorded by extracellular multiunit electrodes. The magnitude of the NMDA response is similar in slices from long and short day animals and in both photoperiods, a plateau was reached during the application.
(C) The magnitude of the acute response to NMDA, measured as the relative increase in discharge rate, was not different between day lengths ($p > 0.3$).

These findings are in contrast to the general assumption that the magnitude of a phase shift is inversely related to the amplitude of the rhythm, i.e. that it is more difficult to shift high amplitude rhythms than low amplitude rhythms. This assumption is based on the theory of limit cycle oscillators, where a perturbation of similar strength changes the phase of an oscillator with low amplitude more than one with higher amplitude, because the perturbation represents a larger fraction of the radius of the circle (Aschoff and Pohl, 1978; Winfree, 2000). The question is how to explain our current findings.

It could be argued, that in long day length, with a wide phase distribution, the neurons have a more diverse phase shifting response to a light input signal, while in short day length, with a narrow phase distribution, neurons may respond more coherent, resulting in a larger overall shift. Simulations were performed in which single unit PRCs were distributed over the light dark cycle according to experimentally obtained distributions of SCN subpopulations (see Supplemental Data and Figure 5.5). We used type 0 and type 1 PRCs as well as the single unit PRC described by Ukai et al. (Ukai et al., 2007).The simulations showed that the amplitude of the long day PRC is considerably smaller than the short day PRC, irrespective of the shape of the single unit phase response curve that was used in the simulations. The results from our simulations accord with our behavioral and electrophysiological results (Figures 5.6 and 5.7). Recent studies have shown that a phase resetting light pulse alters the phase relation between oscillating fibroblasts and SCN neurons (Ukai et al., 2007; Pulivarthy et al., 2007). Our results show that, vice versa, the phase relation between neurons determines the phase response of the ensemble. Together the data indicate a close relation between phase resetting behavior and the synchrony among oscillating cells.

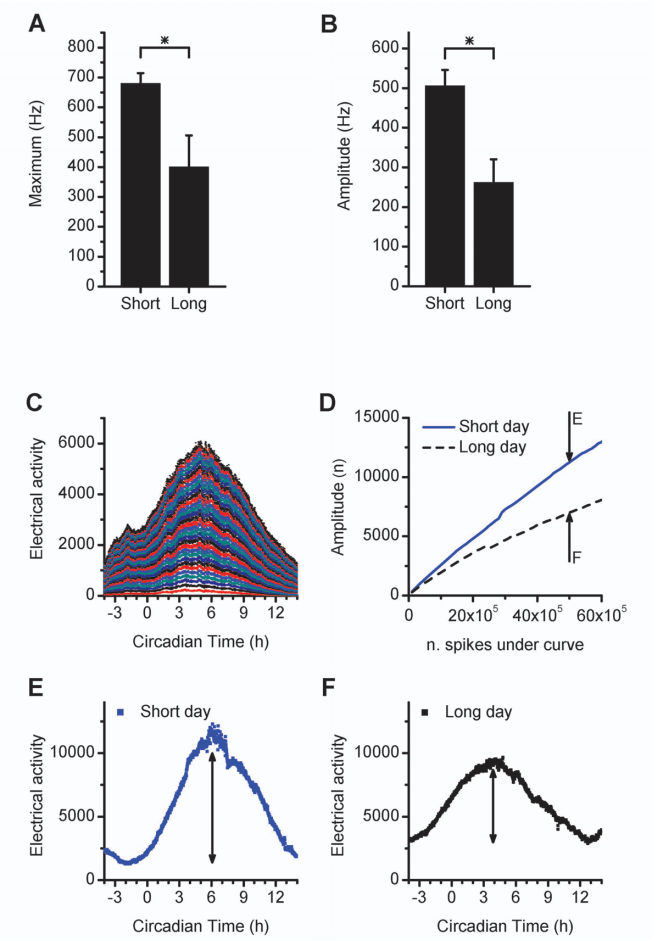

Figure 5.4

Amplitude of the electrical activity peak in short and long days.

(A) Maximal firing frequency in multiunit activity, recorded in slices from animals maintained in short and long days were significantly different ($p < 0.05$).
(B) Amplitudes of the multiunit activity rhythm, defined as the difference between maximal and minimum firing level, were significantly different between the short and long day groups ($p < 0.01$).
(C) An analysis was performed, in which the total number of action potentials contributing to the electrical activity pattern was determined. This allowed for a comparison of rhythm amplitude between the experiments for multiple sizes of subpopulations. Each line represents an increase over the lower line of a total number of 10^5 action potentials included in the recording. Action potentials were counted in 60s bins.
(D) Amplitude of electrical activity rhythms in subpopulations with a selected number of action potentials included in the recording. The amplitude of the electrical activity in the short day group is larger than the amplitude in the long day group for recordings with an equal number of action potentials. For 50×10^5 action potentials (indicated by arrows), examples of subpopulation electrical activity patterns are indicated in E and F. The difference in amplitude between long and short days exists for any number of action potentials contributing to the curve, and thus, for any subpopulation size.
(E, F) Examples of electrical activity patterns obtained in short (E) and long (F) days, with the same total number of action potentials (50×10^5) making up the electrical activity pattern.

While our data suggest that the phase relationship among oscillators determines the response to a shifting pulse, we acknowledge that other mechanisms cannot be ruled out. Our explanation is parsimonious, however, as two major aspects of photoperiodic encoding by the SCN, namely changes in circadian waveform and changes in light resetting properties, can be explained by changes in phase distribution within the SCN.

In summary, our findings indicate that the phase shifting capacity of the SCN expressed in long and short day length is retained in the SCN *in vitro*, offering an attractive model for future investigation. Our data also show that the inverse relation between the phase shifting capacity and the amplitude of the neural activity rhythm may not hold for neuronal networks in which neurons oscillate with different phases. We have shown that such networks respond in fact opposite, and show a maximum phase shifting capacity when the rhythm amplitude is large, and a smaller response when the amplitude is low. The data provide a clear example that neuronal networks are governed by different rules than single cell oscillators. To predict the phase response characteristics of the SCN network, we have taken into account the phase distribution among the single cell oscillators. We realize that a more accurate prediction of the properties of the network can be obtained when the interactions between the single cell oscillators are incorporated (Johnson, 1999; Indic et al., 2007; Beersma et al., 2008). In the past few years a number of synchronizing agents have been proposed such as VIP, GABA, and gap junctions (Colwell et al., 2003; Aton et al., 2005; Welsh, 2007; Albus et al., 2005; Long et al., 2005; Colwell, 2005), and it would be interesting to determine their role in photoperiodically induced changes in the phase resetting properties of the SCN. Our findings may be relevant not only for the photoperiodic modulation of the phase shifting capacity of the circadian system, but may have broader implications and be relevant also to observations of reduced light responsiveness and reduced circadian rhythm amplitude in the elderly.

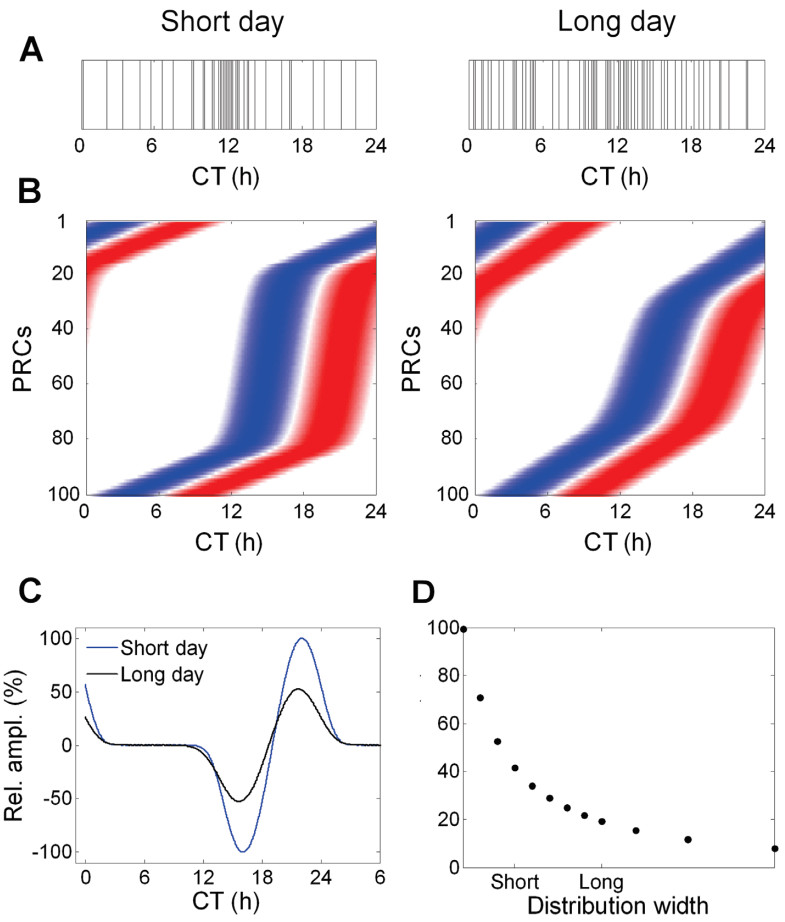

Figure 5.5

Short and long photoperiod PRCs obtained from simulations.

(A) The distributions for short and long day subpopulations were taken from VanderLeest et al., 2007. Each vertical line represents the peak time of a small subpopulation of neurons.
(B) A fitted curve through the long and short day length distribution was used to distribute 100 single unit PRCs. The y-axis represents differently phased single unit PRCs, distributed according to the fitted curve. The blue part of each line represents the delay part of the single unit PRC, the red part represents the advance part of the single unit PRC. The left side shows the distribution for short days and the right side shows the distribution for long days.
(C) The resulting simulated ensemble PRC for short and long days using type 1 single unit PRCs. The long day PRC shows a lower amplitude than the short day PRC.
(D) The area under the curve of the PRC decreases exponentially when the phase distribution of the neurons increases. The area is given relative to the area under the curve when all single unit PRCs coincide, which leads to a maximum amplitude of the PRC of the ensemble, and a maximal working area. On the x-axis, the observed distributions for the short and long day lengths are indicated. The Figure shows the results for type 1 single unit PRCs. The results indicate that the area under the curve for short days is about two times larger than for long days, consistent with experimental results (see also Figure 5.7).

Materials and Methods

Ethics Statement

All experiments were performed in accordance to animal welfare law and with the approval of the Animal Experiments Ethical Committee of the Leiden University Medical Center.

Behavioral Experiments

Mice (C57BL6) were kept under long (16h light, 8h dark) and short (8h light, 16h dark) photoperiods for at least 30 days in clear plastic cages equipped with a running wheel. The animal compartments are light tight and illuminated by a single white fluorescent "true light" bulb with a diffuse glass plate in front. The light intensity at the bottom of the cage was ~180lux. Running wheel activity was recorded with Actimetrics software and the onset of activity was defined as circadian time 12 (CT 12). After at least 30 days in the light regime, the animals were released into constant darkness (DD). On day 4 in DD, the animals received a 30min white light pulse (180lux) at a specific CT. We have previously shown that after 4 days in constant darkness, photoperiodic effects on behavioral activity and on SCN waveform are still fully present (VanderLeest et al., 2007). For each animal in the compartment, the average onset of activity was calculated and the CT of the light pulse was determined. Running wheel activity was recorded for another 14 days after the light pulse. The phase shifts were calculated by comparing activity onset in DD before and after the light pulse. The circadian times at which the light pulses were given were binned in 3h intervals.

In vitro Experiments

Animals were housed under long and short photoperiods, as described before, for at least 30 days. Prior to the *in vitro* experiment, the animals were transferred to a dark compartment for 3 days. Onset of wheel running activity was determined over these 3 days and decapitation and subsequent dissection of the brain was performed at

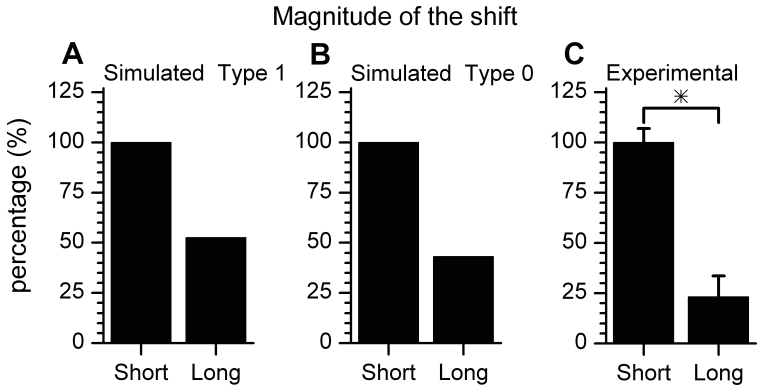

Figure 5.6

Magnitude of the light induced phase shift.

(A) Experimentally obtained subpopulation distributions (VanderLeest et al., 2007) were used to distribute 100 type 1 single unit PRCs. The simulations resulted in high amplitude phase shifts for short days and low amplitude shifts for long days. Short day shifts were normalized to 100% and long day shifts were plotted relative to this value.
(B) The same procedure was followed for type 0 single unit phase response curves. (C) For comparison, the experimentally obtained phase shifts in running wheel activity are depicted with the shift in short days normalized to 100% ($p < 0.001$).

the end of the resting period of the animal (CT 12). Slices of 400µm were prepared with a chopper and were transferred to a laminar flow chamber that was perfused with warmed (35°C) ACSF within 6 min after decapitation (Schaap et al., 2003). The pH was controlled by a bicarbonate buffer in the ACSF and was maintained by gassing the solution and blowing warmed humidified O_2 (95%) and CO_2 (5%) over the slice. The slice was kept submerged and was stabilized with an insulated tungsten fork.

The slices settled in the recording chamber for ~1h before electrode placement. Action potentials were recorded with 90% platinum 10% iridium 75µm electrodes, amplified 10k times and band-pass filtered (300Hz low, 3kHz high). The action potentials crossing a preset threshold well above noise (~5µV) were counted electronically in 10s bins by a computer running custom made software. Time of occurrence and amplitudes of action potentials were digitized by a CED 1401 and stored for off-line analysis. To induce a phase shift, the recording chamber was perfused with ACSF containing 10 or 25µM N-methyl-D-aspartate (NMDA) for 30min. The timing of the NMDA application was in accordance with the light

pulse presentation in the behavioral experiments: The slices were prepared on day 3 in DD and on the fourth night in DD the NMDA pulse was applied at CT 15. The estimation of CT 15 was done one the basis of the activity onsets of the animals in DD, on the days preceding the preparation of the slice.

Data Analysis

Electrophysiological data was analyzed in MATLAB using custom made software as described earlier (VanderLeest et al., 2007). The time of maximum activity was used as marker for the phase of the SCN and was determined on the first peak in multiunit activity, both for control and experimental slices. Multiunit recordings of at least 24h, that expressed a clear peak in multiunit activity, were moderately smoothed using a least squares algorithm (Eilers, 2003) and peak time, half maximum values and amplitude were determined in these smoothed recordings.

For a more detailed analysis of rhythm amplitude, we used the stored times of the occurrence and amplitudes of the action potentials. This analysis allows for an off-line selection of the size of the population of neurons that contributes to the electrical activity rhythm, through a selection of voltage thresholds (see also Schaap et al., 2003 (Schaap et al., 2003) and VanderLeest et al., 2007 (VanderLeest et al., 2007)). In this way, we could describe the circadian activity pattern of larger or smaller subpopulations of SCN neurons. This analysis was performed in slices from long and short day animals, and allowed to compare rhythm amplitudes in both groups with an equal number of action potentials that contributed to the recording over the same time interval (c.f. Figure 5.4). The thresholds were determined so that each trigger level includes 10^5 more spikes than the previous level. For all experiments the deviation from the aimed number of action potentials selected for was <5%.

Statistical analyses were performed in Origin 7 (OriginLab Corporation) and Excel (Microsoft). All values are stated as average ± standard error of the mean (s.e.m.). Whenever the calculated value is

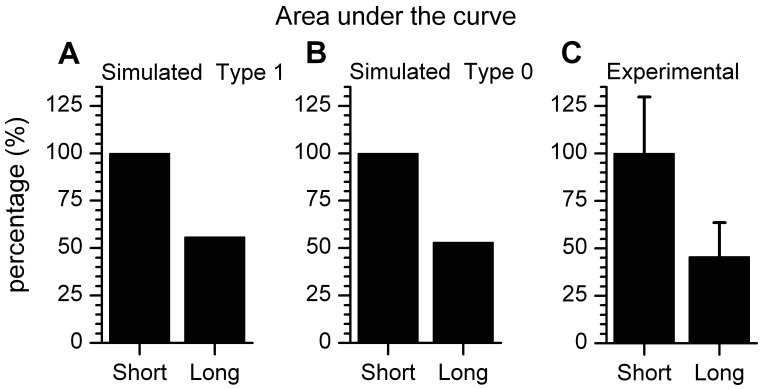

Figure 5.7

Area under the phase response curve.

(A) Quantitative analysis of the PRC based on type 1 single unit PRCs by a measurement of the area under the curve. For short days, the area was normalized to 100% and for long days, the area was plotted as a fraction of this value.
(B) The same procedure was repeated for type 0 single unit PRCs.
(C) The relative area under the curve from experimentally obtained behavioral PRCs. The area under the PRC in long day length is 45% of the normalized area in short day length.

the result of a difference between groups, such as in the calculation of *in vitro* phase shifts, variances were considered unequal, rendering a conservative test. P-values were calculated with a two sided t-test and were considered to be significant when $p < 0.05$.

Supplemental Data - Simulations

Both molecular and electrophysiological studies have provided evidence that photoperiodically induced waveform changes observed at the population level (Mrugala et al., 2000; Sumova et al., 2003) are caused by a reconfiguration of single cell activity patterns (Schaap et al., 2003; Hazlerigg et al., 2005; Inagaki et al., 2007; VanderLeest et al., 2007; Naito et al., 2008). In short day length single units oscillate highly in phase while in long days they are more spread out over the circadian cycle. Because in short days the phase distribution among neurons is narrow, light information will reach SCN neurons at a similar phase of their cycle. When the distribution is broad, however, light information reaches neurons at different phases of their cycle. We performed simulations both with type 1 and with type 0 PRCs in the distributions. When distributing 100 type 1 PRCs, the amplitude

for the long day length PRC is 52.5% of the amplitude for the short day length PRC; for type 0 PRCs, this ratio is 43% (Figure 5.6). The simulations revealed that irrespective of the type of single unit PRC, a broad distribution of cellular oscillations, corresponding to long days, results in a low amplitude PRC of the ensemble, and a narrow distribution, corresponding to short days, results in a high amplitude PRC of the ensemble (Figure 5.5). These results were independent of the number of single unit PRCs that were used in the simulations, although small deviations occurred for low numbers ($n < 40$). The simulated differences in the magnitude of the shifts resembled the experimentally obtained data (Figure 5.6).

We have also measured the area under the delay and advance part of the PRC for long and short day length PRCs for both the simulations and the experimentally obtained data (Figure 5.7). The area under the simulated long day PRC curve is about 50% of the area under the short day PRC. This was true for both types of single unit PRCs that were used to construct the ensemble PRC. For type 1 single unit PRCs, the area under the curve of the simulated long day PRC was 55.9% of the area under the curve of the short day PRC. For type 0 single unit PRCs, the area under the curve of the simulated long day PRC was 53% of the short day PRC. The results from these simulations were independent of the number of single unit PRCs and in accordance with the experimentally obtained data (Figure 5.7).

Simulation Methods

Simulations of a PRC for short day length and long day length were performed in MATLAB by distributing 100 normalized single unit phase response curves over the day. Two types of single unit PRCs were used. The first PRC consisted of a 12h dead-zone (where no phase responses can be induced) and a 12h sinusoidal responsive part, in accordance with the type 1 light pulse PRC (Johnson, 1999). The other single unit PRC was in accordance with a type 0 light pulse PRC, consisting of a 12h dead-zone followed by an exponential function with an asymptote at CT18, and a maximum shift of 12 h

(Johnson, 1999). The distributions that were used for long and short day lengths were taken directly from experimentally described subpopulation distributions in long and short photoperiods (VanderLeest et al., 2007). The peak times of these subpopulations were used to fit a distribution curve. This curve was used to distribute 100 single unit PRCs over the circadian day. In addition, simulations were performed using single unit PRCs without a dead-zone (c.f. Ukai et al., 2007 (Ukai et al., 2007), data not shown).

We have measured the area under the curve, which is the surface of the delay and advance part of the PRC. The surface is an indication for the phase shifting capacity of the circadian system. The equation for this calculation is the first integral of a curve over a certain interval: $\int_a^b f(x)dx$ or $\sum |y| \times \Delta x$ for discrete functions, where the absolute value of y is multiplied by the width on the x-axis.

CHAPTER 6

Discussion & Perspectives

Cellular Communication

The functioning of the SCN as pacemaker relies on the communication between cells. In this thesis it was shown that cellular communication is of great importance for photoperiodic encoding. The SCN cellular network is composed of different cell types with different inputs and outputs. Besides the anatomical and biochemical heterogeneity of SCN cells which was well known, the studies in this thesis have revealed the presence of phase differences between SCN neurons, which give rise to variation in the waveform of the measured population electrical activity peak (Schaap et al., 2001). The plasticity in the phase distribution appears to be of great importance for photoperiodic encoding mechanisms as well as for the phase resetting capacity of the SCN.

In the SCN different regions can be recognized based on neurotransmitter content and afferent and efferent connections. The anatomical distinction based on cell types is however not uniform among all species. In rats there is a clearly defined dorsal region that

contains AVP neurons. This region is commonly referred to as shell. A ventral region that contains VIP is referred to as core. In mice these regions are not that clearly defined with respect to neurotransmitter content and therefore mostly referred to as dorsal and ventral (Moore and Lenn, 1972; Card and Moore, 1984; Abrahamson and Moore, 2001). The differences in anatomical properties of dorsal and ventral SCN cells may reflect a functional difference. Cells in the SCN core may not be intrinsically rhythmic, but may show light driven rhythmicity or are easily reset by light input. The core cells that show light driven rhythmicity are able to reset the phase of pacemaker cells in the shell region that receive no direct light input. Cells in the SCN shell that are intrinsically rhythmic receive no direct light input but are reset by output of the core and communicate phase information to other brain areas (Silver and Schwartz, 2005). Although the functions of the VIP and AVP cells in the different regions are clearly distinct in terms of electrophysiological and biochemical properties, the cytochemical characterization may not fully correspond with the anatomical location of these cells in mice.

Time of preparation does not influence MUA *in vitro*

In chapter 2 of this thesis we presented data to validate the *in vitro* brain slice preparation as a tool for investigating the electrophysiological rhythm of the SCN *ex vivo* (VanderLeest et al., 2009b). To investigate the electrophysiological properties of the SCN, the *in vitro* technique offers a valuable approach. It enables to record direct after effects of a light dark cycle, such as phase shifts, and in the absence of any influence of behavioral activity or activation of brain areas that interfere with the endogenous activity of the SCN. In the *in vitro* situation, it is possible to study both after effects of circadian manipulations, and isolate the SCN from the surrounding tissues and eliminate behavioral artifacts. To study the parameters of single units, it would be best to isolate one unit, by means of either isolating it from the surrounding cells, or by recording the electrophysiological properties with a small electrode. These

recordings would however introduce complications since the stability of the recording does not allow one to follow the electrical activity of a single cell for a long period of time. In our *in vitro* brain slice preparation, we use extracellular electrodes to record the electrical activity of many cells in the surrounding of the electrode tip. These multiunit electrodes enable long-term stable recordings of SCN electrical activity. It is possible to extract the electrical activity of small populations of cells and even from single units from the recorded multiunit data.

We have examined whether the Zeitgeber time of preparation may affect the properties of the electrical activity rhythms of a large population of SCN cells. We have confirmed in this chapter that the time of preparation does not influence the phase or the shape of the recorded electrical activity rhythms. At all preparation times the peak in multiunit activity occurred around midday (ZT 6). Furthermore, the shape of the multiunit electrical activity peak was similar for all preparation times, described by the width of the peak and the time of the half-maximum values. We conclude nevertheless that within one series of experiments, one preferably should restrict the times of preparation to the same time point for all experiments as otherwise it may introduce a greater variability in the recorded parameters. The *in vitro* brain slice preparation offers a robust and valuable technique for determining phase and waveform of a population of SCN cells.

Phase heterogeneity of SCN neurons

In the third chapter of this thesis we have shown that single cells and small populations of about three SCN neurons, have only a short duration of elevated electrical activity (Schaap et al., 2003). The electrical activity peaks of these subpopulations and single units are spread out over the circadian cycle and their distribution determines the population waveform. We did not observe a relation between the time of maximum firing and the anatomical location in the SCN. We introduced the term subpopulation to describe the recordings of small

populations of neurons. The isolation of the activity of subpopulations relies on an offline selection of the voltage threshold for counting action potentials. The action potentials that are produced by neurons in close proximity of the electrode tip are larger in amplitude than action potentials produced by neurons located further from the electrode. This way, a small region around the electrode tip can be recorded from, which corresponds to a subpopulation. The activity of single units was also isolated from the multiunit recordings by a principal component analysis of action potential shape. The resulting clusters were separated using a Gaussian model. An autocorelogram of the event times was used to validate the separated clusters as the activity of a single unit.

We performed a Monte Carlo simulation to determine the phase distribution over the 24h cycle of recorded single unit activity. These simulations were performed with several population sizes, ranging from a subpopulation size of about three neurons, up to a thousand. The simulations resulted in a Gaussian distribution of the phases of the single units with a peak around midday. With smaller population sizes, the standard error in the distribution of peak times became larger, indicating that a certain randomness is dampened in large populations. With small population sizes the randomness in the distribution in the simulation introduced a larger peak width than we recorded. From these results we concluded that the recorded subpopulations consisting of about 3 neurons were tightly coupled together to produce a coherent subpopulation peak. These neurons show a highly synchronized rhythm in their firing activity and are thus strongly coupled in phase.

Recordings from larger subpopulations comprise differently phased subpopulations that are synchronized to some extend. The simulated distribution of the single unit activity over time introduces variability in peak time that is attributable some randomness in the distribution. For the recorded subpopulation activity this is not the case. If the timing would be random, the standard error in the peak width would decrease with a larger population size. However, in our

recordings the standard error in peak width was constant between different recorded population sizes, indicative of regional synchronization and that the timing of the activity of subpopulations in the SCN is not attributable to randomness.

The short duration of electrical activity of single units prompted us to investigate a possible role of phase differences among SCN neurons in photoperiodic encoding in the SCN. We performed additional multiunit electrical activity recordings from rats in short and long photoperiods. In these recordings, we determined the phase, amplitude and width of the activity peak. We furthermore simulated multiunit electrical activity profiles in different day lengths. We used an average single unit electrical activity profile and distributed it linearly over the light period for short days (8h light), normal days (12h light) and long days (16h light). The results from these simulations were compared with the obtained multiunit recordings and showed that the phase distribution among single units can underlie photoperiodic encoding by the SCN.

Photoperiodic Encoding

The results presented in chapter 3 of this thesis, prompted us to test the predictions on photoperiodic adaptation of the SCN in mice (VanderLeest et al., 2007). Behavioral recordings showed that these mice entrained to long and short photoperiods despite the lack of functional melatonin signaling. This indicated that photoperiodic adaptation is present in the SCN. *In vivo* multiunit recordings in freely moving mice revealed that the electrical activity pattern in the SCN was broad in long photoperiods and narrow in short photoperiods. The peak in multiunit discharge occurred 4-5 h before lights off in both photoperiods. This indicates that in long photoperiods the rising phase of the electrical activity is shifted towards earlier times while the declining phase remains locked to lights off, which is consistent with other studies (Mrugala et al., 2000; Sumova et al., 2003; de la Iglesia et al., 2004). The shape and timing

of the electrical activity profiles did not change in constant darkness. This shows that the photoperiod information is stored in the SCN.

The aftereffects of long and short photoperiods remain visible in the *in vitro* preparation as a broader or narrower multiunit electrical activity peak. Using the methods outlined in chapter 3, we confirmed that in mice subpopulations of SCN neurons also have a narrow peak in electrical activity. The peak widths of subpopulations were not different between day lengths. However, larger population sizes showed a significant difference in peak width. With larger population sizes the peak width increases, reaching 75% of the multiunit peak width with only 50 neurons in both long and short day length. The distribution of the subpopulations over time is also significantly different in long and short day length. This shows that photoperiodic encoding in the SCN takes place through a redistribution of the timing of small populations of neurons.

The activity of single units was also determined in both day lengths. The single unit activity profiles were similar between short and long day length. To determine the precise phase distribution of single units we however need to obtain more single unit recordings. Our results show that the electrical activity pattern of a single unit is not altered by day length. Instead photoperiodic encoding takes place at the network level and requires differently phased oscillating units.

Our data have been confirmed by a number of studies. We have shown that the increased synchronization in the SCN is a key element for the SCN to code for short day length, although other mechanisms may also contribute. The short duration of electrical activity and the variability in phases between different populations and single units of SCN neurons have been confirmed in several studies (Brown et al., 2005; Brown et al., 2006). Regional differences in timing and duration of single unit electrical activity has also been observed under different photoperiods, indicating that different regions in the SCN may be synchronized differentially to dawn and dusk (Brown and Piggins, 2009).

Phase differences were furthermore detected using molecular techniques (Yamaguchi et al., 2003; Quintero et al., 2003). Regional differences in phase were found in bioluminescence recordings of Per1 gene expression in different photoperiods. In the anterior SCN temporal reorganization was observed related to the prior photoperiod (Naito et al., 2008). Other studies also show that phase differences between neurons and regions are a key element of encoding day length in the SCN. (Johnston et al., 2005; Inagaki et al., 2007).

Simulations have also contributed to our understanding of photoperiodic encoding and have shown that changes in phase relation between neurons is essential for the SCN to code for day length (Rohling et al., 2006b; Beersma et al., 2008). The simulation studies revealed that, counter intuitively, a narrowing or broadening in the activity pattern of single units does not effectively contribute to the waveform of the population pattern (Rohling et al., 2006a).

Molecular versus Electrical oscillations in the SCN

It should be noticed that molecular expression profiles differ from electrical activity profiles. Neurons communicate with one another by means of electrical activity and therefore the electrical activity profile is transmitted from one part of the SCN to another. Molecular rhythms on the other hand, remain restricted to the individual cell and cannot be transmitted between cells by itself. Differences between electrical and molecular distribution pattern became evident for instance following a phase shift of the light-dark cycle. Expression profiles of Per bioluminescence after a phase shift of the light-dark cycle, showed that the ventral SCN shifts rapidly, and the dorsal part shifts slowly. Electrical activity however, showed both a slow and a fast shifting component in both areas. The data indicate that the electrical information has been transmitted between the dorsal and ventral aspect, and explain the presence of a bimodal electrical activity peak can be observed in the dorsal and in the ventral SCN (Albus et al., 2005). When dorsal and ventral SCN are separated by a knife cut, the electrical activity pattern is similar to the molecular

expression profile. A shifted component is visible in the ventral part and a non-shifted, or slowly shifting component is visible in the more dorsal part of the SCN (see Albus et al., (2005) for a discussion of molecular versus electrical findings).

Another example that shows dissimilar results between regional patterns in molecular and electrical activity is found in the occurrence of splitting. During splitting, molecular expression profiles of the left and right SCN show oscillations that are in anti-phase (de la Iglesia et al., 2000). However, electrical activity recordings in the SCN from animals with split rhythms show 12h oscillations both in the left and in the right SCN (Zlomanczuk et al., 1991), showing that electrical activity is transmitted between the nuclei.

Furthermore, following long photoperiods, electrical activity patterns of SCN neurons show a broad distribution in phase (Schaap et al., 2003; VanderLeest et al., 2007; Brown and Piggins, 2009). The broad phase distribution is present throughout the SCN. However, molecular expression data show regional differences to a larger extend than in electrical activity (Brown and Piggins, 2009). These findings are again in line with the finding that electrical activity is integrated within the SCN.

While the differences in localization between molecular and electrical studies are evident, and understandable, the common aspects of the molecular and electrophysiological findings together, support the idea that photoperiodic encoding is a consequence of the structural heterogeneity within the SCN (Schaap et al., 2003; Hazlerigg et al., 2005; Inagaki et al., 2007; VanderLeest et al., 2007; Vansteensel et al., 2008; Naito et al., 2008; Brown and Piggins, 2009).

Phase shifting responses in long and short photoperiod

In chapter 5 we investigated phase shifting responses in different day lengths (VanderLeest et al., 2009a). It was known that in short day length the phase shifting response in hamsters and mice is larger than in long photoperiods (Refinetti, 2002; Pittendrigh et al., 1984). We investigated the phase shifting response in behavior and

constructed a PRC for light in different day lengths. Our results were similar to earlier observations, with large amplitude phase responses in short day length and small amplitude in long days. These results are somewhat counterintuitive since the area where phase responses can be elicited is in the subjective dark and it can be expected that because of the longer duration of darkness in short days, the phase response curve is stretched while the area under the curve remains the same. This however is not the case since the amplitude of the PRC in short days is actually larger.

An explanation of these observations could be that because of a higher exposure to light in long days, the phase shifting response to light is decreased because of desensitization (Refinetti, 2001; Refinetti, 2002). Therefore we exposed the animals in short day length to the same amount of photons per day as the animals receive in long day length. The animals from short days received a light pulse aimed at the time of maximal phase response, CT 15. The response in short days remained unaltered from the previous lower light intensity light-dark cycle and significantly different from the response in long day length. Animals from long day lengths also received another set of light pulses aimed at the time of maximal delay, CT 15 in this case the light intensity of the pulse was increased, while the intensity of the light-dark cycle remained the same. These results were also not different from the data we obtained with normal light intensity light pulses and remained small and significantly different from both results in short day length. It can be concluded from these experiments that it is unlikely that sensitization and desensitization of the photic input pathways is the mechanism responsible for the difference in phase shifting capacity.

We performed *in vitro* recordings of electrical activity and applied NMDA at the time of maximum delay in both short and long day length. Light information is communicated to the SCN through the RHT of which the most important neurotransmitter is glutamate, which acts on NMDA receptors. The phase shifts induced by NMDA were large in slices from short days and small in slices from long days.

The phase shifts were significantly different between day lengths and the phase shifts were not different between results from behavior and *in vitro*. This shows that the large amplitude phase responses are intrinsic to the SCN and are not caused by desensitization of the circadian visual system in long days.

Limit cycle oscillators

The large phase shifts we observed in slices from short day length were surprising since the amplitude of the SCN rhythm in short days is large. This stands in contrast with the theory of limit cycle oscillators, which can be used to describe characteristics of circadian rhythms. In limit cycle theory, the magnitude of a shift is inversely related to the amplitude of the rhythm. The circadian cycle can be represented as a circle: a high amplitude rhythm has, in this example, a large radius, and a low amplitude rhythm has a small radius. A shifting stimulus of similar strength will change the phase of an oscillator with low amplitude more than one with higher amplitude, because the stimulus represents a larger fraction of the radius of the circle. Our results show the opposite, as high amplitude rhythms from short day length shift to a larger extend to a similar stimulus than low amplitude rhythms from long day length.

An explanation for these paradoxical results can be found at the network level. In short days neurons are highly synchronized in phase, therefore a resetting stimulus will reach SCN neurons at a similar phase of their cycle. In long days, neurons in the SCN have a wider phase distribution and therefore there are more neurons out of phase than in short days. If all neurons would be perfectly aligned in phase, the neurons would have a more consistent phase shift, giving rise to a large phase shift at the network level. In long days the resetting stimulus reaches neurons in more diverse phases of their cycle, leading to more divergent responses, delaying some cells while advancing others, resulting in a smaller overall shift at the network level. This hypothesis is consistent with findings that application of NMDA shifts the electrical activity of SCN neurons differentially

(Brown et al., 2006). We performed a simulation study to test this hypothesis, by distributing putative single unit phase response curves over the 24h cycle, with a distribution that was based on the timing of recorded neuronal subpopulations in the SCN under different photoperiods (VanderLeest et al., 2007). The recorded behavioral PRCs showed asymmetric photoperiodic responses: in both day lengths the delay portion of the PRC showed a significant difference, while the advance part of the behavioral PRC remained at similar amplitude. This asymmetry was not present in the simulated PRCs, where we used a simple approach to calculate a combined response and focused on the amplitude difference. However, the results from these simulations do show that, irrespective of the shape of the single unit response curve, the phase shifting response at the network level indeed shows an increase in amplitude in short photoperiods and a decrease in amplitude in long days, consistent with our hypothesis.

Perspectives

Mechanisms for Synchronization

Photoperiodic information is stored in the SCN by an alteration of the synchrony in the timing of (subpopulations of) neurons (Schaap et al., 2003; VanderLeest et al., 2007; Rohling et al., 2006a; Brown and Piggins, 2009). Although it is now clear that heterogeneity in phases exists within the SCN, the mechanism by which the multitude of cellular clock phases are synchronized to produce rhythms that are well adapted to the environmental light-dark cycles are yet unknown. Several neurotransmitters that are involved in synchronization are known and may play a role in the capability of the SCN to code for day length.

VIP

Vasoactive intestinal polypeptide (VIP) is thought to synchronize neighboring cells, acting upon the $VPAC_2$ receptor (Aton et al., 2005; Vosko et al., 2007; Brown et al., 2007). Cellular electrical activity rhythms are dampened when VIP signaling is absent but compensatory mechanisms (signaling through Gastrin Releasing peptide) may reduce the severity of the absence of this key signaling pathway. To investigate the possible mechanisms that enable the SCN to adapt to different photoperiods, it would be interesting to block synchronizing pathways such as VIP signaling in slices from different day lengths. In short days it can be hypothesized that absence of $VPAC_2$ receptor signaling will result in a loss of synchrony between SCN neurons. This will result in a wider MUA peak over time, while different neurons have a slightly different τ, phase differences will accumulate over time and cells become less synchronized after application of the $VPAC_2$ receptor blocker.

We performed pilot experiments in VIP/PHI deficient mice, where there is no functional VIP signaling, but $VPAC_2$ receptors are present and remaining $VPAC_2$ signaling can rescue some of the

cellular rhythms, enabling some of the animals to remain rhythmic in their behavior (Brown et al., 2007). During entrainment to a short day light-dark cycle the wheel running rhythms of VIP deficient mice showed adaptation to the day length. These wheel running rhythms could however be masked by the light-dark cycle. We therefore exposed the animals to constant darkness to detect the endogenous circadian behavior, but behavioral rhythms were hard to interpret because of an extremely positive phase angle and seemingly arrhythmic behavior. It was shown that slices from behaviorally arrhythmic animals also are arrhythmic in electrical multiunit activity *in vitro* (Brown et al., 2007). In our experiments, electrical activity in slices from VIP/PHI $^{-/-}$ was severely distorted and multiunit recordings yielded only a single MUA peak, out of six slices, which was of very low amplitude. Based on these pilot experiments we are unable to determine the involvement of VIP signaling in day length encoding by the SCN. In an LD cycle, animals may seem rhythmic due to masking effects of the LD cycle, but entrainment is hard to asses. Furthermore, because of a high number of arrhythmic slices, the effect of VIP on the MUA peak cannot be determined by these methods. As an alternative strategy, we propose would perform *in vitro* experiments in slices from WT mice, entrained to a short day length and apply a blocker of the $VPAC_2$ receptor to inhibit VIP signaling.

GABA

Another known synchronizing agent in the SCN is γ- aminobutyric acid (GABA) of which it is shown that it synchronizes the electrical activity between regions (Albus et al., 2005; Liu and Reppert, 2000; Belenky et al., 2008; Choi et al., 2008). In long days, the *in vitro* multiunit electrical activity patterns are broad, because of a broad phase distribution of single units. If GABA is synchronizing SCN neurons, application of a GABA agonist, which increases GABA signaling, will increase the level of synchronization when applied chronically. In behavioral experiments, the GABA agonist midazolam

was shown to acutely increase alpha, consistent with a short day activity profile (Vansteensel et al., 2003a). If GABAergic signaling on the other hand is blocked, a loss of synchrony will occur, leading to an increase in phase dispersion in the timing of neurons, which would lead to an increase in peak width. We entrained mice to a long and short day photoperiod and prepared hypothalamic slices containing the SCN and recorded electrical activity *in vitro*. We chronically applied 20 μM bicuculline in slices from short days and 100 nM midazolam in slices from long days to assess the effects of GABA signaling in the SCN on synchronization between neurons.

Our preliminary results show that chronic application of midazolam did not affect the peak width in slices from long days, indicating that chronic GABA activation does not induce an increased synchronization among the SCN neurons. In slices from short day in which we chronically blocked GABAergic signaling by application of bicuculline, we did not observe an increment in the duration of elevated electrical activity. We furthermore performed experiments in which we increased the concentration of potassium ions in the ACSF, which increases neuronal spiking activity and increases GABA signaling. No differences were found in the width of the multiunit peak. If GABA is essential for day length encoding, we would expect that at least in the slices from long day length a decrease in MUA peak width would be observed when a GABA agonist was applied. However, in all these experiments, we did not observe any changes in MUA activity relative to the control situation. This suggests that GABAergic activity is not involved in the temporal synchronization between neurons needed for photoperiodic encoding, although more experiments are needed to strengthen this conclusion. These results are in agreement with the finding that GABA signaling increases electrical rhythm amplitude and single cell rhythm precision, but does not synchronize between neurons (Aton et al., 2006). However it should be noted that those results were obtained in dispersed cell cultures rather than acute SCN slices. Furthermore, regional synchronization, perhaps by GABA, may play a role in photoperiodic

encoding in a manner we are not able to elucidate by means of stationary extracellular electrodes. The observed change in alpha after application of midazolam (Vansteensel et al., 2003a), mimicking the short day activity profile, may have been induced by GABAergic connections downstream of the SCN (Kalsbeek et al., 2008).

Taken together, our preliminary results do not yet indicate what mechanism in the SCN is responsible for tighter or loser synchronization, by which the SCN is able to code for day length. It is possible that a loss of synchronizing signaling does not lead to an increase in peak width, measurable in about 48h *in vitro*, since the starting point is a tightly synchronized system, and a lack of a synchronizing signal does not necessarily lead to an acutely desynchronized situation, but may take several cycles to become visible

Role of synchronization in the aging SCN

The role of the SCN and circadian rhythmicity in aging is a topic of great interest. With increasing age after reaching adulthood, in many mammals including humans, aging brings about deficits in the behavioral activity rhythm and sleep-wake cycle. An internally and externally well adapted circadian timing system is of importance for well-being. With increasing age, some of the circadian rhythms become less adapted (Van Someren and Riemersma-van der Lek RF, 2007). Common aspects of aging in mammals include a decrease in circadian rhythm amplitude, measurable in body temperature and hormonal levels. Furthermore a decrease in synchrony between hormonal rhythms can be observed, altered phase relationships of rhythms and diminished capacity to respond to timing signals (Duncan, 2006), as it is for instance harder to re-adjust to a jet lag or shift work (Härmä et al., 1994). Some aspects of aging resemble data obtained in long photoperiod where a diminished response to a phase shifting stimulus, and a decrease in rhythm amplitude is also observed (VanderLeest et al., 2009a). In the SCN of mice kept on a

long day length we have shown that these phenomena are attributable to a decreased synchrony in the timing of neurons in the SCN.

A possible explanation for the observed changes in circadian timing at high age is that neurons in the SCN are less synchronized, which may explain the deterioration of circadian rhythmicity at different levels. If at high age neurons in the SCN become less synchronized, it can be hypothesized that there will be a decrease in the rhythm amplitude, as is observed in the SCN of mice entrained to long day length. Downstream physiological processes may become desynchronized from each other because the output of the master pacemaker in the SCN fails to exhibit a large enough amplitude in its rhythmic output for these processes to lock on to (Bao et al., 2008). Some evidence exists that supports the hypothesis of decreased synchronization. In a post mortem study in humans, lower expression levels of VIP and AVP were observed in the SCN of elderly people (Bao et al., 2008; Lucassen et al., 1997). As AVP is most predominant in the dorsal part of the SCN, AVP cells may well be connected to other brain structures as output relays. Both the rhythm in behavioral activity and the expression levels of AVP and can be greatly increased by application of high light intensity during the day (Lucassen et al., 1995; Van Someren et al., 2002). Furthermore, the direct effects of light on the neurons in the SCN may already generate a higher amplitude rhythm which other processes can lock on to (Bao et al., 2008).

Other research focused on GABAergic synapses in the SCN and aging. It was found that at higher age, the number of GABAergic synapses has decreased (Nygård and Palomba, 2006). GABA is involved in synchronizing dorsal and ventral SCN after a shift of the light dark cycle (Albus et al., 2005) and may play a critical role in synchronizing between regions in the SCN. If synchronization between light input and circadian output is dysfunctional, expression of rhythms that are well adapted to the environment are lost. Furthermore, if the SCN is internally not well synchronized, different

output parameters may develop changed phase relationships. The results from this study may also provide evidence for a lack of synchronization between neurons in the SCN.

SCN network rescues molecular clock deficits

The molecular clock mechanism relies on the feedback of clock gene products that inhibit their own transcription. This molecular clockwork is present and oscillates intrinsically in many *in vitro* preparations such as in fibroblasts, liver and lung explants(Yamazaki et al., 2000; Yoo et al., 2004). Molecular deficits in a single clock gene are often not reflected in the behavior of the animal or SCN oscillations. Recent findings show that molecular deficits in the SCN are rescued by the network of neurons. In several different *in vitro* preparations, clock gene expression profiles were followed many days using an mPer2luc bioluminescence marker (Liu et al., 2007). All tissues showed robust circadian rhythmicity that was sustained over several 24h cycles. While several single clock gene knockouts did not introduce any deficits in the rhythmicity in behavior or in the SCN, fibroblasts and explants from lung and liver were more severely affected by these knockouts. Rhythms in peripheral tissues quickly dampened either by a de-synchronization of cellular rhythms or a reduction in rhythmic gene expression or both (Liu et al., 2007). These results pointed towards a mechanism specific to the SCN for rescuing these molecular deficits that were visible in the other preparations but not the SCN. However, when clock gene knockout SCN cells were dissociated and cell signaling was severed, circadian oscillations quickly dampened and resembled the other tissue preparations. This suggests that in the SCN it is not the molecular clock that is more robust than in other tissues, but instead that the network of cells, where electrical activity feeds back on neighboring neurons, rescues deficits in the molecular rhythm. The neuronal structure of the SCN is therefore of great importance, as the network of neurons enforces its intrinsic rhythmicity(Liu et al., 2007; Westermark et al., 2009).

Although many properties of circadian rhythms exist at the cellular level in many tissues and can be explained at the molecular level, circadian rhythms need an intact network in which interactions between neurons give rise to a more robust system. This shows that the SCN neuronal network renders an additional level of organization. The results presented in this thesis underscore the importance of synchronization of neuronal rhythms in the SCN. Intracellular signaling, which is needed for synchronization of clock neurons, is of key importance, for the adaptation to different day lengths and therefore for the adaptation to seasonal changes in the environment. The synchronization of clock neurons is furthermore of importance in setting the capacity of the clock to shift in phase. The neuronal network organization of the SCN is thus of critical importance for the adaptive functioning of the circadian system.

REFERENCES

Abe,M., Herzog,E.D., Yamazaki,S., Straume,M., Tei,H., Sakaki,Y., Menaker,M., and Block,G.D. (2002). Circadian rhythms in isolated brain regions. J. Neurosci. *22*, 350-356.

Abraham,U., Prior,J.L., Granados-Fuentes,D., Piwnica-Worms,D.R., and Herzog,E.D. (2005). Independent circadian oscillations of Period1 in specific brain areas in vivo and in vitro. J. Neurosci. *25*, 8620-8626.

Abrahamson,E.E. and Moore,R.Y. (2001). Suprachiasmatic nucleus in the mouse: retinal innervation, intrinsic organization and efferent projections. Brain Res. *916*, 172-191.

Abrahamson,E.E. and Moore,R.Y. (2006). Lesions of suprachiasmatic nucleus efferents selectively affect rest-activity rhythm. Mol. Cell Endocrinol. *252*, 46-56.

Aida,R., Moriya,T., Araki,M., Akiyama,M., Wada,K., Wada,E., and Shibata,S. (2002). Gastrin-releasing peptide mediates photic entrainable signals to dorsal subsets of suprachiasmatic nucleus via induction of Period gene in mice. Mol. Pharmacol. *61*, 26-34.

Akiyama,M., Kouzu,Y., Takahashi,S., Wakamatsu,H., Moriya,T., Maetani,M., Watanabe,S., Tei,H., Sakaki,Y., and Shibata,S. (1999). Inhibition of light- or glutamate-induced mPer1 expression represses the phase shifts into the mouse

circadian locomotor and suprachiasmatic firing rhythms. J. Neurosci. *19*, 1115-1121.

Albrecht,U., Sun,Z.S., Eichele,G., and Lee,C.C. (1997). A differential response of two putative mammalian circadian regulators, mper1 and mper2, to light. Cell *91*, 1055-1064.

Albus,H., Bonnefont,X., Chaves,I., Yasui,A., Doczy,J., van der Horst,G.T., and Meijer,J.H. (2002). Cryptochrome-deficient mice lack circadian electrical activity in the suprachiasmatic nuclei. Curr. Biol. *12*, 1130-1133.

Albus,H., Vansteensel,M.J., Michel,S., Block,G.D., and Meijer,J.H. (2005). A GABAergic mechanism is necessary for coupling dissociable ventral and dorsal regional oscillators within the circadian clock. Curr. Biol. *15*, 886-893.

Allada,R., Emery,P., Takahashi,J.S., and Rosbash,M. (2001). Stopping time: the genetics of fly and mouse circadian clocks. Annu. Rev. Neurosci. *24*, 1091-1119.

Asai,M., Yamaguchi,S., Isejima,H., Jonouchi,M., Moriya,T., Shibata,S., Kobayashi,M., and Okamura,H. (2001). Visualization of mPer1 transcription in vitro: NMDA induces a rapid phase shift of mPer1 gene in cultured SCN. Curr. Biol. *11*, 1524-1527.

Aschoff,J. and Pohl,H. (1978). Phase relations between a circadian rhythm and its zeitgeber within the range of entrainment. Naturwissenschaften *65*, 80-84.

Aton,S.J., Colwell,C.S., Harmar,A.J., Waschek,J., and Herzog,E.D. (2005). Vasoactive intestinal polypeptide mediates circadian rhythmicity and synchrony in mammalian clock neurons. Nat. Neurosci. *8*, 476-483.

Aton,S.J., Huettner,J.E., Straume,M., and Herzog,E.D. (2006). GABA and Gi/o differentially control circadian rhythms and synchrony in clock neurons. Proc. Natl. Acad. Sci. U. S. A *103*, 19188-19193.

Bao,A.M., Meynen,G., and Swaab,D.F. (2008). The stress system in depression and neurodegeneration: focus on the human hypothalamus. Brain Res. Rev. *57*, 531-553.

Barnard,A.R., Hattar,S., Hankins,M.W., and Lucas,R.J. (2006). Melanopsin regulates visual processing in the mouse retina. Curr Biol *16*, 389-395.

Bayliss,D.A. and Barrett,P.Q. (2008). Emerging roles for two-pore-domain potassium channels and their potential therapeutic impact. Trends Pharmacol. Sci. *29*, 566-575.

Beersma,D.G., van Bunnik,B.A., Hut,R.A., and Daan,S. (2008). Emergence of circadian and photoperiodic system level properties from interactions among pacemaker cells. J. Biol. Rhythms *23*, 362-373.

Belenky,M.A., Yarom,Y., and Pickard,G.E. (2008). Heterogeneous expression of gamma-aminobutyric acid and gamma-aminobutyric acid-associated receptors and transporters in the rat suprachiasmatic nucleus. J. Comp Neurol. *506*, 708-732.

Belle,M.D., Diekman,C.O., Forger,D.B., and Piggins,H.D. (2009). Daily electrical silencing in the mammalian circadian clock. Science *326*, 281-284.

Bendova,Z. and Sumova,S. (2006). Photoperiodic regulation of PER1 and PER2 protein expression in rat peripheral tissues. Physiol. Res. *55*, 623-632.

Bergeron,H.E., Danielson,B., Biggs,K.R., and Prosser,R.A. (1999). TTX blocks baclofen-induced phase shifts of the mammalian circadian pacemaker in vitro. Brain Res. *841*, 193-196.

Berson,D.M., Dunn,F.A., and Takao,M. (2002). Phototransduction by retinal ganglion cells that set the circadian clock. Science *295*, 1070-1073.

Best,J.D., Maywood,E.S., Smith,K.L., and Hastings,M.H. (1999). Rapid resetting of the mammalian circadian clock. J. Neurosci. *19*, 828-835.

Biello,S.M., Golombek,D.A., and Harrington,M.E. (1997). Neuropeptide Y and glutamate block each other's phase shifts in the suprachiasmatic nucleus in vitro. Neuroscience *77*, 1049-1057.

Bouskila,Y. and Dudek,F.E. (1993). Neuronal synchronization without calcium-dependent synaptic transmission in the hypothalamus. Proc. Natl. Acad. Sci. U. S. A. *90*, 3207-3210.

Brown,T.M., Banks,J.R., and Piggins,H.D. (2006). A novel suction electrode recording technique for monitoring circadian rhythms in single and multiunit discharge from brain slices. J. Neurosci. *156*, 173-181.

Brown,T.M., Colwell,C.S., Waschek,J.A., and Piggins,H.D. (2007). Disrupted neuronal activity rhythms in the suprachiasmatic nuclei of vasoactive intestinal polypeptide-deficient mice. J. Neurophysiol. *97*, 2553-2558.

Brown,T.M., Hughes,A.T., and Piggins,H.D. (2005). Gastrin-releasing peptide promotes suprachiasmatic nuclei cellular rhythmicity in the absence of

vasoactive intestinal polypeptide-VPAC2 receptor signaling. J. Neurosci. *25*, 11155-11164.

Brown,T.M. and Piggins,H.D. (2007). Electrophysiology of the suprachiasmatic circadian clock. Prog. Neurobiol. *82*, 229-255.

Brown,T.M. and Piggins,H.D. (2009). Spatiotemporal Heterogeneity in the Electrical Activity of Suprachiasmatic Nuclei Neurons and their Response to Photoperiod. J. Biol. Rhythms *24*, 44-54.

Bunger,M.K., Wilsbacher,L.D., Moran,S.M., Clendenin,C., Radcliffe,L.A., Hogenesch,J.B., Simon,M.C., Takahashi,J.S., and Bradfield,C.A. (2000). *Mop3* is an essential component of the master circadian pacemaker in mammals. Cell *103*, 1009-1017.

Burgoon,P.W., Lindberg,P.T., and Gillette,M.U. (2004). Different patterns of circadian oscillation in the suprachiasmatic nucleus of hamster, mouse, and rat. J. Comp. Physiol. A Neuroethol Sens Neural Behav. Physiol *190*, 167-171.

Cao,G. and Nitabach,M.N. (2008). Circadian control of membrane excitability in Drosophila melanogaster lateral ventral clock neurons. J. Neurosci. *28*, 6493-6501.

Card,J.P. and Moore,R.Y. (1984). The suprachiasmatic nucleus of the golden hamster: immunohistochemical analysis of cell and fiber distribution. Neuroscience *13*, 415-431.

Carr,A.J., Johnston,J.D., Semikhodskii,A.G., Nolan,T., Cagampang,F.R., Stirland,J.A., and Loudon,A.S. (2003). Photoperiod differentially regulates circadian oscillators in central and peripheral tissues of the Syrian hamster. Curr. Biol. *13*, 1543-1548.

Challet,E., Scarbrough,K., Penev,P.D., and Turek,F.W. (1998). Roles of suprachiasmatic nuclei and intergeniculate leaflets in mediating the phase-shifting effects of a serotonergic agonist and their photic modulation during subjective day. J. Biol. Rhythms *13*, 410-421.

Cheng,M.Y., Bullock,C.M., Li,C., Lee,A.G., Bermak,J.C., Belluzzi,J., Weaver,D.R., Leslie,F.M., and Zhou,Q.Y. (2002). Prokineticin 2 transmits the behavioural circadian rhythm of the suprachiasmatic nucleus. Nature *417*, 405-410.

Choi,H.J., Lee,C.J., Schroeder,A., Kim,Y.S., Jung,S.H., Kim,J.S., Kim,d.Y., Son,E.J., Han,H.C., Hong,S.K., Colwell,C.S., and Kim,Y.I. (2008). Excitatory actions of GABA in the suprachiasmatic nucleus. J. Neurosci. *28*, 5450-5459.

Colwell,C.S. (2005). Bridging the gap: coupling single-cell oscillators in the suprachiasmatic nucleus. Nat. Neurosci. *8*, 10-12.

Colwell,C.S., Foster,R.G., and Menaker,M. (1991). NMDA receptor antagonists block the effects of light on circadian behavior in the mouse. Brain Res. *554*, 105-110.

Colwell,C.S., Michel,S., Itri,J., Rodriguez,W., Tam,J., Lelievre,V., Hu,Z., Liu,X., and Waschek,J.A. (2003). Disrupted circadian rhythms in VIP- and PHI-deficient mice. Am. J. Physiol. Regul. Integr. Comp. Physiol. *285*, R939-R949.

Colwell,C.S., Ralph,M.R., and Menaker,M. (1990). Do NMDA receptors mediate the effects of light on circadian behavior? Brain Res. *523*, 117-120.

Daan,S., Merrow,M., and Roenneberg,T. (2002). External time--internal time. J. Biol. Rhythms *17*, 107-109.

Daan,S. and Pittendrigh,C.S. (1976a). A functional analysis of circadian pacemakers in nocturnal rodents. II. The variabilliy of phase response curves. J. Comp. Physiol. *106*, 267-290.

Daan,S. and Pittendrigh,C.S. (1976b). A functional analysis of circadian pacemakers in nocturnal rodents. III. Heavy Water and Constant Light: Homeostasis of Frequency? Journal of Comparative Physiology ? A *106*, 267-290.

Dacey,D.M., Liao,H.W., Peterson,B.B., Robinson,F.R., Smith,V.C., Pokorny,J., Yau,K.W., and Gamlin,P.D. (2005). Melanopsin-expressing ganglion cells in primate retina signal colour and irradiance and project to the LGN. Nature *433*, 749-754.

Dardente,H. and Cermakian,N. (2007). Molecular circadian rhythms in central and peripheral clocks in mammals. Chronobiol. Int. *24*, 195-213.

Dardente,H., Poirel,V.J., Klosen,P., Pevet,P., and Masson-Pevet,M. (2002). Per and neuropeptide expression in the rat suprachiasmatic nuclei: compartmentalization and differential cellular induction by light. Brain Res. *958*, 261-271.

Davidson,A.J., Yamazaki,S., and Menaker,M. (2003). SCN: ringmaster of the circadian circus or conductor of the circadian orchestra? Novartis Found. Symp. *253*, 110-121.

De Jeu,M. and Pennartz,C. (2002). Circadian modulation of GABA function in the rat suprachiasmatic nucleus: excitatory effects during the night phase. J. Neurophysiol. *87*, 834-844.

de la Iglesia,H.O., Meyer,J., Carpino,A., Jr., and Schwartz,W.J. (2000). Antiphase oscillation of the left and right suprachiasmatic nuclei. Science *290*, 799-801.

de la Iglesia,H.O., Meyer,J., and Schwartz,W.J. (2004). Using Per gene expression to search for photoperiodic oscillators in the hamster suprachiasmatic nucleus. Brain Res. Mol. Brain Res. *127*, 121-127.

de Vries,M.J., Treep,J.A., de Pauw,E.S., and Meijer,J.H. (1994). The effects of electrical stimulation of the optic nerves and anterior optic chiasm on the circadian activity rhythm of the Syrian hamster: involvement of excitatory amino acids. Brain Res. *642*, 206-212.

Deboer,T., Vansteensel,M.J., Detari,L., and Meijer,J.H. (2003). Sleep states alter activity of suprachiasmatic nucleus neurons. Nat. Neurosci. *6*, 1086-1090.

DeCoursey,P.J. (1964). Function of a light response rhythm in hamsters. J Cell Physiol *63*, 189-196.

DeCoursey,P.J. and Krulas,J.R. (1998). Behavior of SCN-lesioned chipmunks in natural habitat: a pilot study. J. Biol. Rhythms *13*, 229-244.

DeCoursey,P.J., Krulas,J.R., Mele,G., and Holley,D.C. (1997). Circadian performance of suprachiasmatic nuclei (SCN)-lesioned antelope ground squirrels in a desert enclosure. Physiol. Behav. *62*, 1099-1108.

DeCoursey,P.J., Walker,J.K., and Smith,S.A. (2000). A circadian pacemaker in free-living chipmunks: essential for survival? J. Comp. Physiol. [A]. *186*, 169-180.

Ding,J.M., Chen,D., Weber,E.T., Faiman,L.E., Rea,M.A., and Gillette,M.U. (1994). Resetting the biological clock: mediation of nocturnal circadian shifts by glutamate and NO. Science *266*, 1713-1717.

Doyle,S.E., Castrucci,A.M., McCall,M., Provencio,I., and Menaker,M. (2006). Nonvisual light responses in the Rpe65 knockout mouse: rod loss restores

sensitivity to the melanopsin system. Proc Natl Acad Sci U. S. A *103*, 10432-10437.

Drouyer,E., Rieux,C., Hut,R.A., and Cooper,H.M. (2007). Responses of suprachiasmatic nucleus neurons to light and dark adaptation: relative contributions of melanopsin and rod-cone inputs. J. Neurosci. *27*, 9623-9631.

Dudek,F.E., Kim,Y.I., and Bouskila,Y. (1993). Electrophysiology of the suprachiasmatic nucleus: synaptic transmission, membrane properties, and neuronal synchronization. J. Biol. Rhythms *8 Suppl*, S33-S37.

Duncan,M.J. (2006). Aging of the Mammalian Circadian Timing System: Changes in the Central Pacemaker and Its Regulation by Photic and Nonphotic Signals. Neuroembryology and Aging *4*, 85-101.

Eilers,P.H.C. (2003). A perfect smoother. Anal. Chem. *75*, 3631-3636.

Eskes,G.A. and Rusak,B. (1985). Horizontal knife cuts in the suprachiasmatic area prevent hamster gonadal responses to photoperiod. Neurosci. Lett. *61*, 261-266.

Evans,J.A., Elliott,J.A., and Gorman,M.R. (2004). Photoperiod differentially modulates photic and nonphotic phase response curves of hamsters. Am J Physiol Regul Integr. Comp Physiol *286*, R539-R546.

Fee,M.S., Mitra,P.P., and Kleinfeld,D. (1996). Automatic sorting of multiple unit neuronal signals in the presence of anisotropic and non-Gaussian variability. J. Neurosci. Methods *69*, 175-188.

Foster,R.G., Provencio,I., Hudson,D., Fiske,S., De,G.W., and Menaker,M. (1991). Circadian photoreception in the retinally degenerate mouse (rd/rd). J Comp Physiol A *169*, 39-50.

Gekakis,N., Staknis,D., Nguyen,H.B., Davis,F.C., Wilsbacher,L.D., King,D.P., Takahashi,J.S., and Weitz,C.J. (1998). Role of the CLOCK protein in the mammalian circadian mechanism. Science *280*, 1564-1569.

Gillette,M.U. (1986). The suprachiasmatic nuclei: circadian phase-shifts induced at the time of hypothalamic slice preparation are preserved in vitro. Brain Res. *379*, 176-181.

Gillette,M.U., DeMarco,S.J., Ding,J.M., Gallman,E.A., Faiman,L.E., Liu,C., McArthur,A.J., Medanic,M., Richard,D., and Tcheng,T.K. (1993). The organization of the suprachiasmatic circadian pacemaker of the rat and its

regulation by neurotransmitters and modulators. J. Biol. Rhythms *8 Suppl*, S53-S58.

Gillette,M.U., Medanic,M., McArthur,A.J., Liu,C., Ding,J.M., Faiman,L.E., Weber,E.T., Tcheng,T.K., and Gallman,E.A. (1995). Intrinsic neuronal rhythms in the suprachiasmatic nuclei and their adjustment. Ciba Found. Symp. *183*, 134-144.

Gillette,M.U. and Prosser,R.A. (1988). Circadian rhythm of the rat suprachiasmatic brain slice is rapidly reset by daytime application of cAMP analogs. Brain Res. *474*, 348-352.

Goldman,B.D. (2001). Mammalian photoperiodic system: formal properties and neuroendocrine mechanisms of photoperiodic time measurement. J. Biol. Rhythms *16*, 283-301.

Gorman,M.R., Goldman,B.D., and Zucker,I. (2001). Mammalian Photoperiodism. In Circadian Clocks, J.S.Takahashi, F.W.Turek, and R.Y.Moore, eds. (New York: Kluwer Academic / Plenum Publishers), pp. 481-510.

Green,D.J. and Gillette,R. (1982). Circadian Rhythm of Firing Rate Recorded from Single Cells in the Rat Suprachiasmatic Brain Slice. Brain Res. *245*, 198-200.

Gribkoff,V.K., Pieschl,R.L., Wisialowski,T.A., van den Pol,A.N., and Yocca,F.D. (1998). Phase shifting of circadian rhythms and depression of neuronal activity in the rat suprachiasmatic nucleus by neuropeptide Y: mediation by different receptor subtypes. J. Neurosci. *18*, 3014-3022.

Groos,G. and Hendriks,J. (1982). Circadian rhythms in electrical discharge of rat suprachiasmatic neurones recorded in vitro. Neurosci. Lett. *34*, 283-288.

Groos,G.A. and Meijer,J.H. (1985). Effects of illumination on suprachiasmatic nucleus electrical discharge. Ann. N. Y. Acad. Sci. *453*, 134-146.

Güler,A.D., Ecker,J.L., Lall,G.S., Haq,S., Altimus,C.M., Liao,H.W., Barnard,A.R., Cahill,H., Badea,T.C., Zhao,H., Hankins,M.W., Berson,D.M., Lucas,R.J., Yau,K.W., and Hattar,S. (2008). Melanopsin cells are the principal conduits for rod-cone input to non-image-forming vision. Nature *453*, 102-105.

Hannibal,J. (2002). Neurotransmitters of the retino-hypothalamic tract. Cell Tissue Res. *309*, 73-88.

Hannibal,J. (2006). Roles of PACAP-containing retinal ganglion cells in circadian timing. Int. Rev. Cytol. *251*, 1-39.

Hannibal,J. and Fahrenkrug,J. (2002). Melanopsin: a novel photopigment involved in the photoentrainment of the brain's biological clock? Ann. Med. *34*, 401-407.

Härmä,M.I., Hakola,T., Akerstedt,T., and Laitinen,J.T. (1994). Age and adjustment to night work. Occup. Environ. Med. *51*, 568-573.

Harmar,A.J., Marston,H.M., Shen,S., Spratt,C., West,K.M., Sheward,W.J., Morrison,C.F., Dorin,J.R., Piggins,H.D., Reubi,J.C., Kelly,J.S., Maywood,E.S., and Hastings,M.H. (2002). The VPAC(2) receptor is essential for circadian function in the mouse suprachiasmatic nuclei. Cell *109*, 497-508.

Harrington,M.E., Hoque,S., Hall,A., Golombek,D., and Biello,S. (1999). Pituitary adenylate cyclase activating peptide phase shifts circadian rhythms in a manner similar to light. J. Neurosci. *19*, 6637-6642.

Harrington,M.E. and Rusak,B. (1986). Lesions of the thalamic intergeniculate leaflet alter hamster circadian rhythms. J Biol Rhythms *1*, 309-325.

Harrington,M.E. and Rusak,B. (1988). Ablation of the geniculo-hypothalamic tract alters circadian activity rhythms of hamsters housed under constant light. Physiol. Behav. *42*, 183-189.

Hastings,M.H., Field,M.D., Maywood,E.S., Weaver,D.R., and Reppert,S.M. (1999). Differential regulation of mPER1 and mTIM proteins in the mouse suprachiasmatic nuclei: new insights into a core clock mechanism. J. Neurosci. *19*, RC11.

Hastings,M.H. and Herzog,E.D. (2004). Clock genes, oscillators, and cellular networks in the suprachiasmatic nuclei. J. Biol. Rhythms *19*, 400-413.

Hazlerigg,D.G., Ebling,F.J., and Johnston,J.D. (2005). Photoperiod differentially regulates gene expression rhythms in the rostral and caudal SCN. Curr. Biol. *15*, R449-R450.

Herzog,E.D., Aton,S.J., Numano,R., Sakaki,Y., and Tei,H. (2004). Temporal precision in the mammalian circadian system: a reliable clock from less reliable neurons. J. Biol. Rhythms *19*, 35-46.

Herzog,E.D., Geusz,M.E., Khalsa,S.B., Straume,M., and Block,G.D. (1997). Circadian rhythms in mouse suprachiasmatic nucleus explants on multimicroelectrode plates. Brain Res. *757*, 285-290.

Herzog,E.D., Takahashi,J.S., and Block,G.D. (1998). Clock controls circadian period in isolated suprachiasmatic nucleus neurons. Nat. Neurosci. *1*, 708-713.

Hong,H.K., Chong,J.L., Song,W., Song,E.J., Jyawook,A.A., Schook,A.C., Ko,C.H., and Takahashi,J.S. (2007). Inducible and reversible Clock gene expression in brain using the tTA system for the study of circadian behavior. PLoS Genet. *3*, e33.

Honma,S., Honma,K., and Hiroshige,T. (1984). Dissociation of circadian rhythms in rats with a hypothalamic island. Am J Physiol *246*, R949-R954.

Honma,S., Shirakawa,T., Katsuno,Y., Namihira,M., and Honma,K. (1998). Circadian periods of single suprachiasmatic neurons in rats. Neurosci. Lett. *250*, 157-160.

Inagaki,N., Honma,S., Ono,D., Tanahashi,Y., and Honma,K. (2007). Separate oscillating cell groups in mouse suprachiasmatic nucleus couple photoperiodically to the onset and end of daily activity. Proc. Natl. Acad. Sci. U. S. A. *104*, 7664-7669.

Indic,P., Schwartz,W.J., Herzog,E.D., Foley,N.C., and Antle,M.C. (2007). Modeling the behavior of coupled cellular circadian oscillators in the suprachiasmatic nucleus. J. Biol. Rhythms *22*, 211-219.

Inouye,S. and Kawamura,H. (1982). Characteristics of a circadian pacemaker in the suprachiasmatic nucleus. Journal of Comparative Physiology A: Neuroethology, Sensory, Neural, and Behavioral Physiology *146*, 153-160.

Inouye,S.T. and Kawamura,H. (1979). Persistence of circadian rhythmicity in a mammalian hypothalamic "island" containing the suprachiasmatic nucleus. Proc. Natl. Acad. Sci. U. S. A. *76*, 5962-5966.

Itri,J.N., Michel,S., Vansteensel,M.J., Meijer,J.H., and Colwell,C.S. (2005). Fast delayed rectifier potassium current is required for circadian neural activity. Nat. Neurosci. *8*, 650-656.

Jac,M., Sumova,A., and Illnerova,H. (2000). c-Fos rhythm in subdivisions of the rat suprachiasmatic nucleus under artificial and natural photoperiods. Am. J. Physiol. Regul. Integr. Comp. Physiol. *279*, R2270-R2276.

Jagota,A., de la Iglesia,H.O., and Schwartz,W.J. (2000). Morning and evening circadian oscillations in the suprachiasmatic nucleus in vitro. Nat. Neurosci. *3*, 372-376.

Jiang,Z.G., Yang,Y.Q., and Allen,C.N. (1997). Tracer and electrical coupling of rat suprachiasmatic nucleus neurons. Neuroscience *77*, 1059-1066.

Johnson,C.H. (1999). Forty years of PRCs--what have we learned? Chronobiol. Int. *16*, 711-743.

Johnson,C.H., Mori,T., and Xu,Y. (2008). A cyanobacterial circadian clockwork. Curr Biol *18*, R816-R825.

Johnson,M.S. (1926). Activity and distribution of certain wild mice in relation to biotic communities. J. Mammal. *7*, 245-277.

Johnson,M.S. (1939). Effects of continuous light on periodic spontaneous activity of white-footed mice (*Peromyscus*). J. Exp. Zool. *82*, 315-328.

Johnston,J.D. (2005). Measuring seasonal time within the circadian system: regulation of the suprachiasmatic nuclei by photoperiod. J. Neuroendocrinol. *17*, 459-465.

Johnston,J.D., Ebling,F.J., and Hazlerigg,D.G. (2005). Photoperiod regulates multiple gene expression in the suprachiasmatic nuclei and pars tuberalis of the Siberian hamster (Phodopus sungorus). Eur. J. Neurosci. *21*, 2967-2974.

Kalsbeek,A., Foppen,E., Schalij,I., Van,H.C., van,d., V, Fliers,E., and Buijs,R.M. (2008). Circadian control of the daily plasma glucose rhythm: an interplay of GABA and glutamate. PLoS One. *3*, e3194.

Kalsbeek,A., Palm,I.F., La Fleur,S.E., Scheer,F.A., Perreau-Lenz,S., Ruiter,M., Kreier,F., Cailotto,C., and Buijs,R.M. (2006). SCN outputs and the hypothalamic balance of life. J. Biol. Rhythms *21*, 458-469.

Kim,D.Y., Kang,H.C., Shin,H.C., Lee,K.J., Yoon,Y.W., Han,H.C., Na,H.S., Hong,S.K., and Kim,Y.I. (2001). Substance p plays a critical role in photic resetting of the circadian pacemaker in the rat hypothalamus. J. Neurosci. *21*, 4026-4031.

King,V.M., Chahad-Ehlers,S., Shen,S., Harmar,A.J., Maywood,E.S., and Hastings,M.H. (2003). A hVIPR transgene as a novel tool for the analysis of circadian function in the mouse suprachiasmatic nucleus. Eur. J. Neurosci. *17*, 822-832.

Klein,D.C. and Moore,R.Y. (1979). Pineal N-acetyltransferase and hydroxyindole-O-methyltransferase: control by the retinohypothalamic tract and the suprachiasmatic nucleus. Brain Res. *174*, 245-262.

Ko,C.H. and Takahashi,J.S. (2006). Molecular components of the mammalian circadian clock. Hum. Mol. Genet. *15 Spec No 2*, R271-R277.

Kopp,M.D., Meissl,H., Dehghani,F., and Korf,H.W. (2001). The pituitary adenylate cyclase-activating polypeptide modulates glutamatergic calcium signalling: investigations on rat suprachiasmatic nucleus neurons. J. Neurochem. *79*, 161-171.

Kramer,A., Yang,F.C., Snodgrass,P., Li,X., Scammell,T.E., Davis,F.C., and Weitz,C.J. (2001). Regulation of daily locomotor activity and sleep by hypothalamic EGF receptor signaling. Science *294*, 2511-2515.

Kuhlman,S.J. and McMahon,D.G. (2004). Rhythmic regulation of membrane potential and potassium current persists in SCN neurons in the absence of environmental input. Eur. J. Neurosci. *20*, 1113-1117.

Kuhlman,S.J. and McMahon,D.G. (2006). Encoding the ins and outs of circadian pacemaking. J. Biol. Rhythms *21*, 470-481.

Kuhlman,S.J., Silver,R., Le Sauter,J., Bult-Ito,A., and McMahon,D.G. (2003). Phase resetting light pulses induce Per1 and persistent spike activity in a subpopulation of biological clock neurons. J. Neurosci. *23*, 1441-1450.

Kume,K., Zylka,M.J., Sriram,S., Shearman,L.P., Weaver,D.R., Jin,X., Maywood,E.S., Hastings,M.H., and Reppert,S.M. (1999). mCRY1 and mCRY2 are essential components of the negative limb of the circadian clock feedback loop. Cell *98*, 193-205.

Lee,C., Etchegaray,J.P., Cagampang,F.R., Loudon,A.S., and Reppert,S.M. (2001). Posttranslational mechanisms regulate the mammalian circadian clock. Cell *107*, 855-867.

Lewicki,M.S. (1998). A review of methods for spike sorting: the detection and classification of neural action potentials. Network. *9*, R53-R78.

Lincoln,G., Messager,S., Andersson,H., and Hazlerigg,D. (2002). Temporal expression of seven clock genes in the suprachiasmatic nucleus and the pars tuberalis of the sheep: evidence for an internal coincidence timer. Proc. Natl. Acad. Sci. U. S. A. *99*, 13890-13895.

Linden,A.M., Sandu,C., Aller,M.I., Vekovischeva,O.Y., Rosenberg,P.H., Wisden,W., and Korpi,E.R. (2007). TASK-3 Knockout Mice Exhibit Exaggerated Nocturnal Activity, Impairments in Cognitive Functions, and Reduced Sensitivity to Inhalation Anesthetics. J. Pharmacol. Exp. Ther. *323*, 924-934.

Liu,A.C., Welsh,D.K., Ko,C.H., Tran,H.G., Zhang,E.E., Priest,A.A., Buhr,E.D., Singer,O., Meeker,K., Verma,I.M., Doyle,F.J., III, Takahashi,J.S., and Kay,S.A. (2007). Intercellular Coupling Confers Robustness against Mutations in the SCN Circadian Clock Network. Cell *129*, 605-616.

Liu,C. and Gillette,M.U. (1996). Cholinergic regulation of the suprachiasmatic nucleus circadian rhythm via a muscarinic mechanism at night. J. Neurosci. *16*, 744-751.

Liu,C. and Reppert,S.M. (2000). GABA synchronizes clock cells within the suprachiasmatic circadian clock. Neuron *25*, 123-128.

Liu,C., Weaver,D.R., Jin,X., Shearman,L.P., Pieschl,R.L., Gribkoff,V.K., and Reppert,S.M. (1997a). Molecular dissection of two distinct actions of melatonin on the suprachiasmatic circadian clock. Neuron *19*, 91-102.

Liu,C., Weaver,D.R., Strogatz,S.H., and Reppert,S.M. (1997b). Cellular construction of a circadian clock: period determination in the suprachiasmatic nuclei. Cell *91*, 855-860.

Long,M.A., Jutras,M.J., Connors,B.W., and Burwell,R.D. (2005). Electrical synapses coordinate activity in the suprachiasmatic nucleus. Nat. Neurosci. *8*, 61-66.

Low-Zeddies,S.S. and Takahashi,J.S. (2001). Chimera analysis of the Clock mutation in mice shows that complex cellular integration determines circadian behavior. Cell *105*, 25-42.

Lowrey,P.L., Shimomura,K., Antoch,M.P., Yamazaki,S., Zemenides,P.D., Ralph,M.R., Menaker,M., and Takahashi,J.S. (2000). Positional syntenic cloning and functional characterization of the mammalian circadian mutation tau. Science *288*, 483-492.

Lowrey,P.L. and Takahashi,J.S. (2000). Genetics of the mammalian circadian system: Photic entrainment, circadian pacemaker mechanisms, and posttranslational regulation. Annu. Rev. Genet. *34*, 533-562.

Lucas,R.J., Freedman,M.S., Lupi,D., Munoz,M., vid-Gray,Z.K., and Foster,R.G. (2001). Identifying the photoreceptive inputs to the mammalian circadian system using transgenic and retinally degenerate mice. Behav. Brain Res. *125*, 97-102.

Lucas,R.J., Hattar,S., Takao,M., Berson,D.M., Foster,R.G., and Yau,K.W. (2003). Diminished pupillary light reflex at high irradiances in melanopsin-knockout mice. Science *299*, 245-247.

Lucassen,P.J., Hofman,M.A., and Swaab,D.F. (1995). Increased light intensity prevents the age related loss of vasopressin-expressing neurons in the rat suprachiasmatic nucleus. Brain Res. *693*, 261-266.

Lucassen,P.J., Tilders,F.J., Salehi,A., and Swaab,D.F. (1997). Neuropeptides vasopressin (AVP), oxytocin (OXT) and corticotropin-releasing hormone (CRH) in the human hypothalamus: activity changes in aging, Alzheimer's disease and depression. Aging (Milano.) *9*, 48-50.

Lundkvist,G.B. and Block,G.D. (2005). Role of neuronal membrane events in circadian rhythm generation. Methods Enzymol. *393*, 623-642.

Lundkvist,G.B., Kwak,Y., Davis,E.K., Tei,H., and Block,G.D. (2005). A calcium flux is required for circadian rhythm generation in mammalian pacemaker neurons. J. Neurosci. *25*, 7682-7686.

Mason,R. and Rusak,B. (1990). Neurophysiological responses to melatonin in the SCN of short-day sensitive and refractory hamsters. Brain Res. *533*, 15-19.

Maywood,E.S., Reddy,A.B., Wong,G.K., O'Neill,J.S., O'Brien,J.A., McMahon,D.G., Harmar,A.J., Okamura,H., and Hastings,M.H. (2006). Synchronization and maintenance of timekeeping in suprachiasmatic circadian clock cells by neuropeptidergic signaling. Curr. Biol. *16*, 599-605.

McArthur,A.J., Coogan,A.N., Ajpru,S., Sugden,D., Biello,S.M., and Piggins,H.D. (2000). Gastrin-releasing peptide phase-shifts suprachiasmatic nuclei neuronal rhythms in vitro. J. Neurosci. *20*, 5496-5502.

McArthur,A.J., Gillette,M.U., and Prosser,R.A. (1991). Melatonin directly resets the rat suprachiasmatic circadian clock in vitro. Brain Res. *565*, 158-161.

Meijer,J.H. (2001). Photic Entrainment in Mammals. In Circadian Clocks, J.S.Takahashi, F.W.Turek, and R.Y.Moore, eds. (New York: Kluwer Academic / Plenum Publishers), pp. 183-222.

Meijer,J.H., Groos,G.A., and Rusak,B. (1986). Luminance coding in a circadian pacemaker: the suprachiasmatic nucleus of the rat and the hamster. Brain Res. *382*, 109-118.

Meijer,J.H. and Rietveld,W.J. (1989). Neurophysiology of the suprachiasmatic circadian pacemaker in rodents. Physiol. Rev. *69*, 671-707.

Meijer,J.H., Schaap,J., Watanabe,K., and Albus,H. (1997). Multiunit activity recordings in the suprachiasmatic nuclei: in vivo versus in vitro models. Brain Res. *753*, 322-327.

Meijer,J.H., Thio,B., Albus,H., Schaap,J., and Ruijs,A.C. (1999). Functional absence of extraocular photoreception in hamster circadian rhythm entrainment. Brain Res. *831*, 337-339.

Meijer,J.H., Watanabe,K., Detari,L., and Schaap,J. (1996). Circadian rhythm in light response in suprachiasmatic nucleus neurons of freely moving rats. Brain Res. *741*, 352-355.

Meijer,J.H., Watanabe,K., Schaap,J., Albus,H., and Detari,L. (1998). Light responsiveness of the suprachiasmatic nucleus: long-term multiunit and single-unit recordings in freely moving rats. J. Neurosci. *18*, 9078-9087.

Menaker,M. (1971). Rhythms, reproduction, and photoreception. Biol Reprod *4*, 295-308.

Meng,Q.J., Logunova,L., Maywood,E.S., Gallego,M., Lebiecki,J., Brown,T.M., Sladek,M., Semikhodskii,A.S., Glossop,N.R., Piggins,H.D., Chesham,J.E., Bechtold,D.A., Yoo,S.H., Takahashi,J.S., Virshup,D.M., Boot-Handford,R.P., Hastings,M.H., and Loudon,A.S. (2008). Setting clock speed in mammals: the CK1 epsilon tau mutation in mice accelerates circadian pacemakers by selectively destabilizing PERIOD proteins. Neuron *58*, 78-88.

Meredith,A.L., Wiler,S.W., Miller,B.H., Takahashi,J.S., Fodor,A.A., Ruby,N.F., and Aldrich,R.W. (2006). BK calcium-activated potassium channels regulate circadian behavioral rhythms and pacemaker output. Nat. Neurosci. *9*, 1041-1049.

Messager,S., Hazlerigg,D.G., Mercer,J.G., and Morgan,P.J. (2000). Photoperiod differentially regulates the expression of Per1 and ICER in the pars tuberalis and the suprachiasmatic nucleus of the Siberian hamster. Eur. J. Neurosci. *12*, 2865-2870.

Messager,S., Ross,A.W., Barrett,P., and Morgan,P.J. (1999). Decoding photoperiodic time through Per1 and ICER gene amplitude. Proc. Natl. Acad. Sci. U. S. A. *96*, 9938-9943.

Michel,S., Clark,J.P., Ding,J.M., and Colwell,C.S. (2006). Brain-derived neurotrophic factor and neurotrophin receptors modulate glutamate-induced phase shifts of the suprachiasmatic nucleus. Eur. J. Neurosci. *24*, 1109-1116.

Michel,S., Geusz,M.E., Zaritsky,J.J., and Block,G.D. (1993). Circadian rhythm in membrane conductance expressed in isolated neurons. Science *259*, 239-241.

Michel,S., Manivannan,K., Zaritsky,J.J., and Block,G.D. (1999). A delayed rectifier current is modulated by the circadian pacemaker in Bulla. J. Biol. Rhythms *14*, 141-150.

Miller,J.D., Morin,L.P., Schwartz,W.J., and Moore,R.Y. (1996). New insights into the mammalian circadian clock. Sleep *19*, 641-667.

Moore,R.Y. and Eichler,V.B. (1972). Loss of a circadian adrenal corticosterone rhythm following suprachiasmatic lesions in the rat. Brain Res. *42*, 201-206.

Moore,R.Y. and Klein,D.C. (1974). Visual pathways and the central neural control of a circadian rhythm in pineal serotonin N-acetyltransferase activity. Brain Res. *71*, 17-33.

Moore,R.Y. and Lenn,N.J. (1972). A retinohypothalamic projection in the rat. J. Comp. Neurol. *146*, 1-14.

Morin,L.P. (1994). The circadian visual system. Brain Res. Brain Res. Rev. *19*, 102-127.

Morin,L.P. and Allen,C.N. (2006). The circadian visual system, 2005. Brain Res. Rev. *51*, 1-60.

Mrosovsky,N., Edelstein,K., Hastings,M.H., and Maywood,E.S. (2001). Cycle of period gene expression in a diurnal mammal (Spermophilus tridecemlineatus): implications for nonphotic phase shifting. J. Biol. Rhythms *16*, 471-478.

Mrugala,M., Zlomanczuk,P., Jagota,A., and Schwartz,W.J. (2000). Rhythmic multiunit neural activity in slices of hamster suprachiasmatic nucleus reflect prior photoperiod. Am. J. Physiol. Regul. Integr. Comp. Physiol. *278*, R987-R994.

Nagano,M., Adachi,A., Nakahama,K., Nakamura,T., Tamada,M., Meyer-Bernstein,E., Sehgal,A., and Shigeyoshi,Y. (2003). An abrupt shift in the day/night cycle causes desynchrony in the mammalian circadian center. J. Neurosci. *23*, 6141-6151.

Naito,E., Watanabe,T., Tei,H., Yoshimura,T., and Ebihara,S. (2008). Reorganization of the suprachiasmatic nucleus coding for day length. J. Biol. Rhythms *23*, 140-149.

Nakamura,W., Honma,S., Shirakawa,T., and Honma,K. (2001). Regional pacemakers composed of multiple oscillator neurons in the rat suprachiasmatic nucleus. Eur. J. Neurosci. *14*, 666-674.

Nakamura,W., Yamazaki,S., Takasu,N.N., Mishima,K., and Block,G.D. (2005). Differential response of Period 1 expression within the suprachiasmatic nucleus. J. Neurosci. *25*, 5481-5487.

Nelson,R.J. and Zucker,I. (1981). Photoperiodic control of reproduction in olfactory-bulbectomized rats. Neuroendocrinology *32*, 266-271.

Nitabach,M.N., Blau,J., and Holmes,T.C. (2002). Electrical silencing of Drosophila pacemaker neurons stops the free-running circadian clock. Cell *109*, 485-495.

Nuesslein-Hildesheim,B., O'Brien,J.A., Ebling,F.J., Maywood,E.S., and Hastings,M.H. (2000). The circadian cycle of mPER clock gene products in the suprachiasmatic nucleus of the siberian hamster encodes both daily and seasonal time. Eur. J. Neurosci. *12*, 2856-2864.

Nygård,M. and Palomba,M. (2006). The GABAergic network in the suprachiasmatic nucleus as a key regulator of the biological clock: does it change during senescence? Chronobiol. Int. *23*, 427-435.

Ohta,H., Yamazaki,S., and McMahon,D.G. (2005). Constant light desynchronizes mammalian clock neurons. Nat. Neurosci. *8*, 267-269.

Okamura,H., Miyake,S., Sumi,Y., Yamaguchi,S., Yasui,A., Muijtjens,M., Hoeijmakers,J.H., and van der Horst,G.T. (1999). Photic induction of mPer1 and mPer2 in cry-deficient mice lacking a biological clock. Science *286*, 2531-2534.

Panda,S. and Hogenesch,J.B. (2004). It's all in the timing: many clocks, many outputs. J. Biol. Rhythms *19*, 374-387.

Panda,S., Provencio,I., Tu,D.C., Pires,S.S., Rollag,M.D., Castrucci,A.M., Pletcher,M.T., Sato,T.K., Wiltshire,T., Andahazy,M., Kay,S.A., Van Gelder,R.N., and Hogenesch,J.B. (2003). Melanopsin is required for non-image-forming photic responses in blind mice. Science *301*, 525-527.

Paxinos,G. and Franklin,K.B.J. (2001). The Mouse Brain in Stereotaxic Coordinates, Second Edition. (San Diego: Academic Press).

Pennartz,C.M., de Jeu,M.T., Bos,N.P., Schaap,J., and Geurtsen,A.M. (2002). Diurnal modulation of pacemaker potentials and calcium current in the mammalian circadian clock. Nature *416*, 286-290.

Pickard,G.E., Ralph,M.R., and Menaker,M. (1987). The intergeniculate leaflet partially mediates effects of light on circadian rhythms. J. Biol. Rhythms *2*, 35-56.

Piggins,H.D. and Rusak,B. (1997). Effects of microinjections of substance P into the suprachiasmatic nucleus region on hamster wheel-running rhythms. Brain Res. Bull. *42*, 451-455.

Pittendrigh,C.S. and Daan,S. (1976a). A functional analysis of circadian pacemakers in nocturnal rodents. IV. Entrainment: Pacemaker as Clock. Journal of Comparative Physiology ? A *106*, 291-331.

Pittendrigh,C.S. and Daan,S. (1976b). A functional analysis of circadian pacemakers in nocturnal rodents: V. Pacemaker structure: a clock for all seasons. J. Comp. Physiol. [A]. 333-355.

Pittendrigh,C.S., Elliott,J., and Takamura,T. (1984). The Circadian Component in Photoperiodic induction. In Photoperiodic Regulation of Insect and Molluscan Hormones, R.Porter and J.M.Collins, eds. (London: Pitman), pp. 26-47.

Pittendrigh,C.S., Kyner,W.T., and Takamura,T. (1991). The amplitude of circadian oscillations: temperature dependence, latitudinal clines, and the photoperiodic time measurement. J. Biol. Rhythms *6*, 299-313.

Pitts,G.R., Ohta,H., and McMahon,D.G. (2006). Daily rhythmicity of large-conductance Ca2+ -activated K+ currents in suprachiasmatic nucleus neurons. Brain Res. *1071*, 54-62.

Portaluppi,F., Touitou,Y., and Smolensky,M.H. (2008). Ethical and methodological standards for laboratory and medical biological rhythm research. Chronobiol Int *25*, 999-1016.

Preitner,N., Damiola,F., Lopez-Molina,L., Zakany,J., Duboule,D., Albrecht,U., and Schibler,U. (2002). The orphan nuclear receptor REV-ERBalpha controls circadian transcription within the positive limb of the mammalian circadian oscillator. Cell *110*, 251-260.

Prosser,R.A. (1998). In vitro circadian rhythms of the mammalian suprachiasmatic nuclei: comparison of multi-unit and single-unit neuronal activity recordings. J. Biol. Rhythms *13*, 30-38.

Provencio,I. and Foster,R.G. (1995). Circadian rhythms in mice can be regulated by photoreceptors with cone-like characteristics. Brain Res *694*, 183-190.

Provencio,I., Rodriguez,I.R., Jiang,G., Hayes,W.P., Moreira,E.F., and Rollag,M.D. (2000). A novel human opsin in the inner retina. J Neurosci *20*, 600-605.

Pulivarthy,S.R., Tanaka,N., Welsh,D.K., De,H.L., Verma,I.M., and Panda,S. (2007). Reciprocity between phase shifts and amplitude changes in the mammalian circadian clock. Proc Natl Acad Sci U. S. A *104*, 20356-20361.

Quintero,J.E., Kuhlman,S.J., and McMahon,D.G. (2003). The biological clock nucleus: a multiphasic oscillator network regulated by light. J. Neurosci. *23*, 8070-8076.

Ralph,M.R., Foster,R.G., Davis,F.C., and Menaker,M. (1990). Transplanted suprachiasmatic nucleus determines circadian period. Science *247*, 975-978.

Ralph,M.R. and Menaker,M. (1988). A mutation of the circadian system in golden hamsters. Science *241*, 1225-1227.

Rangarajan,R., Heller,H.C., and Miller,J.D. (1994). Chloride channel block phase advances the single-unit activity rhythm in the SCN. Brain Res. Bull. *34*, 69-72.

Reddy,A.B., Field,M.D., Maywood,E.S., and Hastings,M.H. (2002). Differential resynchronisation of circadian clock gene expression within the suprachiasmatic nuclei of mice subjected to experimental jet lag. J. Neurosci. *22*, 7326-7330.

Reed,H.E., Cutler,D.J., Brown,T.M., Brown,J., Coen,C.W., and Piggins,H.D. (2002). Effects of vasoactive intestinal polypeptide on neurones of the rat suprachiasmatic nuclei in vitro. J. Neuroendocrinol. *14*, 639-646.

Reed,H.E., Meyer-Spasche,A., Cutler,D.J., Coen,C.W., and Piggins,H.D. (2001). Vasoactive intestinal polypeptide (VIP) phase-shifts the rat suprachiasmatic nucleus clock in vitro. Eur. J. Neurosci. *13*, 839-843.

Refinetti,R. (2001). Dark adaptation in the circadian system of the mouse. Physiol. Behav. *74*, 101-107.

Refinetti,R. (2002). Compression and expansion of circadian rhythm in mice under long and short photoperiods. Integr. Physiol. Behav. Sci. *37*, 114-127.

Reppert,S.M. and Weaver,D.R. (2001). Molecular analysis of mammalian circadian rhythms. Annu. Rev. Physiol. *63*, 647-676.

Reppert,S.M. and Weaver,D.R. (2002). Coordination of circadian timing in mammals. Nature *418*, 935-941.

Rohling,J., Meijer,J.H., VanderLeest,H.T., and Admiraal,J. (2006a). Phase differences between SCN neurons and their role in photoperiodic encoding; a simulation of ensemble patterns using recorded single unit electrical activity patterns. J. Physiol Paris *100*, 261-270.

Rohling,J., Wolters,L., and Meijer,J.H. (2006b). Simulation of day-length encoding in the SCN: from single-cell to tissue-level organization. J. Biol. Rhythms *21*, 301-313.

Ruby,N.F., Hwang,C.E., Wessells,C., Fernandez,F., Zhang,P., Sapolsky,R., and Heller,H.C. (2008). Hippocampal-dependent learning requires a functional circadian system. Proc. Natl. Acad. Sci. U. S. A *105*, 15593-15598.

Rusak,B. (1977). The role of the Suprachiasmatic Nuclei in the Generation of Circadian-Rhythms in the Golden-Hamster, *Mesocricetus-auratus*. Journal of Comparative Physiology *118*, 145-164.

Rusak,B. and Boulos,Z. (1981). Pathways for photic entrainment of mammalian circadian rhythms. Photochem Photobiol *34*, 267-273.

Saeb-Parsy,K. and Dyball,R.E. (2003). Defined cell groups in the rat suprachiasmatic nucleus have different day/night rhythms of single-unit activity in vivo. J. Biol. Rhythms *18*, 26-42.

Sato,T.K., Panda,S., Miraglia,L.J., Reyes,T.M., Rudic,R.D., McNamara,P., Naik,K.A., FitzGerald,G.A., Kay,S.A., and Hogenesch,J.B. (2004). A functional genomics strategy reveals Rora as a component of the mammalian circadian clock. Neuron *43*, 527-537.

Schaap,J., Albus,H., Eilers,P.H., Detari,L., and Meijer,J.H. (2001). Phase differences in electrical discharge rhythms between neuronal populations of the left and right suprachiasmatic nuclei. Neuroscience *108*, 359-363.

Schaap,J., Albus,H., VanderLeest,H.T., Eilers,P.H., Detari,L., and Meijer,J.H. (2003). Heterogeneity of rhythmic suprachiasmatic nucleus neurons: Implications for circadian waveform and photoperiodic encoding. Proc. Natl. Acad. Sci. U. S. A. *100*, 15994-15999.

Schaap,J. and Meijer,J.H. (2001). Opposing effects of behavioural activity and light on neurons of the suprachiasmatic nucleus. Eur. J. Neurosci. *13*, 1955-1962.

Schak,K.M. and Harrington,M.E. (1999). Protein kinase C inhibition and activation phase advances the hamster circadian clock. Brain Res. *840*, 158-161.

Schibler,U. and Sassone-Corsi,P. (2002). A web of circadian pacemakers. Cell *111*, 919-922.

Schwartz,W.J., Carpino,A., Jr., de la Iglesia,H.O., Baler,R., Klein,D.C., Nakabeppu,Y., and Aronin,N. (2000). Differential regulation of fos family genes in the ventrolateral and dorsomedial subdivisions of the rat suprachiasmatic nucleus. Neuroscience *98*, 535-547.

Schwartz,W.J., Gross,R.A., and Morton,M.T. (1987). The suprachiasmatic nuclei contain a tetrodotoxin-resistant circadian pacemaker. Proc. Natl. Acad. Sci. U. S. A. *84*, 1694-1698.

Shearman,L.P., Sriram,S., Weaver,D.R., Maywood,E.S., Chaves,I., Zheng,B., Kume,K., Lee,C.C., van der Horst,G.T., Hastings,M.H., and Reppert,S.M. (2000). Interacting molecular loops in the mammalian circadian clock. Science *288*, 1013-1019.

Shearman,L.P., Zylka,M.J., Weaver,D.R., Kolakowski,L.F., Jr., and Reppert,S.M. (1997). Two period homologs: circadian expression and photic regulation in the suprachiasmatic nuclei. Neuron *19*, 1261-1269.

Shibata,S. and Moore,R.Y. (1993). Neuropeptide Y and optic chiasm stimulation affect suprachiasmatic nucleus circadian function in vitro. Brain Res. *615*, 95-100.

Shibata,S., Oomura,Y., Kita,H., and Hattori,K. (1982). Circadian rhythmic changes of neuronal activity in the suprachiasmatic nucleus of the rat hypothalamic slice. Brain Res. *247*, 154-158.

Shibata,S., Tsuneyoshi,A., Hamada,T., Tominaga,K., and Watanabe,S. (1992). Effect of substance P on circadian rhythms of firing activity and the 2-deoxyglucose uptake in the rat suprachiasmatic nucleus in vitro. Brain Res. *597*, 257-263.

Shibata,S., Watanabe,A., Hamada,T., Ono,M., and Watanabe,S. (1994). N-methyl-D-aspartate induces phase shifts in circadian rhythm of neuronal activity of rat SCN in vitro. Am. J. Physiol. Regul. Integr. Comp. Physiol. *267*, R360-R364.

Shimomura,K., Low-Zeddies,S.S., King,D.P., Steeves,T.D., Whiteley,A., Kushla,J., Zemenides,P.D., Lin,A., Vitaterna,M.H., Churchill,G.A., and Takahashi,J.S. (2001). Genome-wide epistatic interaction analysis reveals complex genetic determinants of circadian behavior in mice. Genome Res. *11*, 959-980.

Shinohara,K., Funabashi,T., Mitushima,D., and Kimura,F. (2000a). Effects of gap junction blocker on vasopressin and vasoactive intestinal polypeptide rhythms in the rat suprachiasmatic nucleus in vitro. Neurosci. Res. *38*, 43-47.

Shinohara,K., Honma,S., Katsuno,Y., Abe,H., and Honma,K. (1995). Two distinct oscillators in the rat suprachiasmatic nucleus in vitro. Proc. Natl. Acad. Sci. U. S. A. *92*, 7396-7400.

Shinohara,K., Honma,S., Katsuno,Y., and Honma,K. (2000b). Circadian release of excitatory amino acids in the suprachiasmatic nucleus culture is Ca^{2+}-independent. Neurosci. Res. *36*, 245-250.

Shirakawa,T., Honma,S., Katsuno,Y., Oguchi,H., and Honma,K.I. (2000). Synchronization of circadian firing rhythms in cultured rat suprachiasmatic neurons. Eur. J. Neurosci. *12*, 2833-2838.

Silver,R., LeSauter,J., Tresco,P.A., and Lehman,M.N. (1996). A diffusible coupling signal from the transplanted suprachiasmatic nucleus controlling circadian locomotor rhythms. Nature *382*, 810-813.

Silver,R. and Schwartz,W.J. (2005). The Suprachiasmatic Nucleus is a Functionally Heterogeneous Timekeeping Organ. Methods Enzymol. *393*, 451-465.

Soscia,S.J. and Harrington,M.E. (2004). Neuropeptide Y attenuates NMDA-induced phase shifts in the SCN of NPY Y1 receptor knockout mice in vitro. Brain Res. *1023*, 148-153.

Stephan,F.K. and Zucker,I. (1972). Circadian rhythms in drinking behavior and locomotor activity of rats are eliminated by hypothalamic lesions. Proc. Natl. Acad. Sci. U. S. A. *69*, 1583-1586.

Sumova,A., Jac,M., Sladek,M., Sauman,I., and Illnerova,H. (2003). Clock gene daily profiles and their phase relationship in the rat suprachiasmatic nucleus are affected by photoperiod. J. Biol. Rhythms *18*, 134-144.

Sumova,A., Sladek,M., Jac,M., and Illnerova,H. (2002). The circadian rhythm of Per1 gene product in the rat suprachiasmatic nucleus and its modulation by seasonal changes in daylength. Brain Res. *947*, 260-270.

Sumova,A., Travnickova,Z., and Illnerova,H. (2000). Spontaneous c-Fos rhythm in the rat suprachiasmatic nucleus: location and effect of photoperiod. Am. J. Physiol. Regul. Integr. Comp. Physiol. *279*, R2262-R2269.

Sumova,A., Travnickova,Z., Peters,R., Schwartz,W.J., and Illnerova,H. (1995). The rat suprachiasmatic nucleus is a clock for all seasons. Proc. Natl. Acad. Sci. U. S. A. *92*, 7754-7758.

Takahashi,J.S. (1993). Circadian-clock regulation of gene expression. Curr. Opin. Genet. Dev. *3*, 301-309.

Takahashi,J.S., DeCoursey,P.J., Bauman,L., and Menaker,M. (1984). Spectral sensitivity of a novel photoreceptive system mediating entrainment of mammalian circadian rhythms. Nature *308*, 186-188.

Takahashi,J.S., Hong,H.K., Ko,C.H., and McDearmon,E.L. (2008). The genetics of mammalian circadian order and disorder: implications for physiology and disease. Nat Rev Genet *9*, 764-775.

Takahashi,J.S., Turek,F.W., and Moore,R.Y. (2001). Circadian Clocks. (New York: Kluwer Academic / Plenum Publishers).

Tournier,B.B., Menet,J.S., Dardente,H., Poirel,V.J., Malan,A., Masson-Pevet,M., Pevet,P., and Vuillez,P. (2003). Photoperiod differentially regulates clock genes' expression in the suprachiasmatic nucleus of Syrian hamster. Neuroscience *118*, 317-322.

Ukai,H., Kobayashi,T.J., Nagano,M., Masumoto,K.H., Sujino,M., Kondo,T., Yagita,K., Shigeyoshi,Y., and Ueda,H.R. (2007). Melanopsin-dependent photo-perturbation reveals desynchronization underlying the singularity of mammalian circadian clocks. Nat. Cell Biol. *9*, 1327-1334.

van den Pol,A.N. (1980). The hypothalamic suprachiasmatic nucleus of rat: intrinsic anatomy. J. Comp. Neurol. *191*, 661-702.

van den Pol,A.N. and Dudek,F.E. (1993). Cellular communication in the circadian clock, the suprachiasmatic nucleus. Neuroscience *56*, 793-811.

van der Horst,G.T., Muijtjens,M., Kobayashi,K., Takano,R., Kanno,S., Takao,M., de,W.J., Verkerk,A., Eker,A.P., Van,L.D., Buijs,R., Bootsma,D., Hoeijmakers,J.H., and Yasui,A. (1999). Mammalian Cry1 and Cry2 are essential for maintenance of circadian rhythms. Nature *398*, 627-630.

van Oosterhout,F., Michel,S., Deboer,T., Houben,T., van de Ven,R.C., Albus,H., Westerhout,J., Vansteensel,M.J., Ferrari,M.D., van den Maagdenberg,A.M., and Meijer,J.H. (2008). Enhanced circadian phase resetting in R192Q Cav2.1 calcium channel migraine mice. Ann. Neurol. *64*, 315-324.

Van Someren,E.J., Riemersma,R.F., and Swaab,D.F. (2002). Functional plasticity of the circadian timing system in old age: light exposure. Prog. Brain Res. *138*, 205-231.

Van Someren,E.J. and Riemersma-van der Lek RF (2007). Live to the rhythm, slave to the rhythm. Sleep Med. Rev. *11*, 465-484.

VanderLeest,H.T., Houben,T., Michel,S., Deboer,T., Albus,H., Vansteensel,M.J., Block,G.D., and Meijer,J.H. (2007). Seasonal encoding by the circadian pacemaker of the SCN. Curr. Biol. *17*, 468-473.

VanderLeest,H.T., Rohling,J.H., Michel,S., and Meijer,J.H. (2009a). Phase shifting capacity of the circadian pacemaker determined by the SCN neuronal network organization. PLoS One. *4*, e4976.

VanderLeest,H.T., Vansteensel,M.J., Duindam,H., Michel,S., and Meijer,J.H. (2009b). Phase of the electrical activity rhythm in the SCN in vitro not influenced by preparation time. Chronobiol. Int. *26*, 1075-1089.

Vansteensel,M.J., Deboer,T., Dahan,A., and Meijer,J.H. (2003a). Differential responses of circadian activity onset and offset following GABA-ergic and opioid receptor activation. J. Biol. Rhythms *18*, 297-306.

Vansteensel,M.J., Michel,S., and Meijer,J.H. (2008). Organization of cell and tissue circadian pacemakers: a comparison among species. Brain Res. Rev. *58*, 18-47.

Vansteensel,M.J., Yamazaki,S., Albus,H., Deboer,T., Block,G.D., and Meijer,J.H. (2003b). Dissociation between circadian Per1 and neuronal and behavioral rhythms following a shifted environmental cycle. Curr. Biol. *13*, 1538-1542.

Vitaterna,M.H., King,D.P., Chang,A.M., Kornhauser,J.M., Lowrey,P.L., Mcdonald,J.D., Dove,W.F., Pinto,L.H., Turek,F.W., and Takahashi,J.S. (1994). Mutagenesis and Mapping of A Mouse Gene Clock, Essential for Circadian Behavior. Science *264*, 719-725.

Vitaterna,M.H., Selby,C.P., Todo,T., Niwa,H., Thompson,C., Fruechte,E.M., Hitomi,K., Thresher,R.J., Ishikawa,T., Miyazaki,J., Takahashi,J.S., and Sancar,A. (1999). Differential regulation of mammalian period genes and circadian rhythmicity by cryptochromes 1 and 2. Proc. Natl. Acad. Sci. U. S. A. *96*, 12114-12119.

Vosko,A.M., Schroeder,A., Loh,D.H., and Colwell,C.S. (2007). Vasoactive intestinal peptide and the mammalian circadian system. Gen. Comp Endocrinol. *152*, 165-175.

Warren,E.J., Allen,C.N., Brown,R.L., and Robinson,D.W. (2003). Intrinsic light responses of retinal ganglion cells projecting to the circadian system. Eur. J. Neurosci. *17*, 1727-1735.

Watanabe,K., Deboer,T., and Meijer,J.H. (2001). Light-Induced resetting of the circadian pacemaker: quantitative analysis of transient versus steady-state phase shifts. J. Biol. Rhythms *16*, 564-573.

Webb,A.B., Angelo,N., Huettner,J.E., and Herzog,E.D. (2009). Intrinsic, nondeterministic circadian rhythm generation in identified mammalian neurons. Proc. Natl. Acad. Sci. U. S. A *106*, 16493-16498.

Welsh,D.K. (2007). VIP activates and couples clock cells. Focus on "Disrupted neuronal activity rhythms in the suprachiasmatic nucleus of vasoactive intestinal polypeptide-deficient mice". J. Neurophysiol. *97*, 1885-1886.

Welsh,D.K., Logothetis,D.E., Meister,M., and Reppert,S.M. (1995). Individual neurons dissociated from rat suprachiasmatic nucleus express independently phased circadian firing rhythms. Neuron *14*, 697-706.

Westermark,P.O., Welsh,D.K., Okamura,H., and Herzel,H. (2009). Quantification of circadian rhythms in single cells. PLoS. Comput. Biol. *5*, e1000580.

Winfree,A.T. (2000). The Geometry of Biological Time. (New York: Springer).

Witting,W., Boerma,D., Hoffen,G.C.K., Swaab,D.F., and Mirmiran,M. (1995). Light suppresses frequency and endogenous amplitude of the circadian system in nocturnal animals. Biological Rhythm Research *26*, 477-485.

Woelfle,M.A., Ouyang,Y., Phanvijhitsiri,K., and Johnson,C.H. (2004). The adaptive value of circadian clocks: an experimental assessment in cyanobacteria. Curr Biol *14*, 1481-1486.

Yamaguchi,S., Isejima,H., Matsuo,T., Okura,R., Yagita,K., Kobayashi,M., and Okamura,H. (2003). Synchronization of cellular clocks in the suprachiasmatic nucleus. Science *302*, 1408-1412.

Yamaguchi,S., Kobayashi,M., Mitsui,S., Ishida,Y., van der Horst,G.T., Suzuki,M., Shibata,S., and Okamura,H. (2001). View of a mouse clock gene ticking. Nature *409*, 684.

Yamazaki,S., Alones,V., Irelan,W., and Menaker,M. (1999). Serotonin-containing cell bodies in novel brain locations: effects of light input. Neuroreport *10*, 431-435.

Yamazaki,S., Kerbeshian,M.C., Hocker,C.G., Block,G.D., and Menaker,M. (1998). Rhythmic properties of the hamster suprachiasmatic nucleus in vivo. J. Neurosci. *18*, 10709-10723.

Yamazaki,S., Numano,R., Abe,M., Hida,A., Takahashi,R., Ueda,M., Block,G.D., Sakaki,Y., Menaker,M., and Tei,H. (2000). Resetting central and peripheral circadian oscillators in transgenic rats. Science *288*, 682-685.

Yannielli,P.C. and Harrington,M.E. (2000). Neuropeptide Y applied in vitro can block the phase shifts induced by light in vivo. Neuroreport *11*, 1587-1591.

Yannielli,P.C., Kinley Brewer,J., and Harrington,M.E. (2002). Is novel wheel inhibition of per1 and per2 expression linked to phase shift occurrence? Neuroscience *112*, 677-685.

Yoo,S.H., Yamazaki,S., Lowrey,P.L., Shimomura,K., Ko,C.H., Buhr,E.D., Siepka,S.M., Hong,H.K., Oh,W.J., Yoo,O.J., Menaker,M., and Takahashi,J.S. (2004). PERIOD2::LUCIFERASE real-time reporting of circadian dynamics reveals persistent circadian oscillations in mouse peripheral tissues. Proc. Natl. Acad. Sci. U. S. A. *101*, 5339-5346.

Yoshikawa,T., Yamazaki,S., and Menaker,M. (2005). Effects of preparation time on phase of cultured tissues reveal complexity of circadian organization. J. Biol. Rhythms *20*, 500-512.

Zhou,Q.Y. and Cheng,M.Y. (2005). Prokineticin 2 and circadian clock output. Febs J. *272*, 5703-5709.

Zlomanczuk,P., Margraf,R.R., and Lynch,G.R. (1991). In vitro electrical activity in the suprachiasmatic nucleus following splitting and masking of wheel-running behavior. Brain Res. *559*, 94-99.

SUMMARY

In chapter 1 of this thesis, a general introduction of the mammalian biological clock is given. The biological clock in mammals, which controls 24h rhythms, is located in the suprachiasmatic nucleus (SCN) at the base of the anterior hypothalamus. The SCN is a paired structure and in mice each nucleus contains approximately 10,000 neurons. The SCN is an autonomous pacemaker of circadian rhythms (circa = approximately; dies = day) and has an activity cycle of around 24h. The SCN receives direct light input through a specialized retinal pathway, the retinohypothalamic tract (RHT). The circadian oscillations are the result of a molecular clockwork and can be synchronized to the environment by light. At different phases during the circadian cycle, light has different phase shifting effects that can be summarized in a phase response curve (PRC). In nocturnal animals, a light pulse in the early night induces a delay of the rhythm, so that the animal will become active at a later time, while light at the end of the night induces an advance, causing the animal to become active earlier on the next cycle. These characteristics of the biological clock are intrinsic to the SCN and are preserved in an *in vitro* brain slice preparation.

In chapter 2 of this thesis we studied the effects of the time of brain slice preparation on the phase of the electrical activity rhythm of the SCN. We prepared coronal hypothalamic slices containing the SCN and recorded extracellular electrical activity in brain slices kept submerged in a laminar flow chamber which was perfused with oxygenated ACSF. We found that the SCN in these hypothalamic brain slices continues to show circadian oscillations in electrical activity. Multiunit electrical activity in the SCN in these slices was high during the extrapolated day and low during the subjective night. Preparation of the slices at different phases of the circadian cycle revealed that the timing as well as the waveform of these oscillations are determined by the light dark cycle of the animal and are not influenced by the time the brain slice was prepared. This finding is of importance for the field of rhythm research as the phase of the rhythm at the time of preparation is not always known. The robustness of the waveform is of particular importance in research on seasonal rhythms, where changes in the waveform of the electrical activity are expected to occur. The robustness of the circadian oscillations in the acute *in vitro* brain slice preparation shows that this technique offers a valuable and reliable tool to investigate the phase and waveform of circadian rhythms *ex vivo*.

In chapter 3, we used the brain slice preparation to study the activity pattern of small groups of neurons in the SCN. We recorded extracellular multiunit electrical activity and stored the time, amplitude and shape of action potentials that crossed a preset threshold. For regular multiunit data, containing a large population of neurons, we found that electrical activity was high during the projected day and low during the projected night with very low variability in phase. For smaller populations, we found that there is a large variation in timing of maximum activity between subpopulations in the SCN. Additionally, subpopulations consisting of about 3 neurons that are close to each other are much more synchronized over the 24h cycle than can be explained by random

timing. We furthermore found that electrical activity patterns of single SCN neurons are active for a much shorter duration than large populations of neurons in the SCN. Together the data indicate that a regulated ensemble of SCN neurons determines the waveform of the SCN electrical activity rhythm.

The duration of day light (or "photoperiod") has marked effects on behavior and physiology of animals and in some species induces hibernation. The difference in day length brings about changes in the waveform of the SCN rhythm. Based on our results we questioned whether the phase distribution among neurons is involved in these photoperiodic changes. We recorded electrical activity in slices from animals that were entrained to a long or short photoperiod and found that the length of day is represented in the SCN by an increase or decrease respectively in the width of the electrical activity peak. We hypothesize that in short days, as in winter, the timing of the neurons is distributed over the short duration of the light period, resulting in a highly synchronized output with a narrow and high amplitude peak. In long summer days, the timing of neurons is more spread out over the subjective day because of the longer duration of light, resulting in a lower number of neurons that are highly active at the same time, resulting in a broad, low amplitude multiunit peak. To test this hypothesis, we simulated multiunit activity by linearly distributing single unit activity profiles over the photoperiod. The simulation studies resembled our results and show that the difference in the timing of neuronal activity may indeed provide a mechanism for photoperiodic encoding.

In chapter 4, we performed the experimental test of our hypothesis and empirically tested the proposed mechanism for photoperiodic encoding by the SCN. Mice are nocturnal animals and wheel running activity is restricted to the dark portion of a 24h light dark cycle. The mice showed an adaptation in the duration of wheel running activity that resembled the duration of the dark period, a long duration of wheel running activity in short day length and narrow activity profile

in long day length. We recorded electrical activity in the SCN of freely moving mice and found that the photoperiod is reflected in the duration of elevated electrical activity in the SCN. In continuous darkness, in the absence of light, the oscillations in the SCN remained similar, with a narrow multiunit electrical activity peak in animals from short day length and broad activity peaks in the SCN from long day animals, showing that day length adaptation is not driven by light but encoded in the SCN.

We furthermore prepared brain slices from animals from long and short day length and recorded extracellular electrical activity and stored time and amplitude of action potentials. In brain slices containing the SCN of mice kept on long and short days, we confirmed that the width of the multiunit peak was consistently broad in long day length and narrow in short day length.

To investigate the underlying mechanism by which the SCN is able to change the shape of the electrical rhythm in response to photoperiod, we performed a subpopulation analysis. By changing the threshold for action potential selection, the number of neurons contributing to the electrical activity rhythms can be restricted, resulting in a smaller population of neurons that is recorded from. We found that in small populations of neurons the timing of activity was highly synchronized in the narrow multiunit peaks in slices from short day length. In contrast, the subpopulations showed a broad distribution in slices from long day length. We furthermore extracted single unit activity from these recordings and found that the shape and duration of single unit electrical activity in slices from both day lengths were not different. Based on these results, we were able to make an estimation of population size versus peak width. We found that in both day lengths populations of 50 units already account for 75% of the peak width of the large population. This shows that a small number of neurons can already carry substantial information on day length by a distribution of the phases at which the neurons become active.

In chapter 5, we investigated the phase shifting effects of light in relation to the photoperiod. We found that in the running wheel activity rhythm in animals from long day length, the phase shifts after a light pulse were significantly smaller than from short days. The small shifts in long day length may be attributable to desensitization to light, because of the higher exposure in the light dark cycle. We therefore adjusted the number of photons the animal received during the light dark cycle, and found that despite the higher exposure to light, the animals in short day length did not shift to a lesser extent. This indicates that the lack of large phase shifts in long day length it is not because of desensitization to light.

To investigate whether the photoperiodic modulation of phase shifts is present in the SCN, we prepared hypothalamic brain slices and applied NMDA to mimic the phase shifting effects of light. *In vitro* there were large phase shifts in brain slices from animals entrained to short day lengths and no significant phase shifts in slices from long day lengths, consistent with the behavioral data. We performed an analysis of rhythm amplitude and found that the amplitude of the electrical activity rhythms were different between day lengths. Based on the results shown in chapter 4 we can explain a larger rhythm amplitude in short days by a higher number of synchronized cells. This result seemingly contradicts a dogma that is based on limit cycle oscillators, where an oscillation is represented as a circular shape and the rhythm amplitude is represented as the radius of the circle. In these limit cycle oscillators, high amplitude rhythms are less sensitive to a similar phase shifting stimulus than low amplitude rhythms, because of the larger fraction of radius of the circle. Our results however show the opposite as high amplitude rhythms lead to large phase shifts and low amplitude rhythms to small shifts or absence of shifts.

We performed simulations to investigate these paradoxical results in phase shifting effects of light in more detail. With a phase distribution found in subpopulations of SCN neurons, we distributed single unit PRCs in a similar manner over the 24h cycle. The

population response could be calculated by the summation of the differently distributed single unit PRCs. These simulations showed that a broad phase distribution gives rise to a low amplitude PRC with small shifts, whereas a narrow distribution results in a high amplitude PRC, irrespective of the shape of the single unit PRC. These results show that the limit cycle theory does not apply for multiple oscillators, and that the SCN neuronal network brings about new levels of organization through the amount of synchrony between the pacemaker neurons.

NEDERLANDSE SAMENVATTING

In hoofdstuk 1 van dit proefschrift wordt een algemene inleiding gegeven op de biologische klok van zoogdieren. De biologische klok van zoogdieren, welke 24-uurs ritmen in het lichaam aanstuurt, ligt aan de onderzijde van het voorste deel van de hersenen, in de suprachiasmatische kernen (SCN) van de hypothalamus. De SCN is een gepaarde structuur, dat wil zeggen dat er aan beide zijden van de hersenen een gespiegeld evenbeeld aanwezig is. Iedere kern bestaat uit ongeveer 10,000 neuronen. De SCN genereert circadiane ritmen, wat betekent ritmen van ongeveer (circa) een dag (dies). De SCN ontvangt informatie over de lichtomstandigheden uit de omgeving, via een directe verbinding vanaf het oog, de zogenaamde retinohypothalamic tract (RHT). De circadiane ritmen worden zelfstandig door de SCN geproduceerd en zijn een gevolg van een moleculaire klok welke met de omgeving gelijk gezet kan worden door de invloed van licht.

Op verschillende circadiane fasen, ofwel tijdstippen in de 24-uurs cyclus, heeft licht verschillende fase-verschuivende effecten die kunnen worden samengevat in een fase respons curve (PRC). In nachtdieren veroorzaakt een lichtpuls in de vroege nacht een vertraging van het ritme, zodat het dier de dag volgend op de lichtpuls

op een later tijdstip actief zal worden (delay). Licht aan het einde van de nacht zorgt ervoor dat het ritme vooruit schuift, waardoor het dier de volgende dag eerder actief zal worden (advance). Deze kenmerken van de biologische klok zijn intrinsiek aan de SCN en blijven aanwezig in een *in vitro* preparaat.

In hoofdstuk 2 van dit proefschrift onderzochten we de effecten van het tijdstip waarop het hersenplakje werd geprepareerd. Wij keken hierbij naar de fase van het elektrische activiteits-ritme in de SCN. We prepareerden hersenplakjes uit met daarin de SCN en maakten een opname van de elektrische activiteit in de SCN. Het hersenplakje werd in leven gehouden in een laminaire flowkamer die werd doorstroomd met zuurstofrijke kunstmatige hersenvloeistof (ACSF). Met twee elektroden werd de elektrische activiteit van meerdere cellen tegelijkertijd gemeten. We vonden dat de biologische klok in deze hersenplakjes circadiane ritmen in elektrische activiteit lieten zien. Er was hoge elektrische activiteit tijdens de dag en lage activiteit in de nacht van het dier. We vonden dat de timing en de golfvorm van het ritme worden bepaald door de licht-donker cyclus van het dier, en niet worden beïnvloed door het tijdstip waarop de hersenplakjes werden uitgeprepareerd. Deze bevinding is van belang voor het onderzoek aan de biologische klok, omdat de fase van het ritme bij het uitprepareren niet altijd bekend is. De robuustheid van het ritme en de golfvorm van het ritme is van bijzonder belang in het onderzoek naar seizoensgebonden ritmes, waarbij veranderingen in de golfvorm van de elektrische activiteit te verwachten zijn. Doordat de gemeten ritmes in het preparaat niet afhankelijk zijn van het moment waarop de plakjes werden geprepareerd, is de gemeten activiteit dus het gevolg van het ritme van de biologische klok. Hieruit blijkt dat deze techniek een waardevol en betrouwbaar hulpmiddel is om de fase en golfvorm van circadiane ritmen *ex vivo* te onderzoeken.

In hoofdstuk 3 gebruikten we hetzelfde preparaat als hierboven beschreven. We maakten opnames van de extracellulaire elektrische

activiteit van meerdere neuronen. Hierbij werd het tijdstip, de grootte en de vorm van de elektrische pulsen (actiepotentialen), die een vooraf ingestelde drempel overschreden, opgenomen. Voor de standaard metingen, waarbij er pulsen werden geteld van een grote groep neuronen (multi-unit), vonden we dat de elektrische activiteit hoog was tijdens de subjectieve dag en laag tijdens de subjectieve nacht, met een zeer lage variabiliteit in timing. Voor kleinere groepen cellen (populaties), vonden we een grote variabiliteit in de timing van de maximale activiteit. Daarnaast vonden we dat kleine groepen cellen samen (subpopulaties), die bestaan uit ongeveer 3 neuronen die dicht bij elkaar liggen, veel sterker gesynchroniseerd zijn over de 24-uurs cyclus dan kan worden verklaard door willekeurige timing. Bovendien hebben we vastgesteld dat de elektrische activiteit van een enkele cel in de SCN, veel korter actief is dan het totaal van de cellen in de SCN. Uit deze gegevens samen konden we vaststellen dat de golfvorm van het elektrische activiteitsritme in de SCN wordt bepaald door een gestuurd samenspel van de neuronen in de SCN.

De duur van het daglicht heeft een duidelijke invloed op het gedrag en de fysiologie van dieren en bij sommige soorten induceert een korte daglengte zelfs winterslaap. Het verschil in daglengte tussen zomer en winter brengt veranderingen teweeg in het elektrische activiteitsritme van de SCN. Het vastleggen van deze daglengte-veranderingen in het ritme van de SCN zou kunnen berusten op een verschil in fase van de activiteitspieken van kleine groepen neuronen. Wij hebben de elektrische activiteit in de SCN in hersenplakjes opgenomen van dieren die onder een lange of een korte daglengte werden gehuisvest. We vonden dat de lengte van de dag een verandering teweegbrengt in het elektrische activiteitsritme in de SCN. In een korte dag vonden we smalle pieken en in een lange dag vonden we brede pieken in elektrische activiteit.

Onze hypothese is dat in korte dagen, zoals in de winter, de activiteitsfase van de neuronen verdeeld is over de korte licht periode. Doordat de activiteit van de neuronen overlapt heeft de totale populatie een output met een smalle, hoge amplitude piek. In lange

zomer dagen is de activiteitsfase van de neuronen meer verspreid over de subjectieve dag vanwege de langere duur van het licht. Dit resulteert in een lager aantal neuronen dat op hetzelfde moment actief is en geeft daarmee een brede, lage amplitude piek. Om deze hypothese te toetsen, hebben we de activiteit van vele neuronen samen gesimuleerd. We verdeelden activiteitsprofielen van een enkel neuron over de lengte van de lichtperiode met een lineaire verdeling. De uitkomsten van de simulaties leken sterk op de experimentele resultaten. Dit laat zien, dat het verschil in de timing van de neuronale activiteit inderdaad een mechanisme is waarmee de daglengte kan worden weergegeven en vastgehouden (gecodeerd) in de SCN.

In hoofdstuk 4 hebben we onze hypothese van het mechanisme voor daglengte codering door de SCN experimenteel getoetst. Muizen zijn nachtdieren en hun loopwiel activiteit vindt plaats in het donkere gedeelte van de 24-uurs licht donker cyclus. De muizen vertoonden een aanpassing in de lengte van loopwiel activiteit, die de duur van het donker volgde. Dit betekent een lange activiteitsperiode in korte daglengte en een korte duur van loopwiel activiteit in lange daglengte. Vervolgens registreerden we de elektrische activiteit in de SCN in vrij bewegende muizen en vonden dat de daglengte tot uiting komt in de duur van de verhoogde elektrische activiteit in de SCN. In constant donker, in de afwezigheid van licht, bleef de vorm van de activiteitspieken in de SCN gelijk, met een smalle multi-unit elektrische activiteit piek in de dieren van korte daglengte en brede activiteitspieken in de SCN van dieren op lange dag. Hieruit blijkt dat de daglengte aanpassing gecodeerd is in de SCN.

Hierna onderzochten we de SCN van muizen uit lange en korte daglengte *in vitro* en registreerden de elektrische activiteit in de SCN. Van de elektrische activiteit werd het tijdstip en de grootte van de actiepotentialen opgeslagen. In de SCN van muizen die werden gehouden op verschillende daglengten, vonden we dat de breedte van

de multi-unit piek consequent breed was in lange dag en smal in korte daglengte.

Om het onderliggende mechanisme te onderzoeken waarmee de SCN in staat is om de vorm van het elektrische activiteitsritme te veranderen in reactie op daglengte, voerden we een subpopulatie analyse uit. Actiepotentialen met een verschillende amplitude werden geselecteerd door de selectiedrempel aan te passen. Hierdoor kan het aantal neuronen dat bijdraagt aan de elektrische activiteitsritmen worden beperkt. Dit resulteert in een kleinere populatie van neuronen waarvan de activiteit wordt opgenomen. We vonden dat in kleine populaties van neuronen de timing van de activiteit zeer gesynchroniseerd was in de smalle multi-unit pieken in de SCN van korte daglengte. Daartegenover vertoonden de subpopulaties een brede verdeling van hun activiteitspieken in plakken van lange daglengte. In deze experimenten hebben wij tevens de vorm en het tijdstip van actiepotentialen opgeslagen. Uit deze gegevens hebben wij de elektrische activiteit van enkele neuronen geëxtraheerd. Wij vonden dat de vorm en de duur van de elektrische activiteit van een enkel neuron niet verschillend waren tussen beide daglengtes. Gebaseerd op deze resultaten, konden we een schatting van de populatiegrootte versus piekbreedte maken. We vonden dat in beide daglengten de breedte van de activiteitspiek van gemiddeld 50 neuronen al goed is voor 75% van de totale piekbreedte in de grote populatie. Dit toont aan dat een klein aantal neuronen al veel informatie kan geven over de daglengte door een verdeling van de tijdstippen waarop de neuronen actief worden.

In hoofdstuk 5 onderzochten we de fase verschuivende effecten van licht in relatie tot de daglengte. We vonden dat verschuivingen in het loopwielritme bij muizen in lange daglengte na een lichtpuls beduidend kleiner waren dan bij dieren in korte daglengte. De kleine verschuivingen in lange dag zouden kunnen worden veroorzaakt door een verminderde gevoeligheid voor het licht, als gevolg van de langere blootstelling aan licht overdag. Om voor de blootstelling te corrigeren

hebben wij de hoeveelheid fotonen (lichtdeeltjes) aangepast zodat de dieren in een korte dag per dag evenveel fotonen ontvingen als dieren van een lange dag. Wij vonden dat, ondanks de hogere blootstelling aan licht, de dieren in korte daglengte niet minder verschoven dan de controle groep in korte daglengte. Dit geeft aan dat het ontbreken van grote fase verschuivingen in lange daglengte niet veroorzaakt wordt door een verminderde gevoeligheid voor licht.

Om te onderzoeken wat de rol van de SCN is in de mate van verschuiven in verschillende daglengten hebben wij hersenplakjes van muizen uit lange en korte daglengte geprepareerd en registreerden de elektrische activiteit in de SCN. Wij voegden NMDA toe om de fase verschuivende effecten van het licht na te bootsen. *In vitro* waren er grote fase-verschuivingen in de SCN van muizen van een korte dag lengte. In de SCN van muizen die op een lange daglengte werden gehouden waren er geen significante verschuivingen, in overeenstemming met de gedragsgegevens. Om het achterliggende mechanisme te onderzoeken voerden we een analyse van de amplitude van het ritme uit. We vonden dat de amplitude van de elektrische activiteits-ritmen van verschillende daglengtes op ieder niveau verschillend was. De oorzaak van de grotere amplitude van het ritme in korte daglengte, is een groter aantal cellen dat tegelijkertijd actief is, zoals beschreven in hoofdstuk 4. Dat een ritme met een hoge amplitude meer verschuift dan een ritme met een lage amplitude is in strijd met voorspellingen gebaseerd op limiet cyclus oscillatoren. Hierbij wordt een ritme voorgesteld als een circulaire vorm en de amplitude van het ritme wordt weergegeven door straal van de cirkel. In deze limiet cyclus oscillatoren zijn ritmes met een hoge amplitude minder gevoelig voor een fase verschuiving stimulus dan lage amplitude ritmes, doordat de grootte van de stimulus ten opzichte van de straal van de cirkel bepalend is voor de verstoring van de cyclus. Onze resultaten tonen echter het tegenovergestelde aan: Hoge amplitude ritmen hebben grote fase verschuivingen en lage amplitude ritmen hebben kleine verschuivingen.

We voerden simulaties uit om deze paradoxale resultaten in meer detail te onderzoeken. Hierbij onderzochten we verschillende vormen die de fase-verschuivende effecten van licht op de activiteit van een enkele cel in de SCN kan hebben, een zogenaamde "single-unit PRC". Deze single-unit PRCs verdeelden wij vervolgens over de 24-uurs cyclus met een verdeling zoals we die hebben gevonden in subpopulaties van SCN neuronen (hoofdstuk 4). De fase verschuivingsreactie van de SCN als geheel kon worden berekend door de som te nemen van de single-unit PRCs. Uit deze simulaties bleek dat een brede verdeling over de 24-uurs cyclus een lage amplitude PRC met kleine verschuivingen geeft, terwijl een smalle verdeling resulteert in een hoge amplitude PRC, ongeacht de vorm van de single-unit PRC, in overeenstemming met de resultaten van de gedrags- en *in vitro*-proeven. Dit laat zien dat de limiet cyclus theorie niet van toepassing is op systemen waarin meerdere oscillatoren aanwezig zijn, en dat het neuronale netwerk van de SCN nieuwe organisatie niveaus geeft door synchronisatie tussen de pacemaker neuronen.

GLOSSARY

ACSF	Artificial cerebrospinal fluid
AVP	Arginine vasopressin
Bmal1	Bmal1 gene
BMAL	Bmal1 protein
CHX	Cycloheximide, a protein synthesis blocker
Circadian rhythm	Rhythm of about a day, *circa* = approximately; *dies* = day
Clock	Clock gene
CLOCK	Clock protein
CRY	Crytochrome protein
Cry1	Cryptochrome 1 gene
Cry2	Cryptochrome 2 gene
CSNK1D	Casein kinase 1 δ
CSNK1E	Casein kinase 1 ε
CT	Circadian time, the endogenous state of the pacemaker, or phase φ
DD	Constant darkness
Entrainment	Adjustment to the external time
ex vivo	Tissue taken from living organism
fDR	Fast-delayed rectifier K+-channel
GABA	γ-amino butyric acid
GFP	Green fluorescent protein
GHT	Geniculohypothalamic tract
IGL	Intergeniculate leaflet
in situ	Fixed tissue directly taken from a living organism
in vitro	Living tissue in a controlled environment outside an organism

in vivo	In the living organism
LD	Light-dark
LL	Constant light
MUA	Multi-unit activity, activity of multiple cells
NMDA	N-methyl-D-aspartate
nPas2	Paralogue neuronal PAS domain-containing protein 2 gene
NPY	Neuropeptide Y
Optic chiasm	Crossing of the optic nerves
Organotypic	Culture of a specific part of tissue
PACAP	Pituitary adenylyl cyclase activating peptide, a neuropeptide
PER	Period protein
Per1	Period 1 gene
Per2	Period 2 gene
PHI	Peptide histidine isoleucine
Photoperiod	Length of daylight
PRC	Phase response curve
Rev-erbα	Rev-Erbα gene
REV-ERBα	Rev-Erbα protein
RGC	Retinal ganglion cells
RHT	Retino-hypothalamic tract
RNA	Ribonucleic acid
SCN	Suprachiasmatic nucleus, location of the biological clock in mammals
SUA	Single unit activity, activity of a single cell
Subpopulation	A small number of neurons taken from a larger population
Tau	Internal speed of the clock τ, which is used to describe the free-running period of an animal
TEA	Tetraethylammonium
Tim	Timeless gene of *Drosophila* clock
TIM	Timeless protein of *Drosophila* clock
TTX	Tetrodotoxin, a pharmacological blocker of fast Na+ channels
VIP	Vasoactive intestinal polypeptide
vLGN	Ventral lateral geniculate nucleus
Vm	Membrane potential
VPAC2	Vasoactive intestinal peptide receptor 2
Zeitgeber	External time cues, litterally time-giver
ZT	Zeitgeber time

List of Publications

Schaap,J., Albus,H., VanderLeest,H.T., Eilers,P.H., Detari,L., and Meijer,J.H. (2003). Heterogeneity of rhythmic suprachiasmatic nucleus neurons: Implications for circadian waveform and photoperiodic encoding. **Proc. Natl. Acad. Sci. U. S. A.** *100*, 15994-15999.

Rohling,J., Meijer,J.H., VanderLeest,H.T., and Admiraal,J. (2006). Phase differences between SCN neurons and their role in photoperiodic encoding; a simulation of ensemble patterns using recorded single unit electrical activity patterns. **J. Physiol Paris** *100*, 261-270.

VanderLeest,H.T., Houben,T., Michel,S., Deboer,T., Albus,H., Vansteensel,M.J., Block,G.D., and Meijer,J.H. (2007). Seasonal encoding by the circadian pacemaker of the SCN. **Curr. Biol.** *17*, 468-473.

VanderLeest,H.T., Rohling,J.H., Michel,S., and Meijer,J.H. (2009). Phase shifting capacity of the circadian pacemaker determined by the SCN neuronal network organization. **PLoS One**. *4*, e4976.

VanderLeest,H.T., Vansteensel,M.J., Duindam,H., Michel,S., and Meijer,J.H. (2009). Phase of the electrical activity rhythm in the SCN

in vitro not influenced by preparation time. **Chronobiol. Int**. *26*, 1075-1089.

Meijer,J.H., Michel,S., VanderLeest, H.T., and Rohlin, J.H.T. (2010). Daily and seasonal adaptation of the circadian clock requires plasticity of the SCN neuronal network. **European Journal of Neuroscience**. *In Press*

van Kempen,G.Th.H., vanderLeest,H.T., van den Berg,R.J., Eilers,P. and Westerink,R.H.S. (2010). Three distinct modes of exocytosis revealed by amperometry in neuroendocrine cells *Submitted*

Acknowledgements

This thesis could not have been written without the support of many people. I want to thank all of my colleagues, both past and present, in the neurophysiology group for providing such a good working atmosphere and for the great scientific discussions. A few persons I want to thank specifically. First, I want to thank Joke, for support throughout and scientific guidance. Henk and Stephan, for teaching me electrophysiology in such an inspiring way. Hans, for all the work you do for the group. Jos, for the great time anywhere, anytime. Roman, for our conversations and great discussions. Furthermore, I want to thank the people from the mechanical workshop and electronics, specifically Arie, Huybert, Bram, Jan and Sander. Your help and insights have been crucial for the maintenance and developments in the lab.

The most important people in my life, my family deserve the biggest thanks. Karen, my wife, for being there and supporting me. Suzanne, our daughter for her never ending enthusiasm and the joy she brings. My brother and sister for creating such wonderful cover art of this thesis! All the rest of my family and friends!

Henk Tjebbe

CURRICULUM VITAE

Henk Tjebbe van der Leest werd geboren op 28 juli 1979 in Rotterdam. In 1998 behaalde hij zijn VWO diploma aan de Gereformeerde Scholengemeenschap Randstad te Rotterdam. Hij startte in 1998 de studie Biologie aan de Universiteit Leiden waar hij in 1999 zijn propedeuse behaalde. Als onderdeel van de opleiding volgde hij een stage bij de afdeling diermorfologie van de Universiteit Leiden. Tijdens zijn studie raakte hij geïnteresseerd in de werking van de hersenen en de mogelijkheden die computers bieden hierin inzicht te geven. In 2002 startte hij zijn hoofdstage en legde hij een hoofdvaktentamen af bij Prof. Dr. J.H. Meijer in de groep neurofysiologie van het Leids Universitair Medisch Centrum. Daarin vond hij de uitdagende combinatie van hersenonderzoek en programmeren van analysemethoden. In 2004 heeft hij zijn doctoraalexamen Biologie behaald.

Het werk in het laboratorium, met elektrofysiologische apparatuur en het ontwikkelen van analysemethoden op de computer beviel zo goed, dat op dezelfde afdeling waar hij zijn hoofdstage had gevolgd de start werd gemaakt met het promotieonderzoek waarvan de resultaten beschreven staan in dit proefschrift.

Sinds 2009 heeft hij een aanstelling als postdoctoraal onderzoeker bij het laboratorium voor neurofysiologie, afdeling Moleculaire Celbiologie van het Leids Universitair Medisch Centrum.